DAVID JOEL FIGUEROA CORTÉS

Analysis of power system stability in presence of high levels of wind power penetration

São Paulo
2014
2014

DAVID JOEL FIGUEROA CORTÉS

Analysis of power system stability in presence of high levels of wind power penetration

Dissertação apresentada à Escola Politécnica da Universidade de São Paulo para obtenção do título de Mestre em Ciências

Orientador: Prof.
Mauricio Barbosa de Camargo Salles.

São Paulo

2014

2014

DAVID JOEL FIGUEROA CORTÉS

Analysis of power system stability in presence of high levels of wind power penetration

Dissertação apresentada à Escola Politécnica da Universidade de São Paulo para obtenção do título de Mestre em Ciências

Área de Concentração:
Engenharia Elétrica

Orientador: Prof.
Mauricio Barbosa de Camargo Salles.

São Paulo

2014

2014

Este exemplar foi revisado e corrigido em relação à versão original, sob responsabilidade única do autor e com a anuência de seu orientador.

São Paulo, 12 de agosto de 2014.

Assinatura do autor _____

Assinatura do orientador _____

Catalogação-na-publicação

Figueroa Cortes, David Joel
Analysis of power system stability in presence of high levels of wind power penetration / D.J. Figueroa Cortes. -- versão corr. -- São Paulo, 2014.
130 p.

Dissertação (Mestrado) - Escola Politécnica da Universidade de São Paulo. Departamento de Engenharia de Energia e Automação Elétricas.

1.Energia eólica 2.Sistemas elétricos de potência 3. Estabilidade de sistemas I.Universidade de São Paulo. Escola Politécnica. Departamento de Engenharia de Energia e Automação Elétricas II.t.

I dedicate this work to these people whose encouragement and support were really important in the development and the achievement of the same, maybe without them, none of this would have been successfully completed:

My mom Tati, my dad Mane, my brother and sister, the Mrs. Myriam, my friends Fabio, Débora, Carlos, Miguel, Cristopher, Mauricio, and this special person for me, Luciana.

ACKNOWLEDGEMENTS

- To the professor Mauricio Salles, for the support and orientation during the development of this work;

- To the professors of the Laboratório de Elegtromagnetismo Aplicado (LMAG) for the support;

- To the colleagues with whom I shared in the LMAG during the development of this masters degree;

- To my friends from the Escola Politécnica of the Universidade de São Paulo (USP);

- To the Coordenação de Aperfeiçoamento de Pessoal de Nível Superior (CAPES) and the Fundação de Apoio à Universidade de São Paulo (FUSP) for the financial support;

- To my family and friends for the emotional support and encouragement;

- To Luciana who supported and encouraged me during the end of this stage.

RESUMO

Atualmente, a energia eólica é uma das fontes renováveis mais reconhecidas, e sua penetração em sistemas elétricos de potência está se incrementando consideravelmente. Por consequência, a participação de turbinas eólicas em sistemas elétricos de potência tem se incrementado e pode influenciar o comportamento geral do sistema de potência. Portanto, é importante estudar o desempenho de turbinas eólicas em sistemas elétricos e sua interação com outros equipamentos de geração e cargas. O principal objetivo nesta dissertação é determinar o desempenho dinâmico de diferentes tecnologias ligadas nos sistemas elétricos considerando diferentes níveis de penetração e diferentes perturbações elétricas mediante simulações realizadas usando um *toolbox* de Matlab/Simulink, SimPowerSystems. As tecnologias avaliadas são (a) o gerador de indução duplamente alimentado com fator de potência unitário, (b) o gerador de indução duplamente alimentado com controle de tensão, (c) o gerador de indução de gaiola de esquilo com compensação baseada em condensadores, e (d) gerador de indução de gaiola de esquilo sem equipamentos auxiliares. Os fatores técnicos analisados são perfil de tensão em estado estacionário, as dinâmicas durante afundamentos e elevações de tensão, correntes de curto circuito, e incremento gradual nas cargas do sistema, para verificar a estabilidade de tensão da rede para pequenas perturbações. É proposta uma estratégia para promover uma integração efetiva de turbinas eólicas em sistemas de potência com altos níveis de penetração considerando diferentes normas de operação da rede para sistemas de transmissão e de distribuição. O objetivo nesta estratégia é o cumprimento dos requisitos para conexão de rede com a combinação de tecnologias, minimizando o valor do investimento. Os efeitos na estabilidade de sistemas de potência da fazenda eólica determinada com a metodologia proposta são comparados com os efeitos de uma fazenda eólica de igual capacidade de energia eólica considerando somente geradores de indução duplamente alimentados com controle de tensão. Para as analises realizadas neste trabalho são considerados os sistemas IEEE de 9 e 30 barras.

Palavras-Chave: Altos níveis de penetração de energia eólica. Estabilidade de tensão. Geração de energia eólica. Gerador de indução com gaiola de esquilo. Gerador de indução duplamente alimentado. Normas de operação da rede.

ABSTRACT

Nowadays, wind power is one of the most accepted renewable energy sources, and its penetration in electrical power systems is increasing considerably. Consequently, the participation of wind turbines in electrical power systems has increased and may influence the overall power system behavior. It is therefore important to study the performance of wind turbines in electrical power systems and their interaction with other generation equipment and loads. The main objective of this dissertation is to determine the dynamic performance of different wind turbines technologies connected in electrical system considering different penetration levels and electrical perturbations by simulations performed using a Matlab/Simulink toolbox, SimPowerSystems. The assessed technologies are (a) double fed induction generator with unity power factor, (b) double fed induction generator with voltage control, (c) squirrel cage induction generator with capacitor-based compensation, and (d) squirrel cage induction generator without ancillary devices. The technical factors analyzed are steady-state voltage profile, the dynamics during voltage sags and swells, short-circuit currents, and gradual increase in the system loading, in order to check the network small-disturbance voltage stability. A strategy to promote an effective integration of wind turbines into the power systems with high levels of wind power penetration regarding different grid code requirements in transmission and distribution networks is proposed. The objective in this strategy is fulfilling the grid code requirements with a technology combination, minimizing the invested value. The effects on power system stability of the wind farm, found by the proposed methodology, are compared with the effects that have the same installed capacity of wind power but only considering double fed induction generators with voltage control. The IEEE 9 bus transmission system and the IEEE 30 bus system are regarded for the analysis performed in this work.

Keywords: High wind power penetration levels. Voltage stability. Wind Power generation. Squirrel cage induction generator. Double-fed induction generator. Grid code requirements.

LIST OF FIGURES

LIST OF TABLES

LIST OF ACRONYMS AND ABBREVIATIONS

ABBEolica	Associação Brasileira de Energia Eólica
ASIG	Active Stall Induction Generator
CST	Constant
DC	Direct Current
DFIG	Doubly-Fed Induction Generator
DS	Dynamic Stability
EDV	Electric Drives Vehicles
EMTP	Electromagnetic Transient Programs
FACTS	Flexible Alternating Current Transmission System
GSC	Grid Side Converter
GWEC	Global Wind Energy Council
HPF	Harmonic Power Flow
HVRT	High-Voltage Ride Through
IEA	International Energy Agency
IEEE	Institute of Electrical and Electronics Engineers
LDVS	Large-Disturbance Voltage Stability
LVRT	Low-Voltage Ride Through
OTS	Operator Training Simulators
PCC	Point of Common Coupling
PF	Power Flow
PMSG	Permanent Magnet Synchronous Generator
PU	Per-unit
RES	Renewable Energy Systems
RSC	Rotor Side Converter
SCIG	Squirrel Cage Induction Generator
SDVS	Short-Disturbance Voltage Stability
STATCOM	Static Synchronous Compensator
SVC	Static VAR Compensator
TPF	Transmission Power Flow
TS	Transient Stability
WECC	Western Electricity Coordinating Council
WSAT	Wind Security Assessment Tool
WSCC	Western System Coordinating Council
WWEA	World Wind Energy Association

TABLE OF CONTENTS

1 INTRODUCTION

Throughout the history, mankind has sought different energy sources along its development to counteract the adversities presented by nature. Energy generation to cover basic needs has been the foundation of the modern society. With technological developments, the electrical energy has been used in several applications, from motors in the industry to equipment used in the space. The relationship between energy and life quality is highly related to the technical development of society.

Modern power systems structure is becoming highly complex due to its economic viability and to the search of greenhouse gases emissions reduction using renewable energy sources. In recent years, power demand has increased considerably, while the transmission lines expansion has been limited by environmental restrictions. As result, there are highly loaded transmission lines and the system stability is becoming a limitation for power transfer. Flexible alternating current transmission systems (FACTS) controllers are used to solve some steady-state control problems in power systems, improving the stability and power flow control [1].

Wind power is considered as the most prominent renewable energy source, not just by reducing the emissions of greenhouse gases respect to traditional fuel burning sources, but also by their promissory economic profitability in areas with adequate wind speeds. Wind generators can be installed either on transmission or distribution networks. For these reasons wind power integration in power electric systems has obtained a fast growth in the last decades. Some country governments, such as Denmark, Germany, China, Ireland, USA, Australia, and India have stimulated wind farms connection at existent transmission networks.

In 2012, 100 countries were identified using wind power for electricity generation around the world; surpassing 280.000 MW of installed capacity. This was enough to supply 580 TWh per annum, more than 3% of global electricity consumption [2]-[5]. Although wind power contribution is a small fraction of the total demand relative to the sources of traditional fuel burning, there are statistical data southern Australia, Denmark, Ireland, Northern Germany, Portugal, Spain and Sweden where wind supply has reached significant levels compared to the total demand.

Unlike the conventional generation, the power produced by wind turbines is not constant neither can be determined, but depends on the wind conditions. A sudden change of wind speed can significantly alter the wind power output level and the condition of wind can change within a very short time interval. Due to these characteristics, wind farms integration in the conventional network entails technical implications on the system operation, such as fluctuations in power flow, frequency, voltage and the available generation capacity increasing the complexity of system operation.

The vast majority of large scale wind farms (current and projected) is geographically distant from the consumption centers and linked to the transmission networks. Furthermore, technical restrictions may limit the amount of wind power connected to the network. For these reasons, the importance to perform studies and analysis of the impact of high penetration levels of wind power on electric power systems. Despite large wind farms connected to the network are equipped with double fed induction generators (DFIGs), squirrel cage induction generators (SCIGs) and some synchronous generators are used too. Almost all studies of transient stability analysis of generators connected to the grid are performed considering conventional synchronous generators, but wind turbines dynamic response is different to the response of conventional synchronous generators. Thus, the impact of wind turbines in power systems should not be performed in the traditional way.

In this work, the impact of high penetration levels of wind power on transmission systems has been studied, analyzing technical factors such as steady-state voltage profile, voltage stability, short circuits, and voltage sags. Furthermore, a novel strategy to determine the generators to compose new wind farms fulfilling the grid code requirements is proposed. The study was carried out comparing the mentioned technical factors for different values of wind power generated in different electrical systems and considering different wind turbines technologies and control types. The simulations were performed using a Matlab/Simulink toolbox, SimPowerSystems.

This document is organized as follows. Chapter 2 presents an overview of the wind power around the world. The chapter 3 describes the network component models employed in this project. A review of the grid code requirements in the world is presented in chapter 4. The impacts on the steady-state voltage profile are addressed in chapter 5. Chapter 6 discusses the power system stability in presence of large wind farms. The wind power integration in IEEE 9 bus system with the proposed methodology in the system is determined in chapter 7. Chapter 8 presents the results of the wind power integration considering the proposed methodology in the IEEE 30 bus system. Finally, the chapter 9 summarizes the main conclusions.

2 WIND POWER OVER THE WORLD

Wind power generation has come to a "historical point", where installed wind generator costs are becoming competitive with other conventional technologies [3], [6]. The turnover of the wind sector worldwide reached 60 billion € (78 billion US$) in 2012 [7]. Wind power developing provides positive economic impacts. One of them is the employment generation and economic activity development. Another positive effect is the fossil fuel consumption displacement, and along with it, the environmental and economic costs associated [3], [6]. Table 2.1 presents the estimated number of jobs in the sector and the economic impact in 10 member countries of the International Energy Agency (IEA) and the installed capacity in 2012.

Table 2.1 – Capacity in relation to estimated jobs and economic impact.

Country	Capacity (MW)	Estimated number of jobs	Economic impact (million EUR; million USD)
China	75.324	250	---
United States	60.007	80.7	91.000; 120.000
Germany	31.315	117.9	---
Spain	22.785	16.97	2.894; 3.744
Italy	8.144	30	2.100; 2.768
Canada	6.21	10.5	1.520; 2.003
Portugal	4.517	3.2	---
Denmark	4.162	23	7.400; 9.575
Japan	2.614	2.5	1.582; 2.109
Australia	2.528	1.8	709; 935

Source: International Energy Agency [6]

2.1 MAJOR WIND ENERGY MARKETS

In last two decades China, USA, Germany, Spain and India have driven the increase in installed capacity around the world, representing together more than 70% in worldwide wind capacity, being the top five wind energy markets in the world. The United Kingdom, Italy, France, Canada and Portugal are rounding out the top 10 countries with the greatest installed capacity in the world; these countries owned 86% in overall wind capacity share over the world [2], [7]. Figure 2.1 presents the total installed wind capacity and the cumulative capacity of the top 10 countries in wind power between 2010 and 2012.

Figure 2.1 – Top 10 cumulative capacities (December 2012).

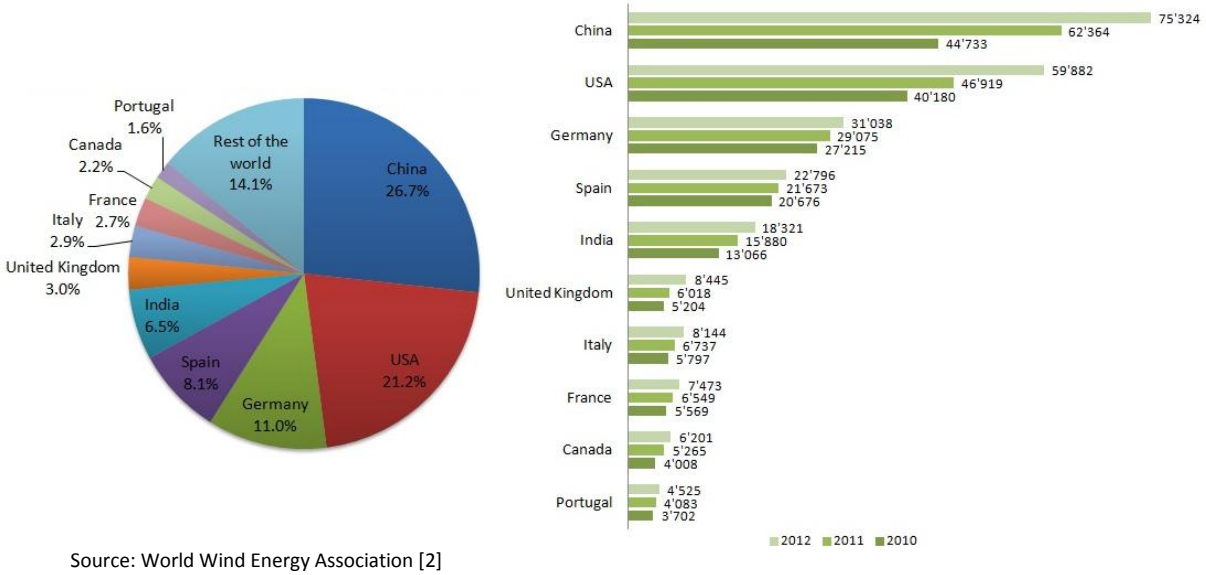

Source: World Wind Energy Association [2]

2.2 OFFSHORE WIND POWER

By the end of 2012, the cumulative offshore wind capacity reached 5.416 MW, out of which 1.903 MW were added during that year, a greater amount than the new installations of 397 MW in 2011 and 1.162 MW in 2010 [2], [4], [7]. According to the most ambitious projections, a total of 80 GW could be installed by 2020 worldwide, with three quarters corresponding to Europe [4]. Thirteen countries have offshore wind farms, eleven of them in Europe as well as China and Japan. Only five countries added new major offshore wind farms in 2012: The United Kingdom, Belgium, Denmark, Germany and China [2], [4], [7]. Figure 2.2 shows the offshore wind power capacities of these countries in 2011 and the installed capacities added in 2012.

Figure 2.2 – Top 5 in offshore wind [MW].

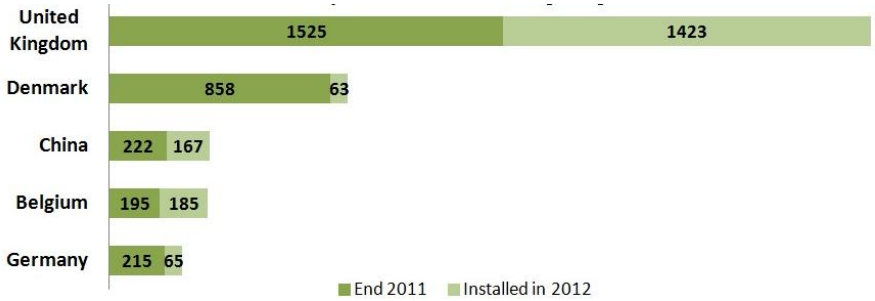

Source: World Wind Energy Association [2]

2.3 CONTINENTAL DISTRIBUTION

Europe was the first continent in installed wind power capacity in 2012, counting with 38% of total capacity. Asia has increased its share in the global wind power industry and is very close to the

European market with 35% of total share. The North American share in the total installed wind power capacity was 23,4% by the end of 2012. Latin America, mainly Brazil, Mexico and Argentina, showed a major progress and increased its share in installed capacity in recent years (1% in 2010, 1,4% in 2011 and 1,8% in 2012). Africa's share in total installed capacity was around 0,4% in 2012 [2], [7]. Figure 2.3 presents the continents' participation in installed wind power capacity between 2009 and 2012.

Figure 2.3 – Continental shares in total capacity [%].

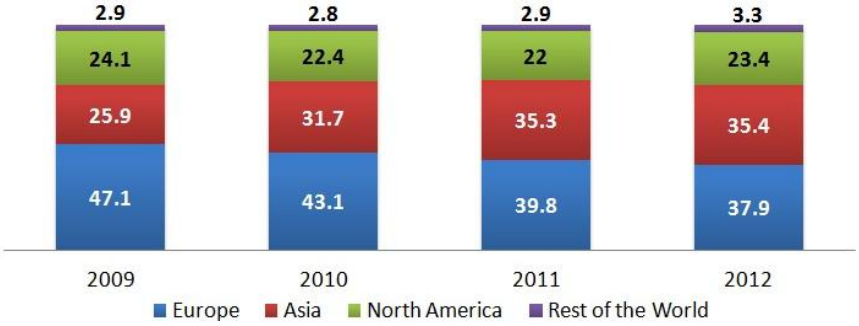

Source: World Wind Energy Association [2]

2.4 HISTORICAL EVOLUTION OF WIND POWER

Between 1973 and 1986, commercial wind turbines market evolved from domestic and agricultural uses (1-25 kW) to interconnected wind farms applications (50-600 kW). In 1979, two Nibe turbines of 630 kW were built. In 1980, the world's first wind farm was built in New Hampshire. The first outbreak of large-scale wind power penetration occurred in California (1,7 GW in total) between 1981 and 1990. Moreover, in Northern Europe, wind farms installation increased steadily in the decades of the 80s and 90s. The high cost of the electricity and the excellent wind resources led to the creation of a small but stable market. Figure 2.4 shows the timeline of principal events in the history of wind power evolution.

Figure 2.4 – Timeline of wind power evolution.

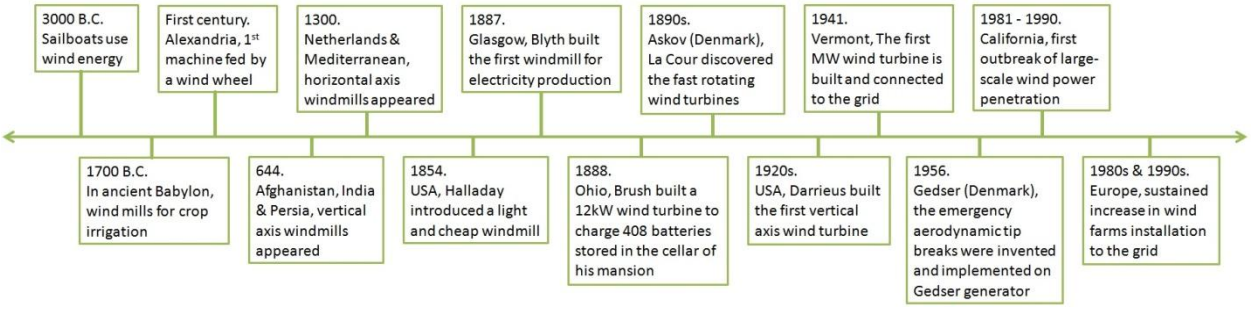

Author

The creation of 55 kW wind turbines, developed between 1980 and 1981, marked an industrial and technological break for the modern wind turbines. The kilowatt-hour (kWh) cost fell by about 50% with the emergence of this new generation. In last 20 years, more than 280 GW in wind power installations have been installed in the world, the growth of installed capacity behavior has been exponential in last years and that tendency is hoped for the coming years. Figure 2.5 presents the installed cumulative capacity in the world between 1990 and 2012.

Figure 2.5 – World total installed capacity [GW].

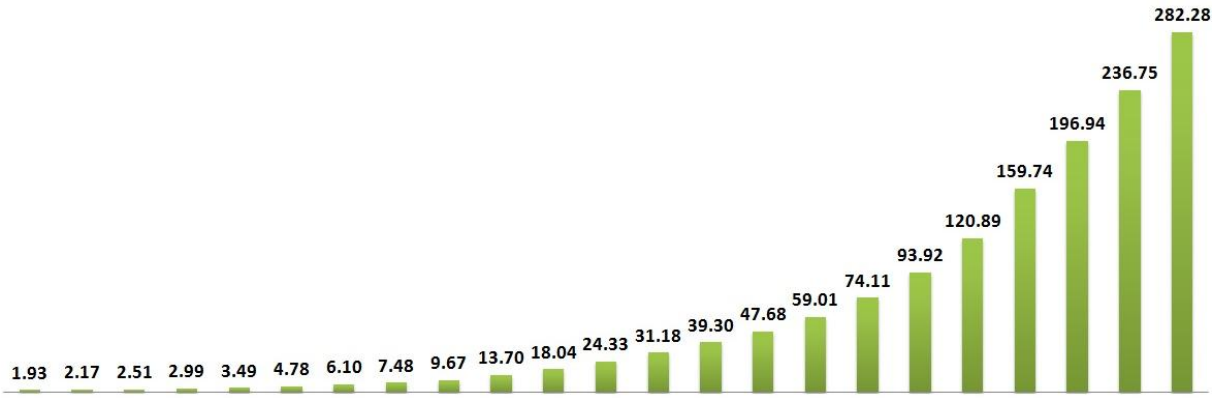

Source: World Wind Energy Association [2]

2.5 COUNTRIES WITH HIGH WIND POWER PENETRATION LEVELS

With the growing interest in wind power and distributed generation (due to market deregulation, technological advances, governmental incentives, and environment impact concerns) [8], significant wind power penetration levels are presented in power systems in some regions of the world and even higher levels are expected in the future. In recent years new records in wind power penetration were found in some countries such as Denmark, Portugal and Spain.

During certain hours of the day, in Denmark the total demand is covered by wind power [9]. In 2011 Ireland presented peaks of wind power penetration exceeding 40% in all months of the year, reaching 53,5% on December 29 [6]. In Sicily (Italy), temporary penetrations up to 62% of the average power per hour were reported. Improved prediction methods have reduced wind forecast errors, helping to handle large wind power penetrations.

In Portugal, a record penetration of 93% of instantaneous power and 70% of energy consumption was set on November 13, 2011. Spain reported 59,6% of national electricity demand was covered by wind power on one November morning in 2011 [6]. On September 3rd 2011, Southern Australia had a penetration level of over 85% of instantaneous power in the early morning hours [10]. In 2012, Denmark supplied nearly 30% of its electricity demand with wind power. Portugal and Spain

supplied almost 20% and Ireland reached 15%. These values are really important considering that the mentioned countries are highly industrialized like Spain, where more than 48 TWh/year were generated. This value exceeded the electricity demand of countries like Ireland and Denmark, as well as the supply of the total electricity demanded by countries such as Greece and Portugal [3]. Table 2.2 shows the wind power penetration levels for ten member countries of the IEA between 2010 and 2012.

Table 2.2 – Percent Contribution of Wind to National Electricity Demand 2010-2012.

Country	2010	2011	2012	Maximum observed
Denmark	21,9	28,0	29,9	100
Portugal	17,0	18,0	20,0	93
Spain	16,4	16,3	17,8	64
Ireland	10,5	15,6	14,5	53.5
Germany	6,0	7,6	7,7	--
United Kingdom	2,6	4,2	6,0	--
Greece	4,0	5,8	5,8	--
Sweden	2,6	4,4	5,0	--
Austria	3,0	3,6	5,0	--
Netherlands	4,0	4,2	4,1	--

Source: International Energy Agency [3], [6].

This work considers some countries with high development and high levels of wind power penetration. The vast majority are European countries due in part to energy constraints and the large wind potential of this continent. Renewable Energy Systems policy (RES) of the European Union aims that 20% of the total energy consumed is going to come from RES by 2020, being wind power the most abundant and profitable resource in Europe [6]. The considered countries are Brazil, Denmark, Germany, Ireland, Japan, Portugal and Spain.

2.5.1 **Brazil**

Brazil is not a country characterized by the wind power utilization within its power supply systems in the past or at present. Instead its energy matrix is mainly based on water resources (over 85%); the wind power share was about 3% in the Brazilian electrical matrix by May 2014 [11]. By May 2014, the country had 181 wind farms and an installed capacity of 4,6 GW. Brazil had its first wind power auction in 2009, as a move to diversify its energy matrix, being wind power and biomass the main alternatives. Beginning the XXI century, a severe drought limited the water at hydroelectric dams in the country, causing a severe energy shortage.

The greatest potential for wind power is during the dry season, so that kind of energy is excellent against low rainfall and the geographical distribution of existing water resources in the

country. The technical potential of wind energy for Brazil is 300 GW. Brazilian Wind Energy Association (Abeeólica) and the government set a target of reaching more than 20 GW of wind power capacity by 2020. According to Abeeólica, the forecast for 2016 is 5.5% wind power share in the Brazilian energy matrix [11]. Figure 2.6 presents the installed capacity of wind power in Brazil since 2003.

Figure 2.6 – Brazilian wind power capacity [MW].

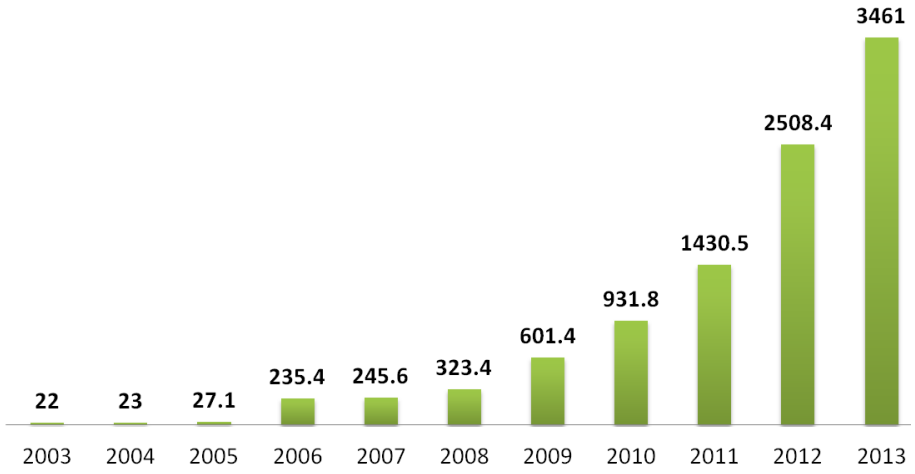

Source: Associação Brasileira de Energia Eólica [11]

2.5.2 **Denmark**

Denmark was a pioneer in wind power industry development during the 70s, and even today, a lot of the turbines in the world are produced by Danish companies such as Vestas and Siemens Wind Power. Wind turbines provided almost 30% of Danish electricity demand in 2012 and 50% in coverage of electricity consumption is expected by 2020. By 2035, 100% of the heat and power sectors would be covered by renewable energy. The expectation for 2050 is that the electricity, heat and transport systems will be converted to 100% of renewable energy [3], [6].

Taxes imposed on oil and coal helped to the competitiveness of wind power plants. Furthermore, tax incentives for generating power for their community and capital grants of up to 30% of the installation costs were offered to Danish families. With the "Energi 2000", fees for electricity generated by wind were established. Thus, only 85% of production and distribution costs were paid by users. Besides, wind projects received a refund from the Danish carbon tax and a partial refund on the energy tax. According the aim of the "Energi 2000" plan, 10% of Danish electricity consumption should have been supplied with wind power in 2005. By 2030, both coal and oil must be removed from power plants and in 2050 half the electricity consumption would be covered by wind power. Figure 2.7 shows the wind power capacity and its share of domestic electricity supply in this country.

Figure 2.7 – Danish wind power capacity and its share of domestic electricity supply.

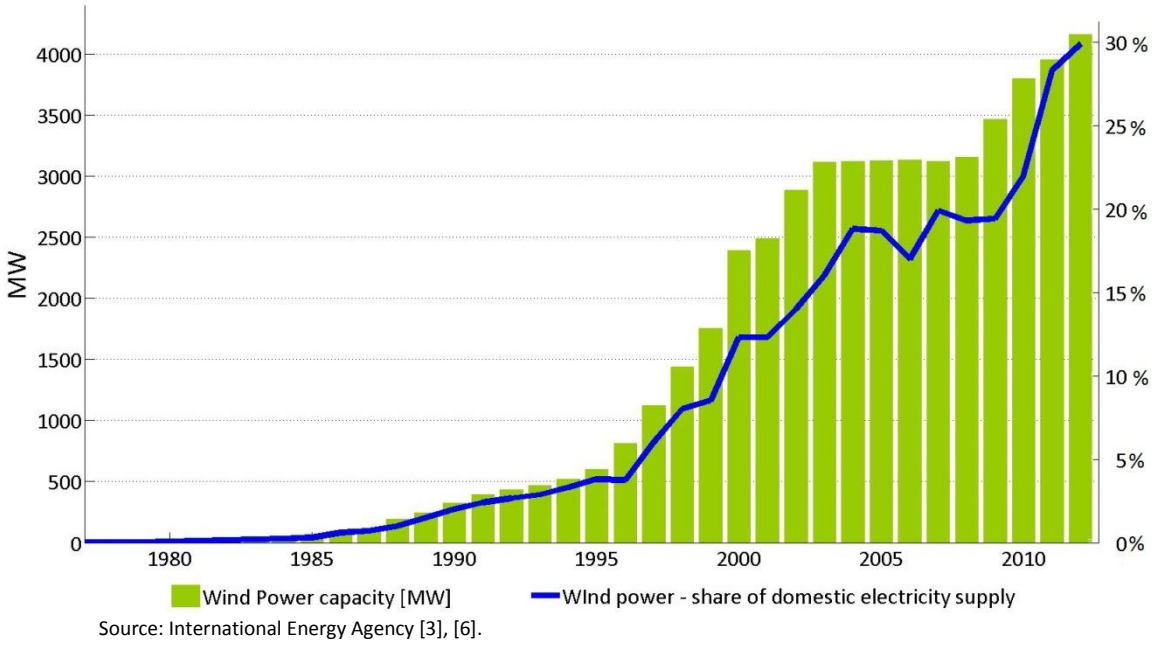

Source: International Energy Agency [3], [6].

2.5.3 **Germany**

Germany has the largest wind energy market in Europe, with an installed capacity over 31 GW in 2012, which supplies about 8% of the local electricity demand. Germany generated more than 45 TWh with wind turbines in 2012, enough energy to meet the electricity demand from countries such as Colombia, Croatia, Denmark, Hungary, Ireland, Portugal, among others. It is the largest industrialized country that decided changing completely its energy supply systems to renewable energy through "Energiewende" (Energy supply transformation, including nuclear energy elimination and shifting to renewable energy).

In Germany, a wind power share between 20 and 25% of the total energy supply, equivalent to 150 TWh, or 45 GW in onshore facilities and 10 GW in offshore, is expected by 2020. According to federal government plans, 50% of electricity consumption will be supplied with wind power by 2050 [3]. It is also decided to phase out nuclear energy production by 2022 [3], [6]. Germany has the tallest wind turbines in the world as the Fuhrländer wind turbine near the village of Laasow. Also most of the most powerful wind turbines are located in this country as the Enercon E126.

Germany presents an interesting market because hundreds of thousands of people participate in it, these people have invested in citizens' wind farms across the country and thousands of small and medium sized enterprises have employed 90.000 people in 2008. The installation of offshore large scale wind farms will allow higher wind power penetration in German electricity system. A practice that takes place in Germany is the repowering of old turbines with larger and modern generators, thus achieving a better utilization of the wind resource in this country. Despite its steady growth in installed

capacity of wind turbines, Germany presented decrease in the energy generated by wind turbines respect to previous year in 2010. Figure 2.8 presents the wind power installed capacity and its share of domestic electricity supply in this country.

Figure 2.8 – German wind power capacity and its share of domestic electricity supply.

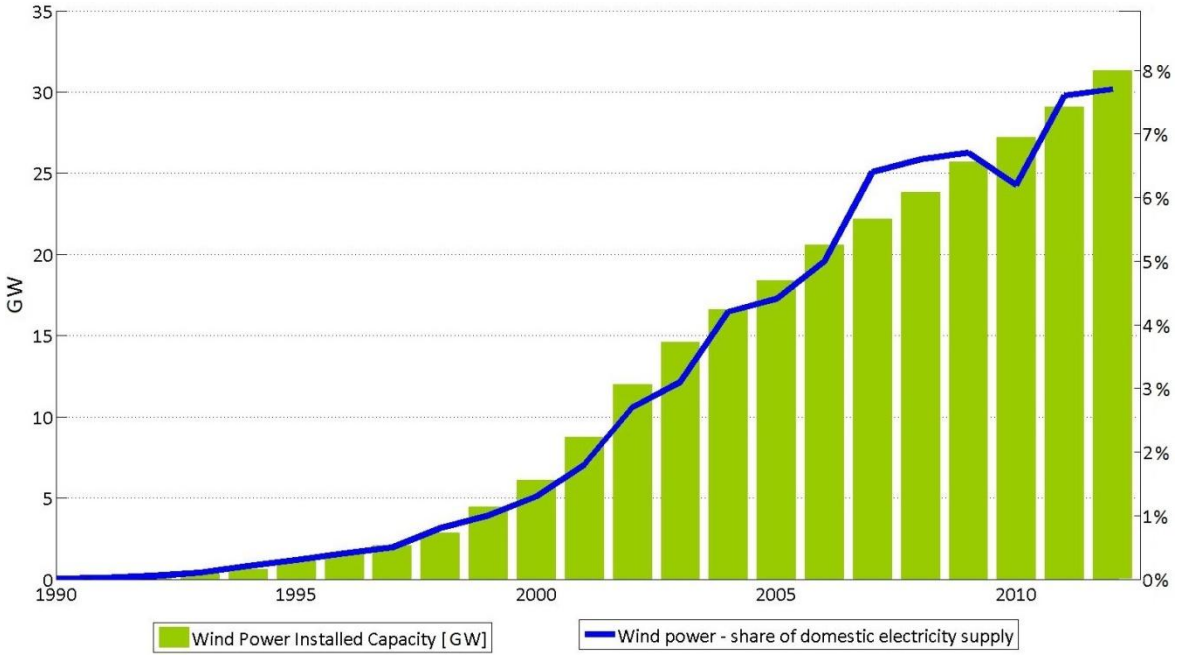

Source: International Energy Agency [3], [6].

2.5.4 **Ireland**

Irish wind power industry has grown significantly after its first wind farm began its operation in October 1992. By the end of 2012, Ireland had an installed wind power capacity nearby to 2 GW. In 2012, wind power supplied 14,5% of electricity demand in the country [3]. Wind power instantaneous penetration exceeded 40% in every month during 2011 reaching 53,5% on December 29. The Irish system operator has a rule limiting wind power penetration to 50%.

Ireland's objective is a contribution of 40% of renewable sources by 2020. It is expected that this objective will be achieved largely by wind power. Developments in interconnection, power system operation and demand management are ongoing or planned in order to maximize the wind resources utilization in Ireland through research and development studies to advance in wind power matter. High levels of wind power penetration (60 to 80%) could be accommodated within the system implementing some corrective measures. These measures include changes in the system policies (including reserves operation and demand side management), the implementation of tools within the system (near real-time wind assessment: WSAT) and developing system performance (reactive power, inertia, etc.) [6]. Figure 2.9 presents the wind power installed capacity and its share of domestic electricity supply in this country.

Figure 2.9 – Irish wind power capacity and its share of domestic electricity supply.

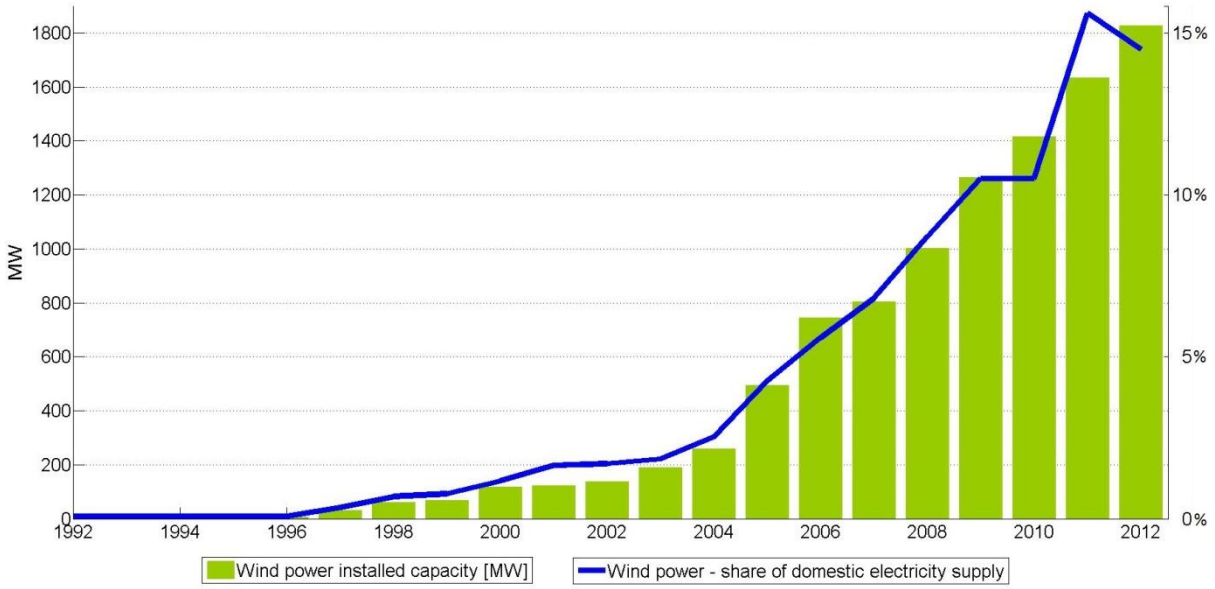

Source: International Energy Agency [3], [6].

2.5.5 **Japan**

Japan is not a country characterized by the renewable energy use within its power supply systems in the past or at present. Instead its energy matrix is mainly based on fossil fuels burning (over 60%) and nuclear power (almost 30%), the latter was expected to supply 50% of the electricity consumed in the country [12]. However, with the Fukushima nuclear plant accident, a greater interest in renewable energy was provoked, especially in wind power, which was pushed to the forefront as a safer and more reliable alternative to meet the country's future energy requirements and together with solar and geothermal energies, is expected to replace nuclear energy [12], [13].The 54 nuclear power plants were shut down between May and June 2012, many of them definitely [2], [7].

In 2012, Japan had an installed wind power capacity of 2,6 GW, covering only 0,52% of the demanded electricity [3]. Japan’s official target for 2020 is an installed capacity of 5 GW. However, due to the Fukushima accident, a higher capacity is expected, especially considering that 80% of Japanese wind infrastructure survived the earthquake and tsunami [13]. Since October 2013, Fukushima's coast waters, where the rugged nuclear plant in 2011 is located, hosted the activities of a powerful floating wind turbine and its transformer substation, symbols of Japanese commitment to renewable energy after the nuclear tragedy. The Mirai turbine and Kizuna substation are located about 20 kilometers from the coast and have been designed as pilot of an offshore wind farm of 140 large wind turbines with an installed capacity equivalent to that of a nuclear reactor, a project that could be working at full capacity by 2020 [14]. Figure 2.10 presents the installed capacity of wind power in Japan since 1989.

Figure 2.10 – Japanese wind power capacity [MW].

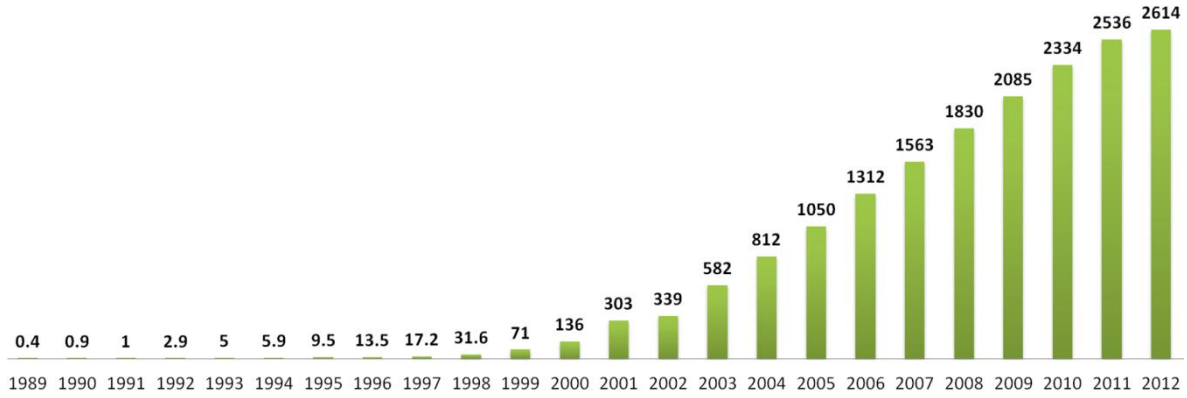

Source: International Energy Agency [3], [6].

2.5.6 **Portugal**

Portugal is in the group of the tenth countries with the largest installed wind capacity with more than 4.500 MW. In 2012, Portugal became the second country with the highest wind power levels in share of domestic electricity supply (20%), just behind Denmark. The target for 2020 is 5.300 MW of installed wind power capacity, being 75 MW offshore [15]. Figure 2.11 shows the values of installed wind power capacity and the percentage of it in the local power supply.

Figure 2.11 – Portuguese wind power capacity and its share of domestic electricity supply.

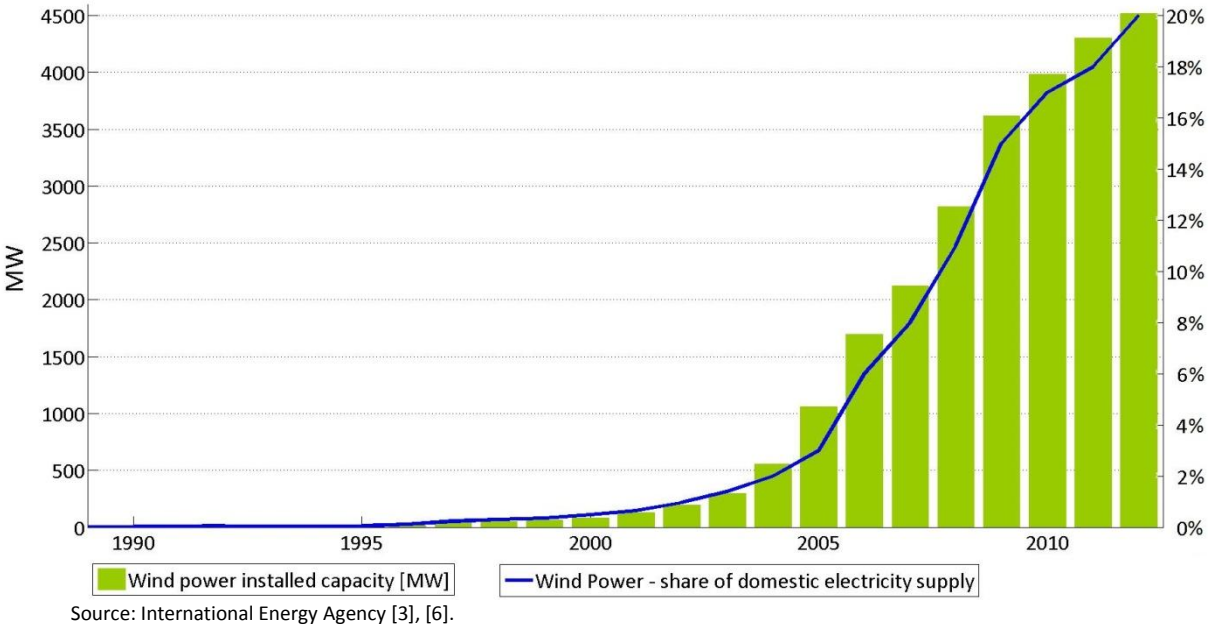

Source: International Energy Agency [3], [6].

The largest instantaneous wind penetration was recorded on November 13, 2011 at 4:30 am with a value of 93% [6]. On December 14, 2012 the maximum instantaneous power in the system was achieved with 3.754 MW. That day, 84 GWh were generated by wind power, equivalent to 54% of the demanded electricity [3], [16]. The first quarter of 2013 was promissory for Portugal, covering 70% of

its electricity needs from renewable sources. The wind power supplied 27% of total demand [17]-[19]. In late October, wind power covered 23% of the demanded power [20].

2.5.7 **Spain**

Spain is the second European country with the largest installed wind power capacity and the fourth one in the world. By the end of 2012, it counted with 22,8 GW of installed capacity and generated 48,16 TWh of energy (17,8% of national demand). The objective established for 2020 is 35.000 MW of installed wind power capacity onshore and 750 MW offshore, 29.000 MW of these must be installed by 2016 [3], [6], [21].

Since 2000, wind energy has risen dramatically, encouraged by legislation that strongly stimulated research and investment in this sector (Royal Decree 661/2007, of May 25) through premiums. After 2007 the growth has been lower due mainly to the economic crisis affecting the country. Figure 2.12 shows the values of installed wind power capacity and the percentage of it in the local power supply.

Figure 2.12 – Spanish wind power capacity and its share of domestic electricity supply.

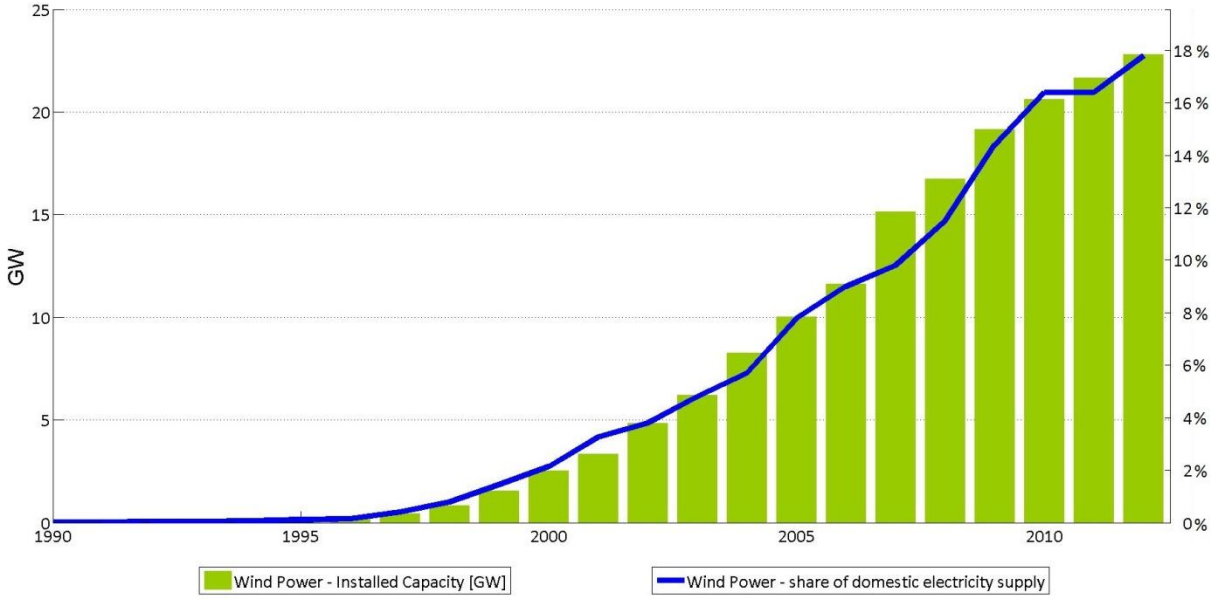

Source: International Energy Agency [3], [6].

In 2012, the maximum production value of wind power was achieved. On September 24, wind power contribution exceeded 64% of demand coverage. On April 18 instantaneous wind production reached 16.636 MW, and 334.850 MWh were generated [22], [23]. On February 6, 2013, the record high value of instantaneous production was exceeded with 17.014 MW. Likewise, the maximum daily production occurred with 344.000 MWh that same day, which meant overcoming nuclear energy

production by almost 2,5 times [24]. This is a higher power (more than twice) than the generation capacity of the six existing nuclear reactors in Spain (7.742,32 MW).

2.6 FUTURE BROADCAST

Based on the 2011 and 2012 growth rates, the WWEA revised its expectations for the future global wind capacity growth, and expects a worldwide installed capacity of 500 GW by 2015. At least, 1.000 GW are expected worldwide by the end of 2020 [2], [7]. The GWEC also made their forecasts for growth in installed capacity until 2017. This forecast is lesser optimistic than the previous one and expects about 420 GW (16,26% less) of installed capacity in the world by 2015. Figure 2.13 presents installed capacity forecasts provided by the WWEA and the GWEC until 2017.

Figure 2.13 – Installed wind power capacity forecasts.

	2012	2013	2014	2015	2016	2017
WWEA	282.28	336.67	420.10	496.67	600.10	681.97
GWEC	282.60	322.40	367.70	418.70	474.90	536.13

Source: World Wind Energy Association [2] and Global Wind Energy Council [4].

3 POWER SYSTEMS AND WIND TURBINES MODELS

Traditionally, power systems use synchronous machines for electricity generation. Nevertheless, in recent years the introduction of renewable energy sources like wind power, has expanded at a large rate. Such generation systems use asynchronous machines with low voltage direct current link or with electronic converters. This combination of synchronous and asynchronous generators is expected to change the power system performance and behavior following disturbances such as voltage sags and short-circuits [25].

3.1 SYSTEM ELEMENT MODELS

Due to small load changes, switching actions, and other transients are always occurring, most of the variables change with the time. Short circuits are not in steady state conditions and they can start dynamic phenomena on the system, whereby dynamic models are needed. To calculate the fault currents in the system, appropriate static models can be used. Fault currents have a transient part and a steady state one [26].

3.1.1 **Loads**

In power system analysis, the load can be considered as active and reactive power connected to different buses on the network model. Load can be represented by constant power, constant current or constant impedance models [27]. Among numerous devices and appliances connected to the system that are considered as loads appear distribution system feeders, shunt capacitors, transformers, voltage controlling devices, voltage regulators, etc. The model used to represent loads can be divided according to its applications in two categories: static and dynamic applications [28]. The fundamental starting point for the load modeling is at the distribution level. Thus, the applications outside of power system can be as follows:

- Static applications: this model considers only voltage dependent characteristics
    - Power flow (PF)
        - Harmonic power flow (HPF)
        - Transmission power flow (TPF)
    - Voltage stability
- Dynamic applications: considers both voltage and frequency dependent characteristics
    - Transient stability (TS)
    - Dynamic stability (DS)
    - Operator training simulators (OTS)

In this work different load models were used depending on the type of analysis to be performed as recommended in [29]. In the steady-state studies, the loads were represented by constant power models, as is usual in load flow programs. On the other hand, the dynamic studies, active power loads were represented by constant current models and reactive power loads were represented by constant impedance models.

Loads in steady-state studies

Generally, in static applications, loads are characterized considering separately the active power P and the reactive power Q. Otherwise, P and Q are represented by combining constant impedance (resistance or reactance), constant current, and constant power elements [30]. The simplest load model is the static mode and it is used for the steady-state analysis. The loads are considered like three-phase impedances connected in Y configuration modeled as constant active and reactive power as shown in Figure 3.1. In this model the load current will change when the voltage varies and it is determined by:

$$I_{a,b,c} = \left(\frac{S_{nom_{a,b,c}}}{V_{(a,b,c)n}}\right)^* = \frac{|S_{nom}|_{a,b,c}}{V_{(a,b,c)n}} \angle \delta_{a,b,c} - \theta_{a,b,c} \tag{2.1}$$

Figure 3.1 – Wye connected load for static analysis.

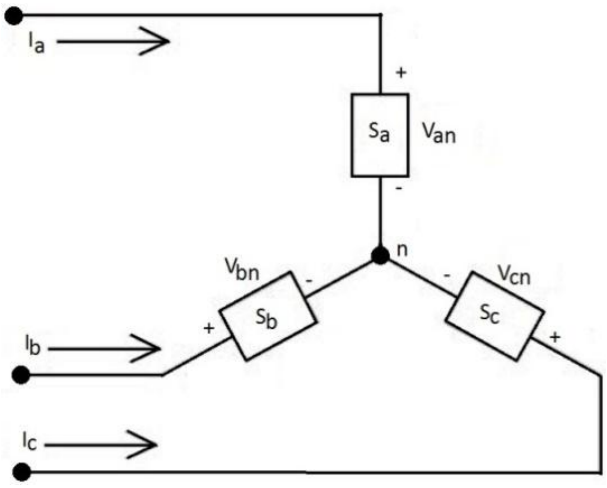

Author

Loads in dynamic studies

In dynamics studies no frequency variations are taken account, the most commonly accepted model represents the active power as constant current and the reactive power as constant impedance as shown in Figure 3.2. The constant current represents a mix of resistive and motor devices (nearly constant MVA) in the active power. This representation may be shifted more towards constant impedance or constant MVA, if the load is known to be more resistive or more motor-driven, respectively. This representation for an average load is reasonably well supported by the data in [29].

In this model the load current is a sum of the active component current (constant) and the reactive component, which depends of voltage variations. Thus, the load current is determinate by:

Figure 3.2 – Wye connected load for dynamic analysis.

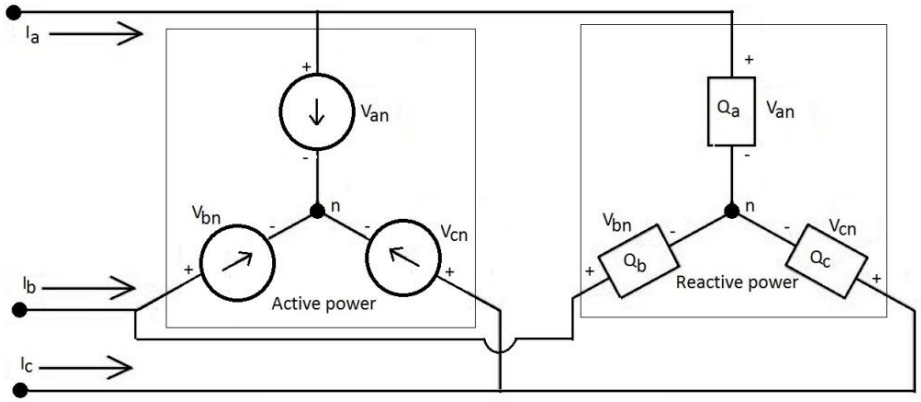

Author

$$I_{a,b,c} = \frac{P_{nom_{a,b,c}}}{V_{nom_{(a,b,c)n}}} + j\left(\frac{V_{(a,b,c)n}\ Q_{nom_{a,b,c}}}{V_{nom_{(a,b,c)n}}^{\ 2}}\right) = \left(\frac{1}{V_{nom_{(a,b,c)n}}}\right)\left(P_{nom_{a,b,c}} + \frac{V_{(a,b,c)n}\ Q_{nom_{a,b,c}}}{V_{nom_{(a,b,c)n}}}\right) \quad (2.2)$$

3.1.2 **Transmission lines and transformers**

Transmission lines are implemented like a balanced three-phase transmission line model with parameters lumped in a π section as shown in the Figure 3.3. In the implemented block in Simulink [31] the line parameters R, L, and C are specified as positive and zero sequence parameters (R_1, L_1, C_1, R_0, L_0 and C_0) to considerate the inductive and capacitive couplings between the three phase conductors, as well as the ground parameters. This method of specifying line parameters assumes that the three phases are balanced. Self and mutual resistances (R_s, R_m), self and mutual inductances (L_s, L_m) of the coupled inductors, as well as phase capacitances C_{phase} and ground capacitances C_g, are deduced from the positive and zero sequence RLC parameters as follows:

$$R_s = \frac{2R_1 + R_0}{3} \quad (2.3)$$

$$L_s = \frac{2L_1 + L_0}{3} \quad (2.4)$$

$$R_m = \frac{R_0 - R_1}{3} \quad (2.5)$$

$$L_m = \frac{L_0 - L_1}{3} \quad (2.6)$$

$$C_{phase} = C_1 \quad (2.7)$$

$$C_g = \frac{3C_1C_0}{C_1 - C_0} \quad (2.8)$$

Figure 3.3 – Transmission line π model.

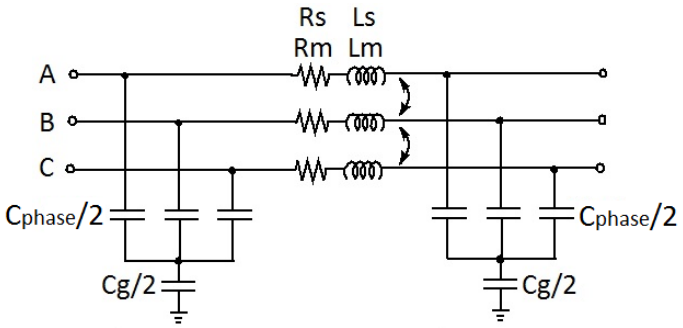

Author

The power transformers are the link between the generators of the power system and the transmission lines, and between lines of different voltage levels. They are highly (nearly 100%) efficient and very reliable [32]. The equivalent circuit for a single-phase transformer of the used model is showed in Figure 3.4. In this model the losses on primary and secondary windings, the losses in the core by heat, hysteresis and eddy currents are considered. Further, the inductances related to the windings, the flux in the core and the disperse flux, are also included in this model.

Figure 3.4 – Equivalent circuit for a single-phase transformer with an ideal transformer of turns ratio $= \frac{N_1}{N_2}$.

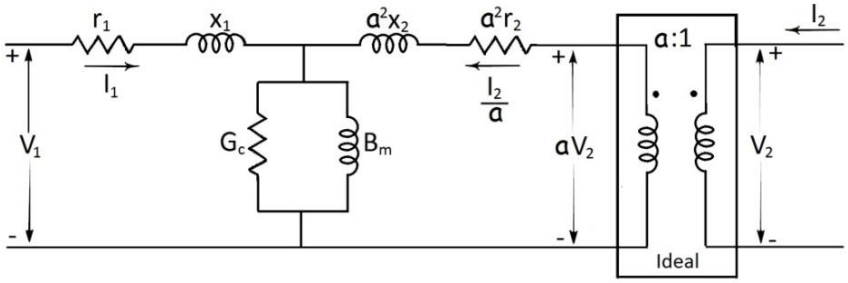

Author

3.1.3 Generators and synchronous condensers

Inside the simulated power systems there are ideal generators that act at swing bus or PV bus in the power flow. This is the case of generators and synchronous condensers used in the systems implemented in this work. Using this generator model implies that in the case of excess or deficiency of active and reactive power, this generator will absorb or supply the necessary power. In dynamic studies, this model may alter the results due to its quick and effective response. The block implemented in Simulink is a balanced three-phase voltage source with internal RL impedance. The three voltage sources are connected in Y with a neutral connection [31]. The model has the internal resistance and inductance (R and L) values of the source, specifying the inductive short-circuit level and X/R ratio. Furthermore, the bus type and specifications of active and reactive power can be set for

each generator. The simplified model for generator and synchronous condenser are presented in Figure 3.5.

Figure 3.5 – Equivalent circuit for a single-phase generator or synchronous condenser.

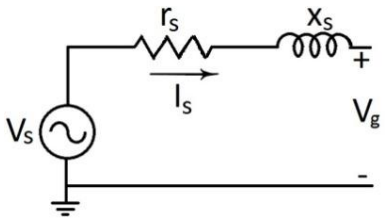

Author

3.1.4 **Hydraulic synchronous generator**

The main objective of this work is understand and analyze the wind turbines behavior in power systems when there is high wind power penetration level and their interaction with other generators. A hydraulic plant with electrical excited synchronous generator, hydraulic turbine and excitation system was simulated to emulate the behavior and performance of the real hydraulic plants. The electrical model of the synchronous machine is represented by a sixth-order state-space model. The model considers the dynamics of the stator, field, and damper windings. The model equivalent circuit is represented in the rotor reference frame (qd frame). All rotor parameters and electrical quantities are referred to the stator. The electrical model of the machine can be found in [31] and is presented in Figure 3.6. The subscripts used are defined as follows:

- d, q: d and q axis quantities
- r, s: rotor and stator quantities
- l, m: leakage and magnetizing inductance
- f, k: field and damper winding quantity

The model equations are:

$$V_d = R_s i_d + \frac{d}{dt}\varphi_d - \omega_r \varphi_q \tag{2.9}$$

$$\varphi_d = L_d i_d + L_{md}\left(i'_{fd} + i'_{kd}\right) \tag{2.10}$$

$$V_q = R_s i_q + \frac{d}{dt}\varphi_q - \omega_r \varphi_d \tag{2.11}$$

$$\varphi_q = L_q i_q + L_{mq} i'_{kq} \tag{2.12}$$

$$V'_{fd} = R'_{fd} i'_{fd} + \frac{d}{dt}\varphi'_{fd} \tag{2.13}$$

$$\varphi'_{fd} = L'_{fd} i'_{fd} + L_{md}(i_d + i'_{kd}) \tag{2.14}$$

$$V'_{kd} = R'_{kd} i'_{kd} + \frac{d}{dt}\varphi'_{kd} \tag{2.15}$$

$$\varphi'_{kd} = L'_{kd} i'_{kd} + L_{md}\left(i_d + i'_{fd}\right) \quad (2.16)$$

$$V'_{kq1} = R'_{kq1} i'_{kq1} + \frac{d}{dt}\varphi'_{kq1} \quad (2.17)$$

$$\varphi'_{kq1} = L'_{kq1} i'_{kq1} + L_{mq} i_q \quad (2.18)$$

$$V'_{kq2} = R'_{kq2} i'_{kq2} + \frac{d}{dt}\varphi'_{kq2} \quad (2.19)$$

$$\varphi'_{kq2} = L'_{kq2} i'_{kq2} + L_{mq} i_q \quad (2.20)$$

Figure 3.6 – Equivalent circuit of synchronous generator.

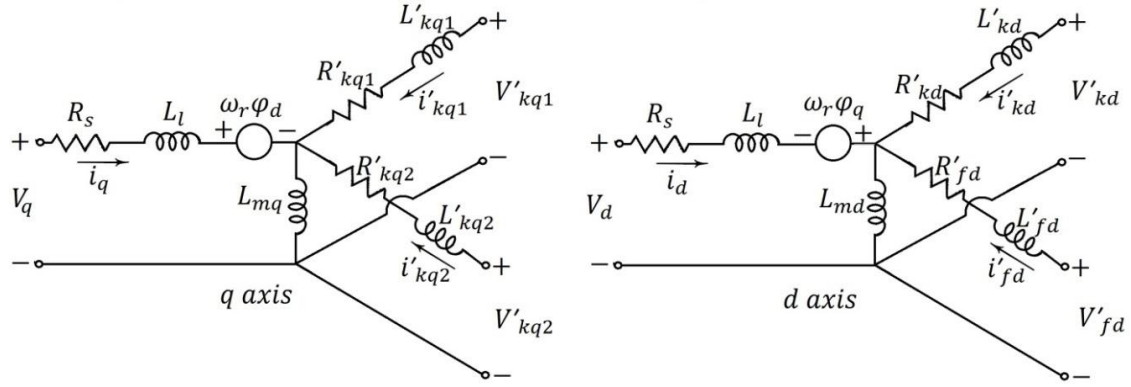

Author

3.1.5 **Induction generators**

Large-sized wind farms connected to grid are equipped with squirrel cage induction generators (SCIG), double fed induction generator (DFIG) and some synchronous generators. The most common wind turbine technology installed in systems is the DFIG. Even though few SCIG unities are still in operation, but it is not common to find them in new wind farms [33]. DFIGs have power electronics converters that can regulate their own reactive power and operate with constant power factor or constant voltage output.

Squirrel cage induction generators (SCIG)

This is the cheapest and the simplest wind turbines technology to generate electricity. These generators are defined as fixed speed generators. This is one of the technologies that have been used for longer in wind turbines connected to distribution systems [34]. In this work, the Simulink model of SCIG was used. This model contains a squirrel cage induction generator represented by a fourth-order model. All the electrical variables are referred to the stator, which are indicated by the prime signs in the machine equations. All stator and rotor quantities are represented in the arbitrary two-axis

reference frame (dq frame), as is shown in [31]. Figure 3.7 presents the SCIG wind power turbine used in this work.

Figure 3.7 – SCIG wind power system topology.

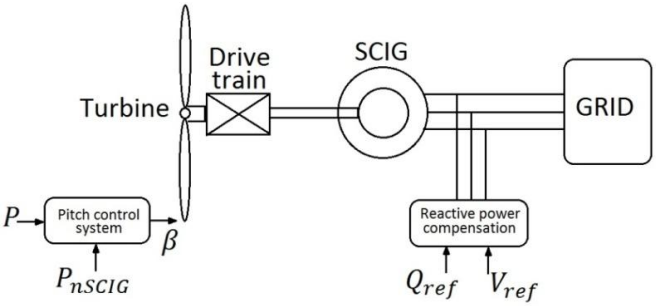

Author

The model equations are:

$$V_{qs} = R_s i_{qs} + \frac{d}{dt}\varphi_{qs} + \omega\varphi_{ds} \tag{2.21}$$

$$\varphi_{qs} = L_s i_{qs} + L_m i'_{qr} \tag{2.22}$$

$$V_{ds} = R_s i_{ds} + \frac{d}{dt}\varphi_{ds} - \omega\varphi_{qs} \tag{2.23}$$

$$\varphi_{ds} = L_s i_{ds} + L_m i'_{dr} \tag{2.24}$$

$$V'_{qr} = R'_r i'_{qr} + \frac{d}{dt}\varphi'_{qr} + (\omega - \omega_r)\varphi_{dr} \tag{2.25}$$

$$\varphi'_{qr} = L'_r i'_{qr} + L_m i_{qs} \tag{2.26}$$

$$V'_{dr} = R'_r i'_{dr} + \frac{d}{dt}\varphi'_{dr} - (\omega - \omega_r)\varphi_{qr} \tag{2.27}$$

$$\varphi'_{dr} = L'_r i'_{dr} + L_m i_{ds} \tag{2.28}$$

$$T_e = 1.5p\left(\varphi_{ds} i_{qs} - \varphi_{qs} i_{ds}\right) \tag{2.29}$$

$$L_s = L_{ls} + L_m \tag{2.30}$$

$$L'_r = L'_{lr} + L_m \tag{2.31}$$

Figure 3.8 illustrates the electric model of an induction generator. In the SCIG the rotor voltages V'_{dr} and V'_{qr} (equations 2.25 and 2.27) are equal to zero.

Figure 3.8 – Equivalent circuit of the induction machine.

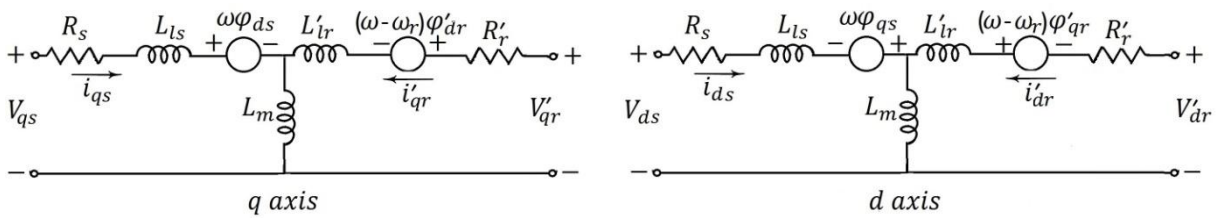

Author

where:

R_s, L_s are the stator resistance and the leakage inductance;
L_m, L_s are the magnetizing and the total stator inductances;
V_{qs}, i_{qs} are the q axis voltage and current;
V_{ds}, i_{ds} are the d axis voltage and current;
φ_{qs}, φ_{ds} are the stator q and d axis fluxes;
ω is the reference frame angular velocity;
ω_m is angular velocity of the rotor;
p is the number of pole pairs;
ω_r is the electrical angular velocity ($\omega_m p$);
T_e is the electromagnetic torque;
L'_r is the total rotor inductance;
R'_r, L'_{lr} are the rotor resistance and the leakage inductance;
V_{qr}, i_{qr} are the q axis voltage and current;
V_{dr}, i_{dr} are the d axis voltage and current;
and φ_{qr}, φ_{dr} are the stator q and d axis fluxes;

Double fed induction generator (DFIG)

With time passage, DFIGs have positioned as the most attractive technology for wind turbine manufacturers, showing themselves as an effective, economic and reliable solution. Until the mid-nineties, most of the wind turbines installed in the world were of fixed speed, using principally SCIGs and being connected to the grid directly. Thanks to technologic innovations, the panorama has changed and now most of wind turbines installed are variable speed, using DFIG [35]. In DFIG, the stator is directly connected to the grid and the rotor is feeding through a bidirectional converter, which also is connected to the grid as shown in Figure 3.9. The applied induction generator model is the same that presents Figure 3.8, with its respective equations (equations 2.21 to 2.31).

Using vector control techniques, the bidirectional converter ensures energy generation with voltage and frequency of the grid, to compensate the difference between the rotor speed and the synchronous speed through the slip control, thereby allowing the turbine to work into a range of wind speeds considerably. Also, by controlling the alternating voltages generated by both converters, network side as the side of the generator rotor; it is possible to control the active and reactive power flow through the rotor and stator [31].

Figure 3.9 – DFIG wind power system topology.

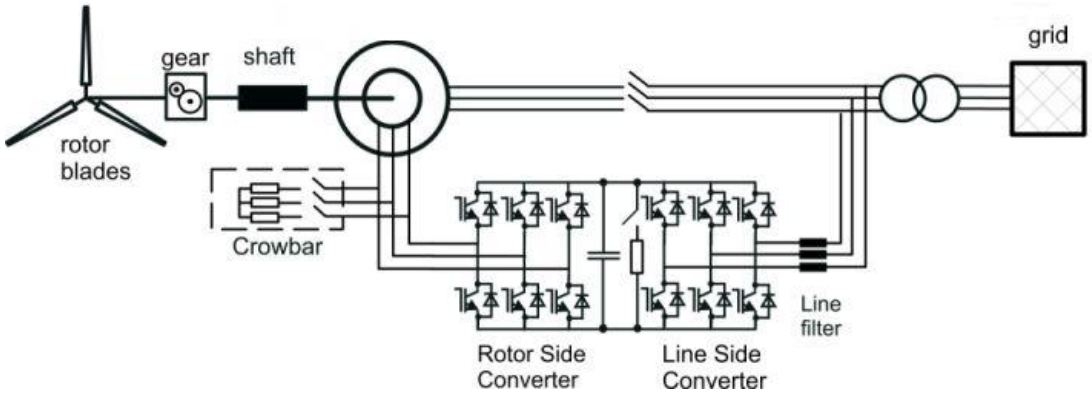

Source: Kiel University, Faculty of Engineering [36].

3.2 WIND FARMS MODELS

Large wind farms are represented for investigations of transient voltage stability with two models as follow:

- Aggregated models: with representation of a turbines group in the farm with similar characteristics, with detailed representation of the internal network and the transformers connecting the generators in the internal grid.
- Reduced models: in which a large number of wind turbines contained in the farm is given by a re-scaled equivalent, e.g. one wind turbine model representing the total group of wind turbines.

Modeling details of large wind farms depends on the study purposes. In relation to transient voltage stability analysis, Akhmatov classifies in [37] the following:

1. Investigation of the mutual interaction between electricity-producing wind turbines within a large wind turbine.
2. Wind turbines response to disturbances occurred in the internal grid of the wind farm.
3. Studies of the wind farm response to short-circuit faults in the entire power system.
4. Voltage stability analysis of the power grid with large wind farms and its dynamic reactive compensation.

In both first and second case, the detailed aggregated model of the wind farm and its internal network is required; in the other cases the reduced models can be successfully applied. In analysis with incorporation of the dynamic compensation unit, the use of the reduced model of large wind farm will be normally preferred instead of the aggregated wind farm. This is because the reduction of the complexity of simulations and the study scope.

The reduced models give the wind turbines response inside the wind farm as the integrated whole. This response does not distinguish specific operational conditions or details of each wind turbine within the wind farm. Therefore, reduction to the reduced equivalent must be achieved with sufficient accuracy. Detailed examples of the aggregated model and equivalent reduced model are found in [37]-[43].

3.3 STABILITY OF SYSTEMS WITH HIGH WIND POWER LEVELS

The first studies of wind power impact on power systems date back to the early 1990s. Also, in West Denmark, the first experiences from large penetration levels occurred around this time. Several integration studies were published over the following decade with different issues and objectives. Hence, there are diverse results and conclusions. Comparisons are difficult to make owing to the approaches, results presentation and system topologies. In [3], [6] and [44] there are detailed methodologies for wind integration studies, considering economical and technical requirements as well as constraints.

So far, the integration of large wind power amounts in power systems has been studied mainly in theoretical way, because wind power penetration is still rather limited in the most countries and power systems. The main objective of power systems is to supply network customers with electricity whenever they demand for it with certain characteristics as shown in [3], [6] and [44]. So, with wind power integration the main aim must still be fulfilled.

Several works have been performed to know and understand the behavior of electrical power systems with wind farms integration. Following some of the works studied: A complete modeling and simulation of wind power systems based on the SCIG and DFIG is presented in [45]. The effect of different values of crowbar resistor in DFIGs and the effect of the DC chopper is discussed in detail in [46]. The fault ride through capability of DFIG turbines is presented in [47].

A detailed methodology to assess the impact of wind generation on the voltage stability of a power system is provided by [33]. It will also demonstrate the value of using time-series ac power flow analysis techniques in assessing the behavior of a power system showing how the voltage stability margin of the power system can be increased through the proper implementation of voltage control strategies in wind turbines. Automatic procedures to generate potential contingencies based on wind power measurements and forecasts to reduce the simulation numbers and to make less complex the contingency analysis is performed in [48].

The impact of DFIGs during grid disturbances are discusses in [49] where a strategy is proposed to operate the DFIG grid-side converter (GSC) as a static synchronous compensator

(STATCOM) during a fault, supporting the local voltage, while the DFIG operates as a SCIG. Conclusions about the dynamic security of non-interconnected power systems with high wind power penetration are provided in [50] and [51], considering DFIGs, permanent magnet synchronous generator (PMSG) and active stall induction generator (ASIG). Other interesting study was develop in [52], considering the introduction of electric drive vehicles (EDV) as flexible loads can improve the system operation injecting power to the system in peak hours.

3.3.1 **Contradictory cases found in literature**

Considering that the issue of high penetration levels of wind power in electric systems is a "novel" theme and the behavior of the system with wind generators is still in study, previous works were sought where simulations of the wind generators impact were performed. Two studies with comparative analysis of DFIGs and synchronous generators were analyzed.

The first one ([53]) concluded that synchronous generators have better performance than DFIGs for the post-fault voltage recovery. It considers a 69 Bus system with sixteen generators. The total load is $\boldsymbol{P_L = 17,62\ GW}$, $\boldsymbol{Q_L = 1,97\ GVAr}$. The total power generated is $\boldsymbol{P_G = 18,41\ GW}$, and the system losses are $\boldsymbol{152,2\ MW}$.

Figure 3.10 – 69 Bus system considering 16 generators.

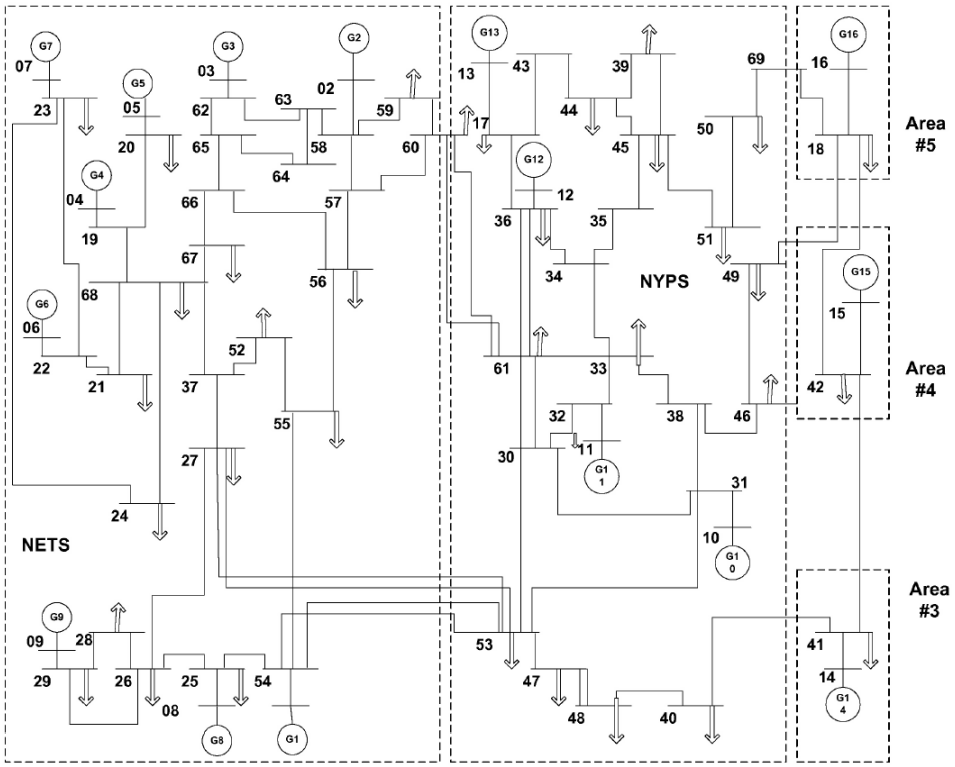

Source: IEEE SYSTEMS JOURNAL [53].

Considering that statically the DFIGs do not supply as much reactive power as synchronous generators do and dynamically they cannot produce the same short circuit currents. Therefore the post-fault voltage support of a DFIG is worse than a synchronous generator. During voltage sags synchronous generators deliver more reactive current than DFIGs. For that reason synchronous generator gives better reactive power support to the grid. DFIGs consume reactive power during transient phenomena reducing the voltage stability margin.

In this study, two cases were performed. In the first one the reactive power output of the synchronous generator (G10) under faulted condition is determined, and then this synchronous generator was replaced by the same capacity DFIG and then its reactive power output was compared to that of the synchronous generator under the same operating conditions. Figure 3.11 shows the reactive power supply by the same capacity synchronous generator (G10) and DFIG during a three phase fault at the middle of line 60–61.

Figure 3.11 – Reactive power for three-phase fault at middle of one of lines 60–61 (solid line synchronous generator and dashed line DFIG).

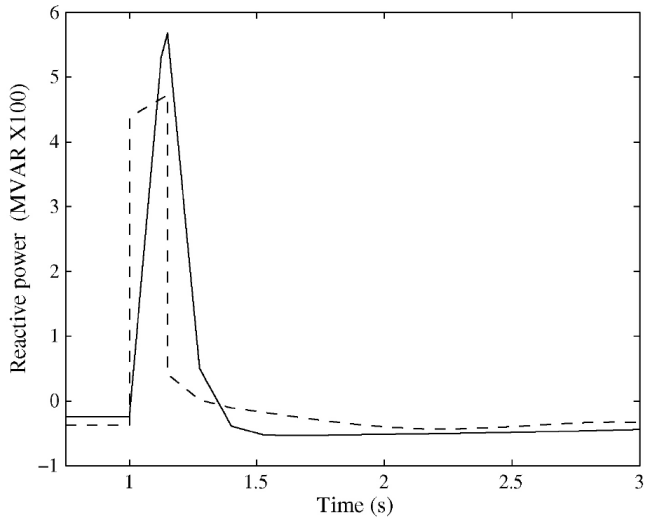

Source: IEEE SYSTEMS JOURNAL [53].

The second case considers the same fault that the previous case for the system with synchronous generators only and a combination of 60% DFIG and 40% synchronous generator. The voltage transients in the bus 49 for the described scenarios are showed in Figure 3.12. The synchronous generator supplies more reactive power and thus provides better performances in contrast to DFIG to recover post-fault voltage. In some countries, the grid codes are so rigid that the DFIGs must be combined with STATCOMs in order to achieve a similar behavior as the one of synchronous generators. In these cases, the wind generation can be considered as equal to a conventional generation.

Figure 3.12 – Voltage at bus 49 for three-phase fault at middle of one of lines 60–61 (solid line synchronous generator, and dashed line 60% DFIGs and 40% SGs).

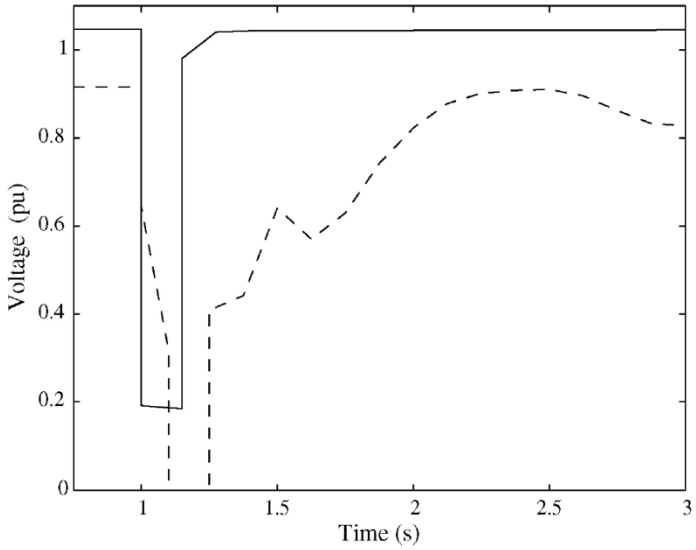

Source: IEEE SYSTEMS JOURNAL [53].

In the second study ([54]) is concluded that the use of DFIGs has better performance than synchronous generators. The WSCC 3 generators 9 bus test system showed in Figure 3.13 was used with three generators and three loads, there is a large-scale wind farm based on DFIGs.

Figure 3.13 – WSCC 3-gen-9-bus test system.

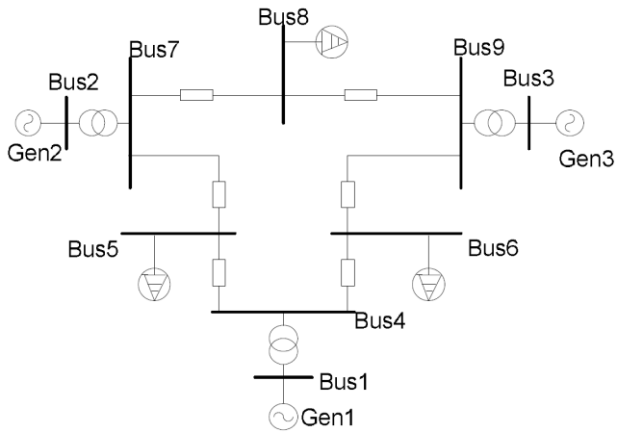

Source: Power & Energy Society General Meeting, 2009 [54].

Wind farms located in Bus 3 with only synchronous generators and with DFIGs were considered for this study. A solid three-phase fault at bus 9 was simulated and by comparison of the two scenarios established the study was carried out. Figure 3.14 gives the active power output, rotor speed, reactive power output and terminal voltage curves of the wind farm and the replaced synchronous generator Gen3 considering the 6th generator model and the constant impedance load model, respectively. The solid line corresponds to the DFIG and the dashed line to synchronous.

Figure 3.14 – Transient behavior curves of the wind farm.

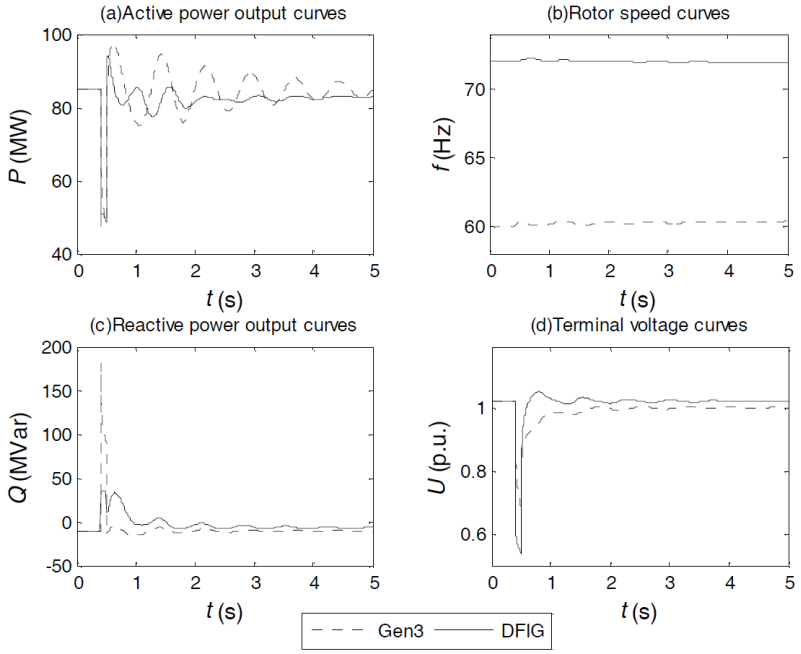

Source: Power & Energy Society General Meeting, 2009 [54].

The study showed that DFIGs introduction does not affect significantly the oscillations damping time after a fault. Instead the amplitudes of the oscillations are smaller and differently shaped. The principal conclusion in this work is that DFIGs introduction could be beneficial to the system, even better than with synchronous generator, with the adequate measures.

The development of this work was based on the contrast and the conclusions of these studies, trying to analyze the impact of high penetration levels of wind power and their interaction with synchronous generators into the system. Understanding and analyzing the operational states that may have the elements of electrical systems is important to study the phenomena that can occur in them. Knowledge of stationary and transient conditions allows the sizing of protection against unwanted situations, which are responsible for the safety and reliability of the system holistically.

3.4 INFORMATICS TOOL USED

Time-domain simulation programs are an integral part of the power system analysis tools. With these simulation programs, the dynamic response to disturbances of power systems or changes in their states can be calculated by using the appropriate mathematical models and numerical algorithms. The dynamic phenomena in power systems are classified into different time ranges in [55] and [56] as depicted in Figure 3.15. The time range of power system transients varies from microseconds (lightning) to hours and days (long term dynamics).

Figure 3.15 – Time frame of power system transients.

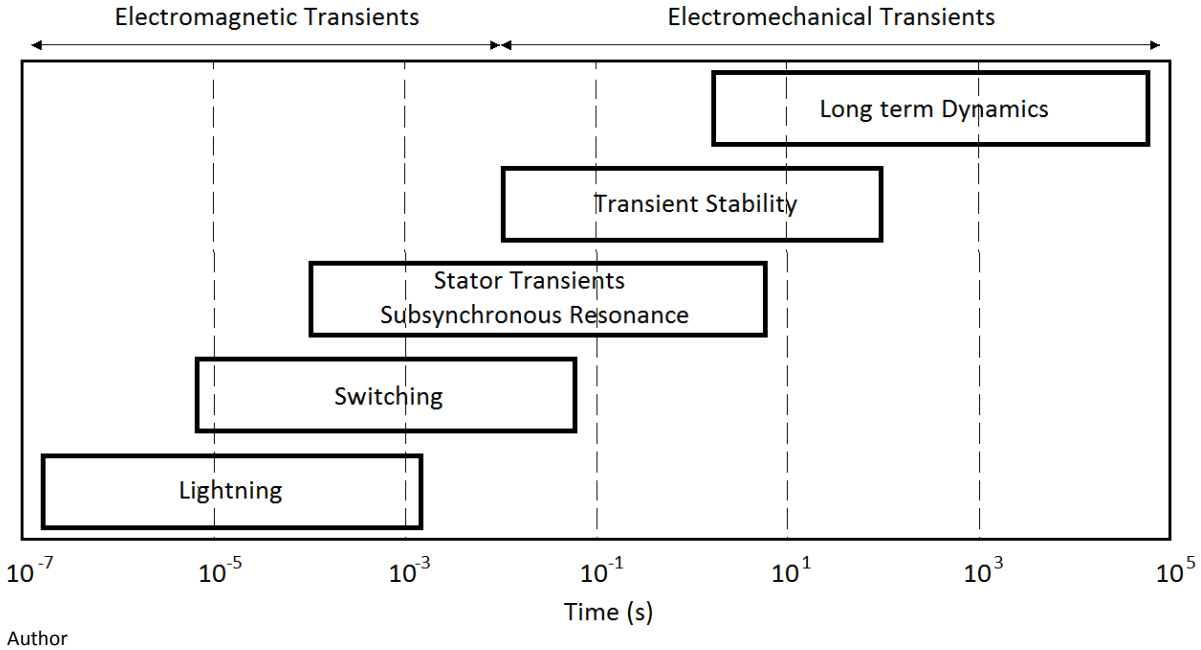

Author

The overall time range of power system transients is classified into fast electromagnetic transients and slow electromechanical transients. Thus, the power system is seen as a coupled electromechanical and electromagnetic system with wide range of time constants. There are fast electromagnetic transients due to the interaction between the magnetic fields of inductances and electrical fields of capacitances. Also, there are slower electromechanical transients due to the interaction between the mechanical energy stored in the rotating machines. Different time-domain simulation tools are used for studying the different dynamic phenomena in power systems.

Electromagnetic transient phenomena are usually triggered by changes in the grid configuration, as closing or opening action of circuit breakers or power electronic equipment, or by equipment failures or faults. These fast electromagnetic transients are studied with the Electromagnetic Transients Programs (EMTP) [57]. The simulation step size is of the order of tens of microseconds but can even be smaller depending on the study. Because of the long time constants associated with the dynamics of generators and turbines, simplified models of these are often sufficient for the time frame of typical electromagnetic transient's studies.

All simulations presented in this work were performed using the SimPowerSystems models developed in conjunction with the user environment using Matlab/Simulink. SimPowerSystems software is a modern design tool that allows build models that simulate power systems "easily". It uses the Simulink environment, allowing the models building using a simple click and drag procedures. Drawing the circuit topology rapidly is possible, and furthermore the circuit analysis can include its interactions with mechanical, thermal, control, and other disciplines [31].

The set of libraries is fairly complete, providing models of several network components e.g. RLC loads, non- linear loads, models of electric machines and associated controls, transmission lines models (π model equivalent and Bergeron model) circuit breakers, components of power electronics and their respective controls, etc. Such components may be used in conjunction with existing models in Simulink, as well as models developed by the user using Simulink, Matlab files (.m), FORTRAN or C language. An important feature of the version 5.6 of the package programming, employed in this work, is to undertake studies of electromagnetic simulation, where the network variables are represented by instantaneous values, and studies of the transient stability, where the variables are represented by phasors. Furthermore, there is a mechanism for initializing the variable of the electrical machines and associated controls using a load flow. The logical structure of SimPowerSystems is discussed in [31] and [34].

4 REVIEW OF INTERNATIONAL GRID CODES FOR WIND POWER

Regulations of grid codes are defined by system operators to describe the rights and responsibilities of all generators and loads connected to the transmission and distribution systems. Due to the low wind power participation in electric systems, grid codes for wind turbines were not needed at the beginning. However, with the increased presence of wind turbines in power systems, significant penetration levels are reached.

Grid codes establishment was necessary and required to ensure the safety and reliability of the systems. The shift from conventional sources to wind power raises concerns about the impacts of large-scale wind farms on the stability of the existing electricity networks considering the fluctuating and intermittent wind power nature. To guarantee a safe grid operation, the system operators established technical requirements for large-scale wind farms. Modern grid codes provide that wind devices must remain connected to the network in case of fault and also contribute to network stability like the conventional units [58].

Although each country must adapt its grid codes according to the own characteristics of its system, such as robustness, reliability, wind power penetration level, spinning reserve, etc., there are similarities in the demanded features to generating units. With a fault occurrence somewhere in the network, the system voltages drop to the lower levels until protection units detect and isolate the affected area. As a consequence of this, wind devices terminals, as well as the other components will experience voltage sags like consequence. In the past, wind turbines could be disconnected from the network due to stability issues that can arise in case of those disturbances. An incident of this type occurred in Western Europe on November 4, 2006 when 4.892 MW of wind power were disconnected from the grid [59]. When the wind power share is important, wind farm disconnection is unacceptable. For that reason modern grid codes require the continuous operation of wind turbines under various fault conditions following some given voltage–time profiles.

A grid code review performed by [60] shows that the technical requirements enforced on large wind generators can be broadly classified into five groups: (1) fault ride-through requirements, (2) active and reactive power responses following disturbances, (3) reactive power control or voltage regulation capability, (4) extended variation range for the voltage–frequency, and (5) active power control or frequency regulation support. In this work just the first three groups are considered. This chapter is based on [60]-[64].

4.1.1 **Fault ride-through requirement**

Low voltage ride through (LVRT) or fault ride through is the capability of electrical devices, mainly wind generators, to operate through of lower grid voltages than the operating limits. Also high voltage ride through (HVRT) exists for voltage swell conditions during which the operation above the established voltage limits is expected. Wound rotor generators designs use electrical current flowing through the windings to produce the magnetic field required for operation. These generators may have minimum and maximum working voltages, out of which they do not work properly, or have lower efficiency. Some generators will cut themselves out of the system when this situation occurs. This effect is more severe in the doubly-fed induction generators (DFIG), which have two sets of powered magnetic windings, than in squirrel-cage induction generators (SCIG) which have only one. [65].

Generation elimination by undervoltage may cause the voltage drops lower even more causing a cascading failure [66]. Modern large-scale wind turbines (1 MW and larger) require the inclusion of systems that allow them to operate during an event of this kind. Depending on the application, the generator may be required during and/or after the dip to:

- ✓ disconnect temporarily from the grid, but reconnect and continue operation after the dip
- ✓ stay operational and not disconnect from the grid
- ✓ stay connected and support the grid with reactive power

LVRT curves included in international grid codes are similar to the presented in Figure 4.1.

Figure 4.1 – Danish LVRT requirement.

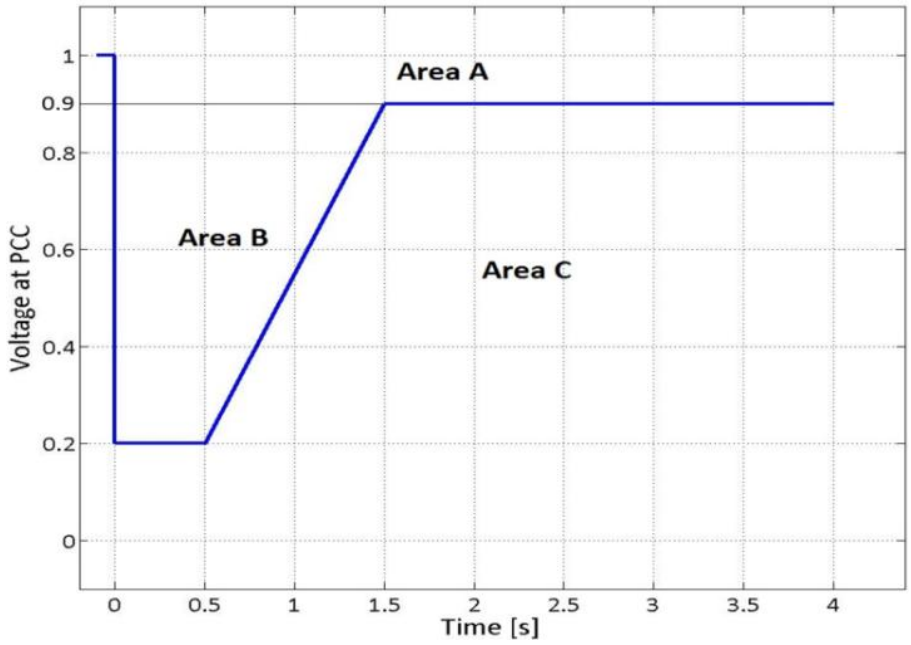

Source: Energinet [66].

However, depending on the regulations of each country, that curve may present some variations. Figure 4.1 shows the LVRT curve of Danish system operator where wind farms are required to withstand faults with voltage drops that reach 0,2 PU during 500 ms, followed by a voltage restoration at 0,9 PU in the next second.

Australian grid code is the most severe considering LVRT curves requiring to the wind farms withstand symmetrical and asymmetrical sags with the voltage down to zero during 100 ms and 400 ms respectively. Furthermore, the supply voltage must be restored to 0,7 PU within 2 s and to 0,8 before 10 seconds. German grid code requires ride-through capability for three-phase faults with voltage drops to zero during 150 ms, followed by the voltage recovery to 0.8 PU in 1,5 s. The old German grid code version was adopted by Ireland and USA.

LVRT curve parameters for some countries are summarized in Table 4.1. Countries like Australia, Canada, Germany, New Zealand and Spain require withstand solid faults at point of common coupling (PCC) with restoration of voltage higher to 60% in less than 2 s, being the Canadian and the Spanish grid codes the most exigent in the voltage recovery time.

Table 4.1 – LVRT requirements in international grid codes.

Grid code country	During fault		Fault clearance	
	V_{min} (PU)	T_{max} (s)	V_{min} (PU)	T_{max} (s)
Australia	0	0,1	0,7	2
Brazil	0,2	0,5	0,85	1
Canada	0	0,15	0,85	1
Denmark	0,2	0,5	0,9	1,5
Germany	0	0,15	0,9	1,5
Ireland	0,15	0,625	0,9	3
New Zealand	0	0,2	0,6	1
Portugal	0,2	0,5	0,8	1,5
Spain	0	0,15	0,85	1
United Kingdom	0,15	0,14	0,8	1,2
USA (WECC)	0	0,15	0,9	1,75

Author

HVRT capability is required by grid codes of Australia, Denmark, Germany, Spain and the United States. Table 4.2 presents the HVRT requirements of some grid codes. Voltage swells could occur by switching off large loads in the system, energizing capacitor banks, maneuvers and some faults on the grid. The most onerous requirements are in Australia and Spain, where the wind farms are required to withstand voltage swells of 1,3 PU. The longest exposure is present in the regulation of USA in which the wind farm must withstand the overvoltage during one second.

Table 4.2 – HVRT requirements in international grid codes.

Grid code country	During swell	
	V_{max} (PU)	T_{max} (s)
Australia	1,3	0,06
Denmark	1,2	0,1
Germany	1,2	0,1
Spain	1,3	0,25
USA (WECC)	1,2	1

Author

4.1.2 Active and reactive power responses of wind turbines under network disturbances

Grid codes set stringent regulations regarding the responses of active and reactive power of generation plants in case of faults on the network. Such regulations are established to ensure system stability following different types of disturbances. Regulations on the active power response of generators assist the network to maintain its short-term frequency stability, while the reactive power support can strengthen the limits of voltage stability on the grid. In countries with important wind power penetration levels, the response of this type of generation plants must be regulated and included within the grid codes. For example, Portuguese grid requires large wind farms to support the transient voltage stability of the network injecting reactive current according to the characteristic shown in Figure 4.2.

Figure 4.2 – Reactive power support requirement enforced by Portuguese grid code.

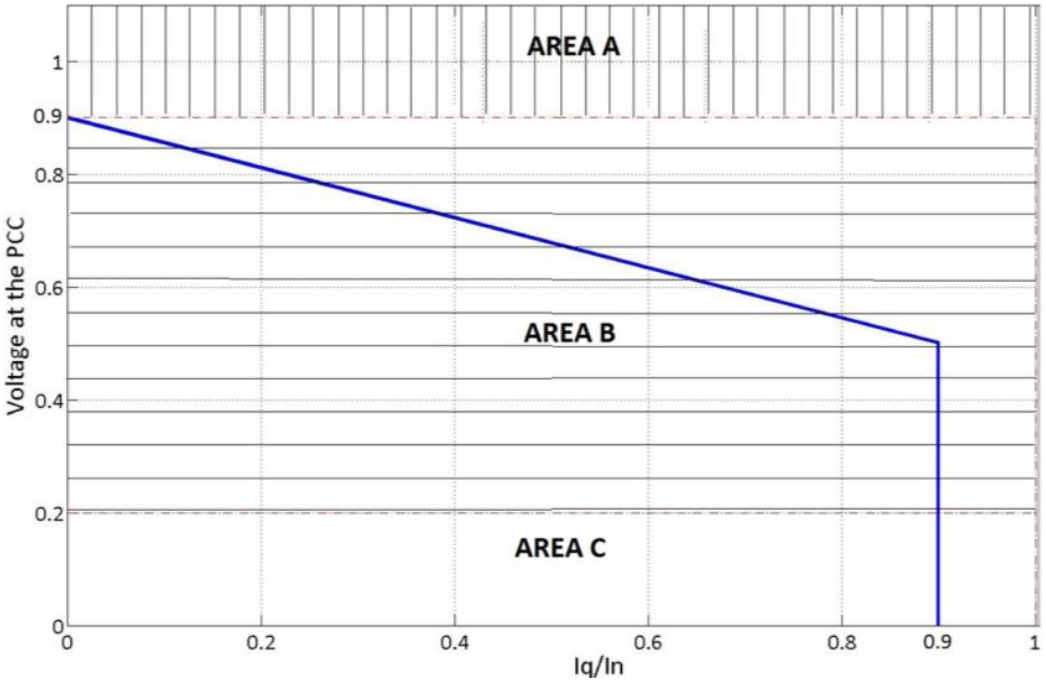

Source: Redes elétricas nacionais [68].

Australia, Denmark, Germany, Ireland, Portugal, Spain and the United Kingdom include regulations on the reactive power support by wind farms during voltage disturbances. Australian grid code requires wind farms to provide capacitive reactive current equal to 4% of their maximum continuous current for each 1% reduction in the PCC voltage, when the voltage drops to less than 0,9 PU. This means that wind turbines must generate their maximum reactive current when the PCC voltage is reduced more than 25%. Danish, German and Portuguese grid codes have similar requirement, but they demand for 2% of the reactive current injection for each percent reduction in the PCC voltage, i.e., maximum reactive current will be needed when the PCC voltage drops to less than 0,5 PU.

Spanish grid code states that wind farms must be equipped with a voltage control loop to inject reactive current during three-phase faults according to the features shown in Figure 4.3. The adopted control loop must reach its set-points within two fundamentals periods after the fault beginning. In Ireland and the United Kingdom, the grid codes establish that wind farms must produce their maximum reactive current during a voltage sag caused by a network fault without compromising wind turbines safety.

Figure 4.3 – Reactive power support requirement enforced by Spanish grid code.

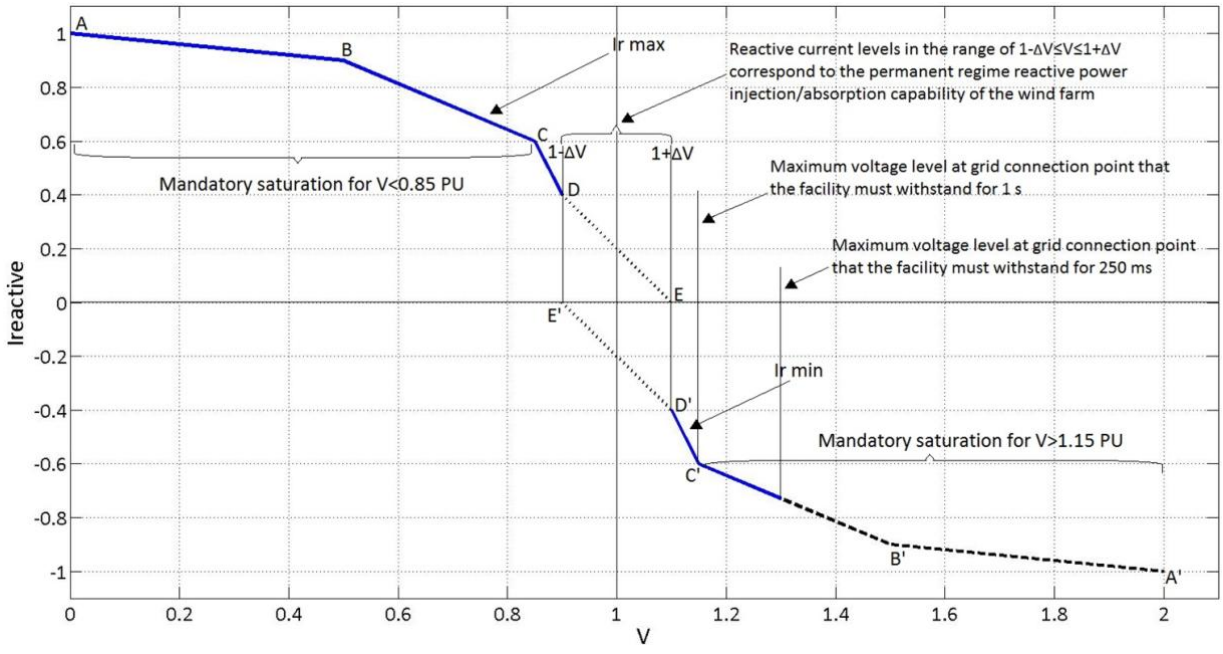

Source: Red eléctrica de España [69].

Regulations on the active power recovery of wind farms are defined in Australia, Denmark, Ireland, Germany, Portugal, Spain and the United Kingdom. Australian grid code requires wind farms to restore their active power at 95% of pre-fault value within 100 ms after the fault clearance. Danish grid code states that wind farms shall produce the rated power no later than 10 seconds after the

voltage is above 0,9 PU again. During the voltage dip the active power in the connection point shall meet the following condition:

$$P_{current} \geq k_p \cdot P_{t=0} \left(\frac{U_{current}}{U_{t=0}} \right)^2$$

where:

$P_{current}$: Current active power measured in the connection point

$P_{t=0}$: Power measured in the connection point immediately before the voltage sag

$U_{t=0}$: The voltage in the connection point immediately before the voltage sag

$U_{current}$: Current voltage measured in the connection point

$k_p = 0.4$: Reduction factor considering any voltage sags to the generator terminals.

German Grid Code stipulates active power restoration to the pre-fault value immediately after the fault clearance, with a gradient larger than 20% of the rated power per second. In Ireland, wind farms must continue the active power production during the fault period in proportion to the retained voltage. Also, the active power output must restore to 90% of the maximum available power within 1 s after the voltage recovery to 0,9 PU. Portugal establishes in its grid code that after fault clearance and PCC voltage recovery, active power must be restored with a rate no lower than 5% of rated power. In Spain, the wind farms are not allowed to consume active power during the fault and the voltage recovery periods. Furthermore, wind farms must retain the active power generation during the fault period in proportion to the remnant voltage. British grid code sets that wind farms must restore their active power output to 90% of the pre-fault value within 500 ms after the supply voltage recovery to 90% of the nominal value.

Considering the above requirements, it can be observed that there are situations in which wind turbines have to be overloaded to meet the requirements demanded by the grid codes. In these circumstances, one of the current components, either the active current component or the reactive current component must be prioritized to constrain the output current of generator within the machine limits. In Australia, Denmark, Germany and Portugal the reactive current component has the highest priority under fault condition. The opposite situation applies to the grid codes of Ireland, Spain and the United Kingdom.

4.1.3 **Reactive power control and voltage regulation**

Modern grid codes require wind farms to control their reactive power generation and provide voltage regulation service to the network. Thus they must be able to operate continuously at a range of capacitive/inductive power factor. Figure 4.4 presents the requirements of reactive power and power factor for a wind farm in Denmark.

Figure 4.4 – Reactive power and power factor requirements enforced by Danish grid code.

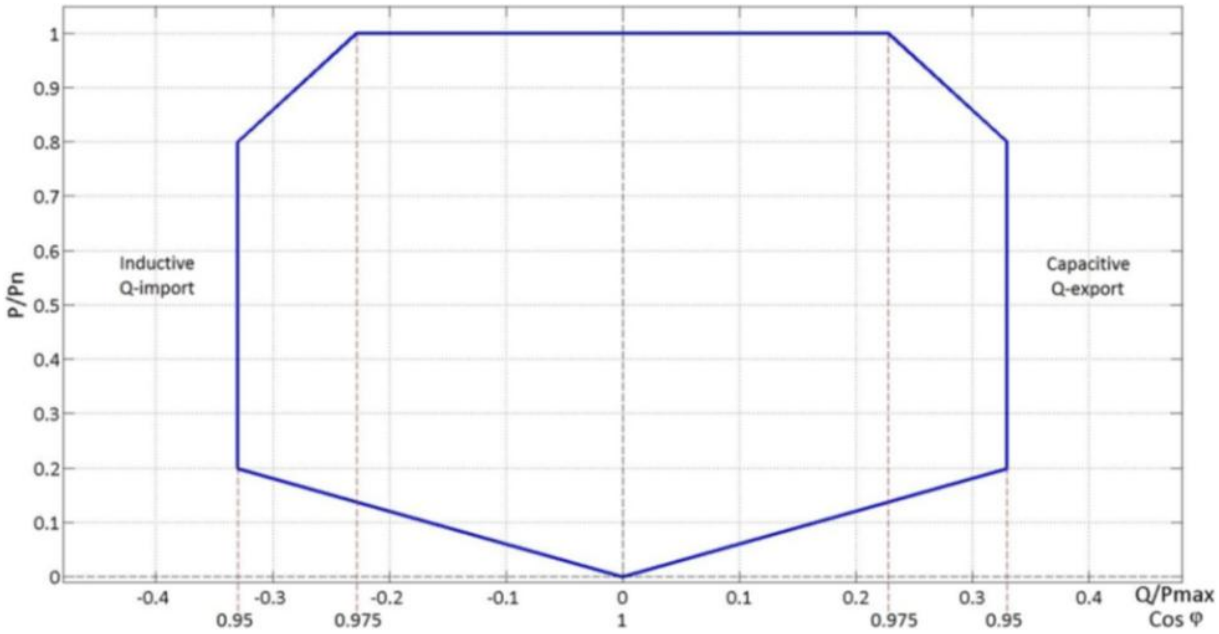

Source: Energinet [66].

This requires wind farms to operate with a power factor interval of 0,95 capacitive to 0,95 inductive when wind farm production represents more than 20% of the rated power. Besides, wind farms must be designed in such a way that the operating point can lie anywhere within the enclosed area in Figure 4.5 to assist steady-state voltage regulation.

Figure 4.5 –Voltage regulation requirement enforced by Danish grid code.

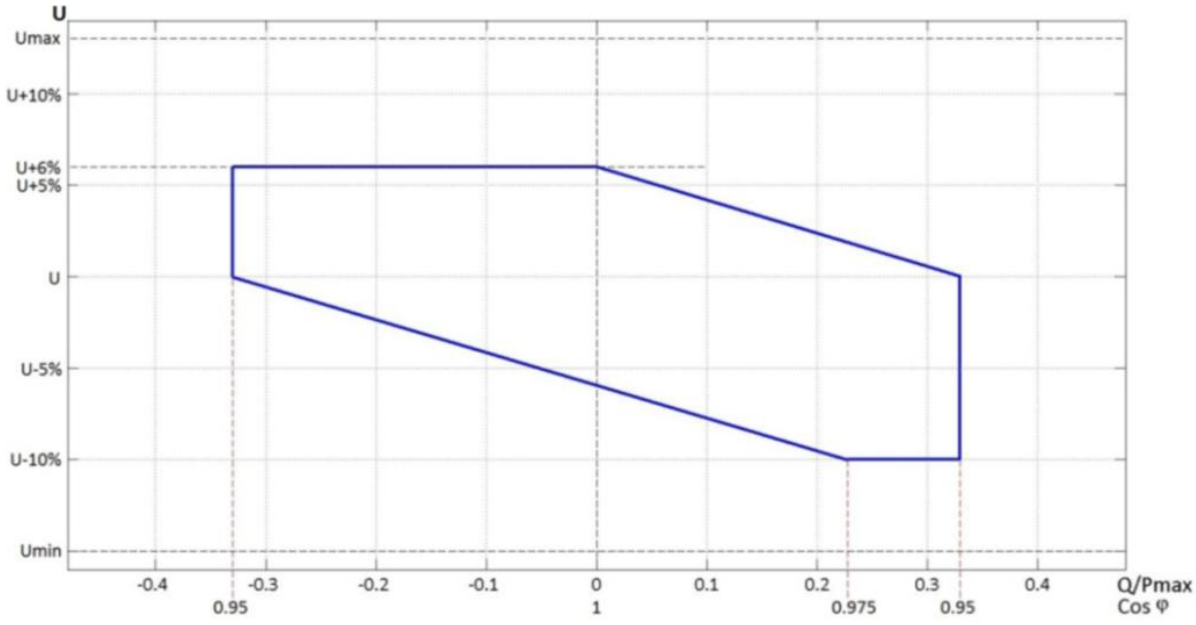

Source: Energinet [66].

Grid code regulation in Australia requires wind farms to be able to continuously operate at their rated output power with power factor variation from 0,93 capacitive to 0,93 inductive, based on the command signal received from the system operator. In Canadian grid code, the reactive power requirements are defined under continuous and dynamic operating conditions. Wind farms must be able to continuously work with a power factor variation from 0,9 capacitive to 0,95 inductive, whereas the minimum range for dynamic conditions varies from 0,95 capacitive to 0,985 inductive. This grid code also requires wind generators to have a voltage regulation system that acts under the voltage set-point control mode. This control loop must be adjusted to reach 95% of the reference reactive power before 1 s after the step change in the voltage set-point. German grid code establishes that wind farms must be able to operate with power factor varying from 0,95 inductive to 0,925 capacitive depending on the PCC voltage, as observed in Figure 4.6.

Figure 4.6 – Power factor control requirement enforced by German grid code.

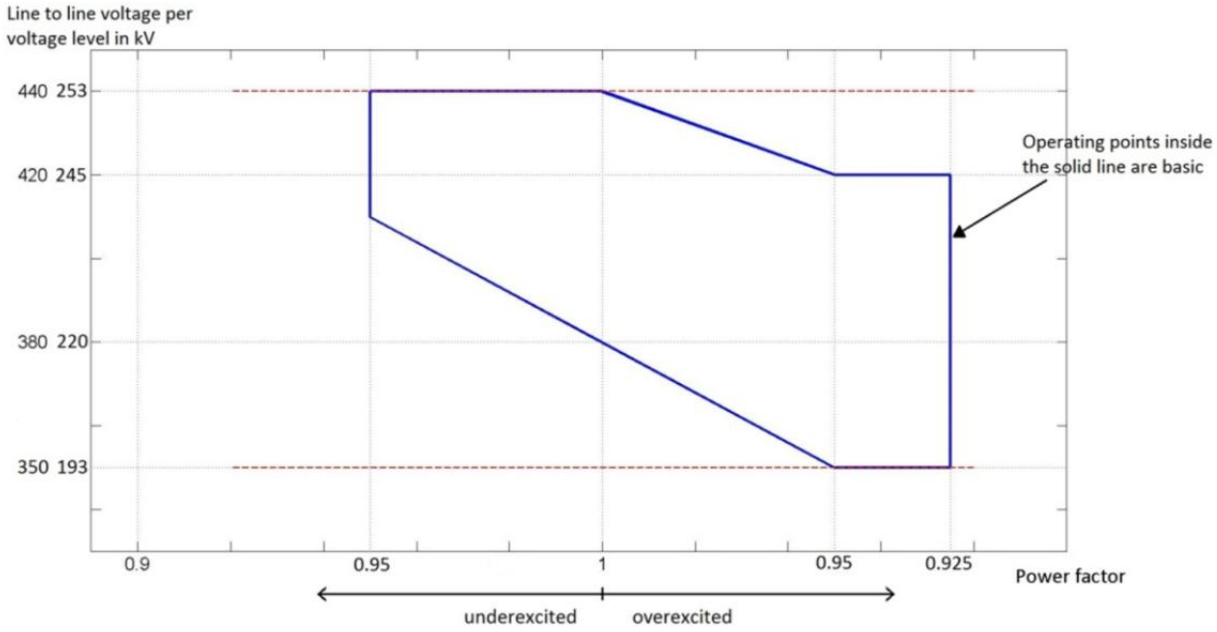

Source: E.ON Netz GmbH [70].

Reactive power regulations for other countries are summarized in Table 4.3. Germany, Spain, and the United Kingdom present reactive power control changes depending on the nominal value of PCC voltage. Accordingly, a comparison of the regulations concerning to the reactive power control is not possible.

Table 4.3 – Power factor limits in international grid codes.

Grid code country	Power factor	
	Capacitive	Inductive
Australia	0,93	0,93
Brazil	0,95	0,95
Canada	0,9	0,95
Denmark	0,95	0,95
Germany	0,95	0,925
Ireland	0,95	0,95
New Zealand	0,95	0,95
Portugal	0,98	0,98
Spain	0,91	0,91
United Kingdom	0,95	0,95
USA	0,95	0,95

Author

5 STEADY-STATE VOLTAGE PROFILE ANALYSIS

The connection of wind turbines in electrical power systems is progressing in several countries where water resources are uncommon and the use of alternative energy sources is sought. Consequently, the usage of wind power in electric systems is increasing and may begin to influence the overall system behavior. Therefore, the study of wind turbines behavior in electrical power systems, and their interaction with other generators and loads is really important.

The most common technology in installed wind turbines is the doubly-fed induction generator (DFIG); nowadays just few of the old squirrel cage induction generators (SCIG) are still in active service. Also there are some synchronous generators operating in wind turbines. These both types of induction machines contribute with asynchronous power to the system, and therefore, the wind power generation impacts over the system stability, particularly in voltage stability, due to the high penetration levels. In this chapter the analysis of the steady-state voltage profile for different scenarios of a power system is performed.

5.1 TRANSMISSION SYSTEM MODEL

In this work a methodology by comparing the impact of different levels of active power generated by wind turbines on the transmission grid. The IEEE 9 bus system was used, including a 163 MW wind farm at bus 2. The single line diagram of the system is shown in Figure 5.1.

Figure 5.1 – IEEE 9 transmission system with wind power generators.

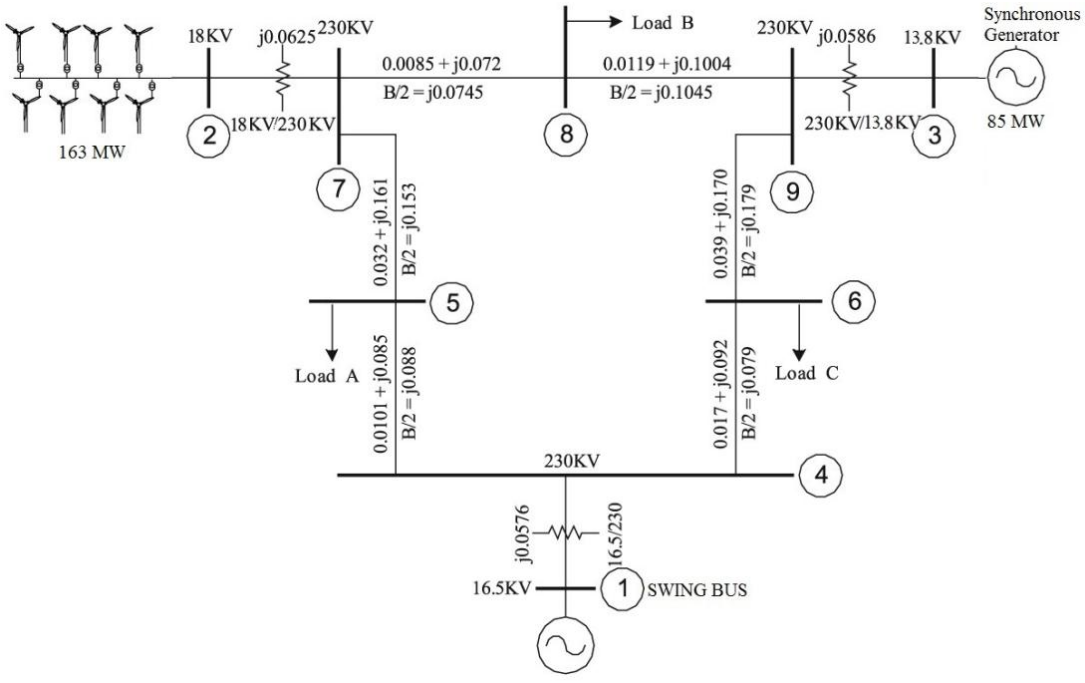

Author

This grid consists of a ring transmission system of 230 kV and 60 Hz, with three generators (buses 1, 2 and 3), three power transformers (between buses 1 and 4, buses 2 and 8, and buses 3 and 6) and three loads (buses 5, 7 and 9). Considering a wind farm of 163 MW (180 MVA representing 50% of the active power demanded) at the bus 2 and a hydraulic synchronous generator of 85 MW (100 MVA) at the bus 3 to supply the three charges. The load values are: load A 125 MW and 50 MVAr, load B 90 MW and 30 MVAr, and load C 100 MW and 35 MVAr.

5.2 STEADY-STATE VOLTAGE PROFILE

The presence of wind turbines in electric power systems may produce voltage violations at the distribution as wells as transmission level, which at the end may affect the loads and the other system components safety. The amount of wind power installed in power systems can be limited due to such violations. Before the installation of wind turbines in power systems, the worst operational scenarios must be analyzed to guarantee, that the inclusion of these will not affect the system. In this sense, the scenarios were characterized by [71] as following:

- no generation and maximum demand;
- maximum generation and minimum demand.

In this work the effects of different wind penetration levels on the system using DFIG, SCIG and synchronous generator are studied. The wind power penetration levels considered are 30%, 50%, 70% and 90%, whose are based on situations existing in some countries around the world. For example, in Portugal a penetration of 93% instantaneous wind power was set on November 13, 2011 [72]; therefore the probability to acquiesce all the other lower levels is really high. In Ireland, peaks of instantaneous penetration exceeding 40% are presented in least monthly, even reaching 53,5% on 29th of December of 2011. Furthermore, in Ireland studies concluded that high levels of instantaneous wind power penetration, such as between 60% and 80% can be allowed in the system taking corrective measures in them [6]. Spain reported that 59,6% of national power demand was covered by wind energy on November 6, 2011 [6]. Denmark is a country that in hours of low demand, the wind power can provide all its electricity, reaching a general supply of 30% of domestic demand in 2012 [3].

5.2.1 **30% of wind power penetration**

This penetration level was achieved by reducing the output power of the wind farm to 96 MW. Leading to a steady-state voltage profile of the grid as presented in Figure 5.2. Wind farms composed by wind generators of the following features are used in bus 2:

- DFIG with reactive power control using generators with unity power factor;

- DFIG with voltage control using generators with output voltage 1,0253 PU;
- SCIG without ancillary devices;
- SCIG with capacitor banks of one third of rated value;
- SCIG with STATCOM of one third of rated value in voltage control;
- and synchronous generator.

Figure 5.2 – Steady-state voltage profile for 30% of wind power penetration.

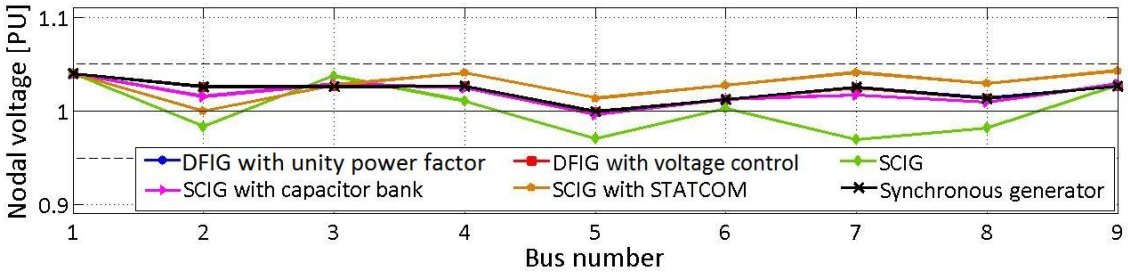

For this penetration level the bus voltage values are almost the same for both control modes of DFIG and the synchronous generator. Using SCIG, the voltage in bus 2 is lower than the ones presented in the other cases, the performance of the SCIG with capacitor bank is similar than the cases with DFIG and synchronous generator. The SCIG without any ancillary equipment demands reactive power leading the other generators to inject this reactive power and the voltage values in the other buses are lower due to the voltage regulation by high currents in the lines. The SCIG with STATCOM injects high reactive power and causes the voltage values in all the buses are higher than with the other generators. The output power values of the system generator devices are found in Table 5.1.

Table 5.1 – Output power values of the system generator devices for 30% of wind power penetration.

Generator	OUTPUT POWER					
	Swing bar (bus 1)		Wind farm (bus 2)		Hydraulic generator (bus 3)	
	Active power (MW)	Reactive power (MVAr)	Active power (MW)	Reactive power (MVAr)	Active power (MW)	Reactive power (MVAr)
DFIG with unity power factor	138,84	25,26	95,33	0	85,01	-19,41
DFIG with voltage control	138,65	25,38	95,34	-0,19	85,01	-19,00
SCIG	121,83	36,35	95,26	-50,11	85,02	21,88
SCIG with capacitor bank	136,70	27,10	94,05	-9,98	85,01	-11,60
SCIG with STATCOM	138,98	26,73	90,90	-11,10	85,01	-9,26
Synchronous generator	138,30	25,41	96,90	-0,35	85,01	-19,45

5.2.2 **50% of wind power penetration**

This penetration level is the “nominal” for this transmission system and consists of a 163 MW wind farm in the bus 2 with a hydraulic synchronous generator of 85 MW at bus 3. The load values are

set to their rated values. The steady-state voltage profile of the grid is presented in Figure 5.3 for DFIGs with voltage control and unity power factor, for SCIG with and without ancillary devices, and for synchronous generator. Wind farms in the bus 2 with the same features of previous case are used.

Figure 5.3 – Steady-state voltage profile for 50% of wind power penetration.

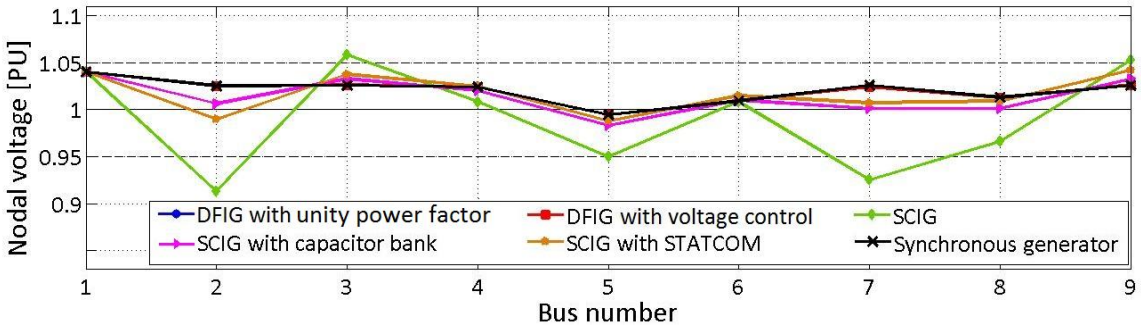

The bus voltage values for this penetration level are about the same for both DFIG control modes and synchronous generator. By using the SCIG without auxiliary devices the bus 2 voltage is close to 0.9 PU because of the high reactive power demanded by this generator and the voltages from the nearby buses are also lower than those presented in the cases of DFIGs. The SCIG with both STATCOM and capacitor bank has a performance similar to those shown in situations with DFIGs but with lower voltages on the buses 2 and 7 (wind farm connection points) than those presented in the DFIG cases, it due to the reactive power consumption of the wind turbines at this point. The output power values of the system generator devices are found in Table 5.2.

Table 5.2 – Output power values of the system generator devices for 50% of wind power penetration.

Generator	OUTPUT POWER					
	Swing bar (bus 1)		Wind farm (bus 2)		Hydraulic generator (bus 3)	
	Active power (MW)	Reactive power (MVAr)	Active power (MW)	Reactive power (MVAr)	Active power (MW)	Reactive power (MVAr)
DFIG with unity power factor	72,88	28,30	162,75	0	85,01	-18,48
DFIG with voltage control	72,93	28,27	162,75	0,15	85,01	-18,61
SCIG	39,95	49,47	163,23	-87,12	84,92	72,59
SCIG with capacitor bank	62,87	34,05	163,15	-25,88	85,02	3,86
SCIG with STATCOM	57,45	36,06	166,40	-31,39	85,01	10,13
Synchronous generator	72,76	28,14	163,21	0,85	85,01	-19,66

5.2.3 **70% of wind power penetration**

To achieve this penetration level the load values were reduced to 55% of their rated value and the output power of the wind farm was adjusted to 126 MW. The steady-state voltage profile of the network for the DFIG with voltage control and unity power factor, for the SCIG with and without

ancillary devices and for the synchronous generator is presented in Figure 5.4. Wind farms in the bus 2 with the same features of the previous cases are used.

Figure 5.4 – Steady-state voltage profile for 75% of wind power penetration.

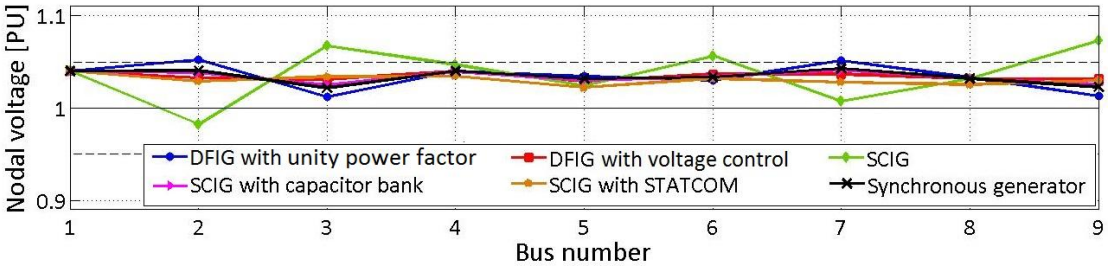

The voltage values for all the technologies except SCIG are oscillating between 1,01 and 1,06 PU. In the case of DIFG with unity power factor the voltage values are higher than 1.05 PU at buses 2 and 7. The voltage profile behavior is alike for the synchronous generator and the SCIG with capacitor bank. The voltage profile behavior is similar for the DFIG with voltage control and the SCIG with STATCOM. The SCIG presents a voltage value lesser than 1.0 PU at the bus 2 and greater than 1.05 PU at the buses 3, 6 and 9 because power flows presented in the system. The output power values of the system generator devices are shown in Table 5.3.

Table 5.3 – Output power values of the system generator devices for 75% of wind power penetration.

Generator	OUTPUT POWER					
	Swing bar (bus 1)		Wind farm (bus 2)		Hydraulic generator (bus 3)	
	Active power (MW)	Reactive power (MVAr)	Active power (MW)	Reactive power (MVAr)	Active power (MW)	Reactive power (MVAr)
DFIG with unity power factor	52,57	-70,98	126,92	0	0	0
DFIG with voltage control	44,69	-41,25	127,62	-24,23	0	0
SCIG	36,63	13,87	125,84	-74,41	0	0
SCIG with capacitor bank	66,90	-56,27	126,06	-18,87	0	0
SCIG with STATCOM	37,86	-28,50	129,60	-34,11	0	0
Synchronous generator	39,77	-51,89	125,36	-13,56	0	0

5.2.4 **90% of wind power penetration**

This penetration level was achieved adjusting the wind farm to 100% to its rated value (163 MW) and the loads were adjusted to 55% of its nominal value. The steady-state voltage profile of the network for the DFIG with unity power factor or voltage control, and for the synchronous generator is presented in Figure 5.5.

Figure 5.5 – Steady-state voltage profile for 90% of wind power penetration.

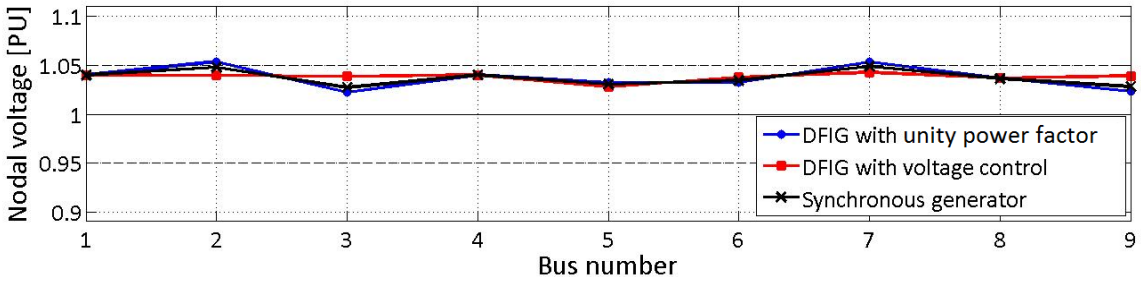

SCIG technology is not considered in this level because this scenario is not real and the reactive power demanded by these generators is very high. For this penetration level the voltage buses present values close to 1.04 PU in all buses exceeding the voltage limits for distribution systems of 1,05 PU on buses 2 and 7 for the DFIG with unity power factor and voltage control and synchronous generator. The output power values of the system generator devices are shown in Table 5.4.

Table 5.4 – Output power values of the system generator devices for 90% of wind power penetration.

Generator	OUTPUT POWER					
	Swing bar (bus 1)		Wind farm (bus 2)		Hydraulic generator (bus 3)	
	Active power (MW)	Reactive power (MVAr)	Active power (MW)	Reactive power (MVAr)	Active power (MW)	Reactive power (MVAr)
DFIG with reactive power control	24,86	-55,28	162,38	0	0	0
DFIG with voltage control	25,83	-32,48	162,77	-18,73	0	0
Synchronous generator	15,54	-44,76	163,21	-7,04	0	0

5.2.5 **Effect of wind power penetration**

Figure 5.6 presents the steady-state voltage profiles by wind penetration level for the six technologies of wind turbines. Among the different wind penetration levels, the two highest levels (70% and 90%) showed higher bus voltages when compared to the other two cases (30% and 50%), further, for the cases of DFIGs in both control modes and synchronous generator. The SCIGs cases either in presence or absence of ancillary elements, and with 70% of wind penetration level, presented the highest nodal voltages in the system. This fact may be explained by the reduction in the loads, below 60% of their rated values, which requires less apparent power. Therefore, there are lower currents circulating in the system in comparison with the full loads, representing a case of lower voltage regulation.

For the cases of DFIG and synchronous generator with 30% and 50% of wind penetration into the system, the nodal voltage values are closely related, because the powers and currents flowing on the system. In the other hand, the SCIGs cases with 30% and 50% of wind penetration into the system, shows and inversely relation between the nodal voltage values and the wind penetration level. It can

be seen an increase in the reactive power demanded by the SCIG together with the penetration level. The ancillary elements can increase the nodal voltage values in the system by reactive power injection; this improvement on the voltage profile is more representative by the greater capacity of the ancillary equipment to inject reactive power.

Figure 5.6 – Resume of the steady-state voltage profiles.

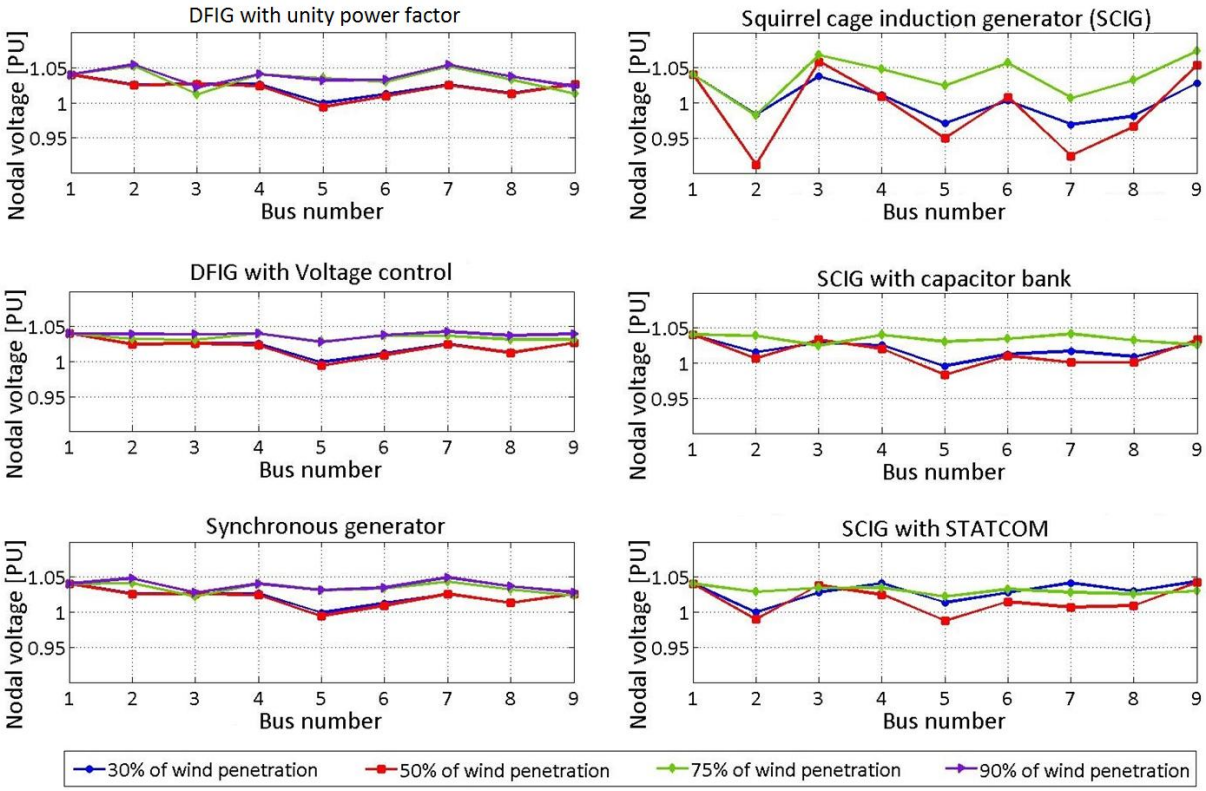

5.3 CONCLUSIONS

The electrical system used has low reactive power exchange between the wind generators and the network because the capacitive characteristic of the transmission lines. Analyzing the developed steady state simulation results, one can verify that the performance of DFIG devices and synchronous generators are similar for all wind penetration levels.

In contrast, the use of SCIG presents a more sensibility. The squirrel cage induction generators demand reactive power from the grid during operation, when no ancillary devices are used to compensate this consumption of reactive power. By consequence, the terminal voltages of the generators are lower because the excessive demand from reactive power. For this reason, the utilization of ancillary devices improves the steady state voltage profile when SCIGs are implemented.

In general, for higher wind power penetration levels, the variations of voltage levels and the reactive power exchanges are higher. The different wind penetration levels in this analysis were found by variations of load percentage and the power delivered by the wind farm.

Any technology may be used in electrical systems during the steady-state operation regarding the voltage limits. However, due to the reactive power consumption, the use of SCIGs without reactive power support could represent higher currents and low voltage values in the system. Therefore, the use of DFIGs, synchronous machines, and STATCOM and SVC represents an effective option considering the power exchange between the grid and the wind farms for all penetration levels.

6 POWER SYSTEM STABILITY IN PRESENCE OF LARGE WIND FARMS

Power system stability is the ability of power systems to remain in operating equilibrium state under normal operating conditions and to retrieve acceptable state of equilibrium after disturbances. Instability in power systems may be manifested in different ways depending on its configuration, topology and operation mode; for instance: with a loss of synchronism (dynamics of generator rotor angles and power-angle relationship), and with collapse of load voltage (stability and voltage control) [28]. During the evaluation of stability the major concern is usually the power system behavior when experiences transient disturbances. These disturbances may be small, showing up in form of continuous load changes and system can change conditions to adjust itself, moreover these disturbances may be large, such as faults on transmission lines, loss of large loads and generators, and loss of ties between subsystems.

The study of power system stability as a single problem is impractical, mostly because the instability may take different forms and be influenced by different factors. Analyses of stability problems, cover the identification of essential factors that contribute to instability, and formation of methods for improving a stable operation. These analyses are facilitated by the classification of stability in categories based on the following considerations:

- Physical nature of the instability;
- size of the disturbance considered;
- devices, processes, and time considered to determine stability;
- and the most appropriate method of calculation and stability prediction.

The most common classification for stability analysis of power systems given by [28] is:

- Rotor angle stability: ability of interconnected synchronous machines in a power system to keep the synchronism. The problem involves the study of electromechanical oscillations inherent to power systems.
- Mid-term and long-term stability: This analysis includes problems associated with the dynamic response of power systems to severe upsets. Severe system upsets result in large excursions of voltage, frequency, and power flows that invoke the actions of slow processes, controls, and protections not considered in traditional transient stability studies.
- Voltage stability: ability of the power system to maintain steady acceptable voltages at all system buses under normal operating conditions and after being exposed to a disturbance.

Figure 6.1 presents an overall classification of the power system stability problems, although within this work just the voltage stability is considered. Voltage stability is generally classified in two

subclasses. The first one is the large-disturbance voltage stability (LDVS) that considers the system ability to control voltage following large disturbances such as faults, loss of generation, or circuit contingencies. The second one is the small-disturbance voltage stability (SDVS) that considers the ability of power systems to control voltages following small perturbations such incremental changes in system load.

Figure 6.1 – Classification of power system stability.

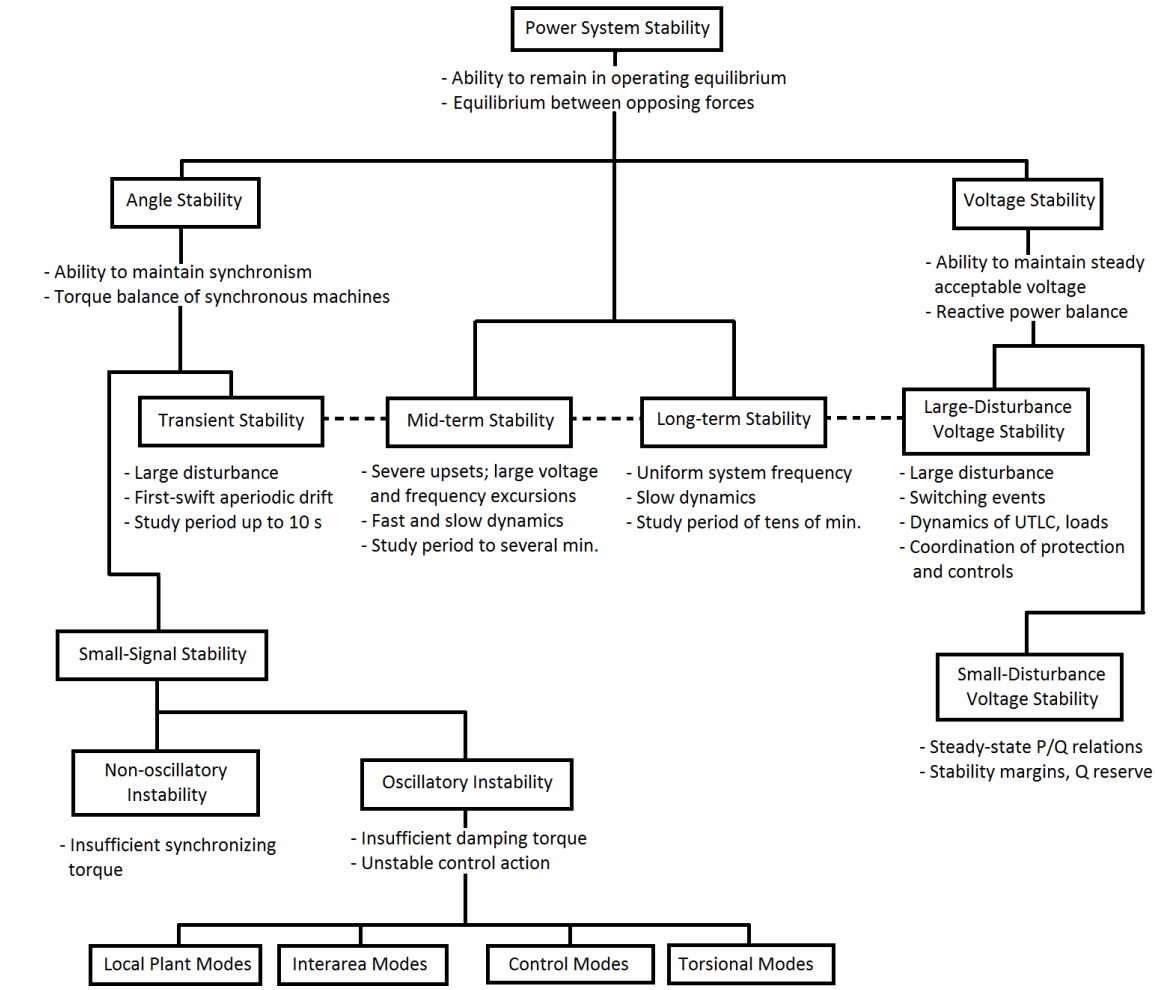

Author

6.1 DYNAMIC ANALYSIS OF DFIGS WITH UNITY POWER FACTOR

Most of the modern wind turbines are based on DFIG, with a back to back power converter connecting the rotor to the grid. Voltage sags at generator terminals can cause overcurrents in the rotor windings, endangering the converter integrity. Protection system and different strategies are suggested in literature with some solutions (crowbar in rotor circuit, chopper in DC link, dynamic voltage restorer, series resistor in the stator circuit, and demagnetizing current control). When some

disturbances are presented on the system, reactive power injection by the DFIGs of the wind farm could be demanded to maintain the system in safe operating limits.

This section discusses three control strategies for wind farms based on DFIGs with unity power factor are illustrated. Analyses to voltage sag and swell, and short circuit are performed to observe the response and help to determine the best option choosing the more appropriated. IEEE 9 bus system was used considering 50% of wind power penetration level (See section 5.2.2).

1. **First strategy** is the most common in distribution systems, shortly the generator maintain its injected reactive power in 0 PU during any disturbance but it is tripped if endangering its own integrity by disconnection of the system.
2. **Second strategy** consists in switch the operation mode to voltage control if terminal voltage are outside the range 0,9 and 1,1 PU injecting or absorbing reactive power to set a safe voltage value. Whether terminal voltage is stable and reactive power value is close to 0 PU, the control mode can be switched again to reactive power control mode. When the DFIG security is in danger it is tripped.
3. **Third strategy** includes the crowbar resistor to protect the DFIG converters during grid faults. In case of fault detection, the crowbar operates during 100 ms after half a cycle to protect the converters and inject reactive power changing its operation control mode to voltage control later, it to reestablishes the voltage quickly and "ride through" the low voltage during the fault. Furthermore this strategy has the second strategy characteristics to switch DFIG control mode during voltage sags and swells.

The graphic representation of the control mode switching that happens during voltage disturbances for the strategies 2 and 3 of the DFIG with unity power factor is represented in the Figure 6.2.

Figure 6.2 – Control mode switching representation for strategies 2 and 3.

6.1.1 Voltage swell

A voltage swell with magnitude of 35% (In this work, voltage swell magnitude refers to the increase of the voltage respect to the nominal one) and a second of duration at bus 1 is considered for this analysis. Wind farm voltage response is presented in Figure 6.3.

Figure 6.3 – Wind farm voltage response to a 35% swell at bus 1.

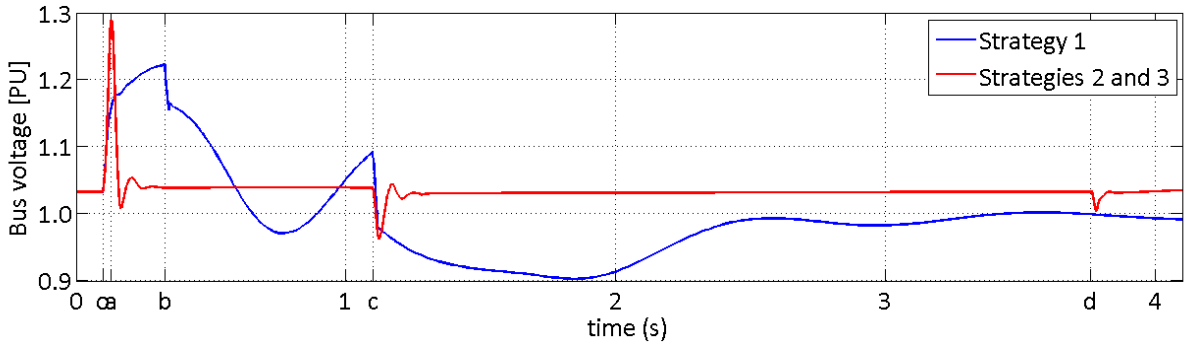

Voltage swell begins in point *o* and wind farm voltage reaches a value greater than 1,1 PU, which is the safe operation limit and is also higher than 1,2 PU that is the set voltage for overvoltage protection trip. For the strategy 1, the voltage exceeds the set voltage in the protection tripping out the wind farm 100 ms (delay protection) after the disturbance begins (point *b*). The bus voltage follows the system dynamic imposed by the other generators. In point *c* the voltage swell ends and system voltages decrease instantaneously following the hydraulic generator dynamic.

Strategies 2 and 3 have the same response for this kind of disturbance. In point *a* the control switch is done to voltage control mode reestablishing the bus voltage to the pre-fault value, through reactive power absorption during the disturbance. In point *c* the voltage swell finishes and voltage value returns to the pre-fault value after a quick transient. Wind farm current response is presented in Figure 6.4.

Figure 6.4 – Wind farm current response to a 35% swell at bus 1.

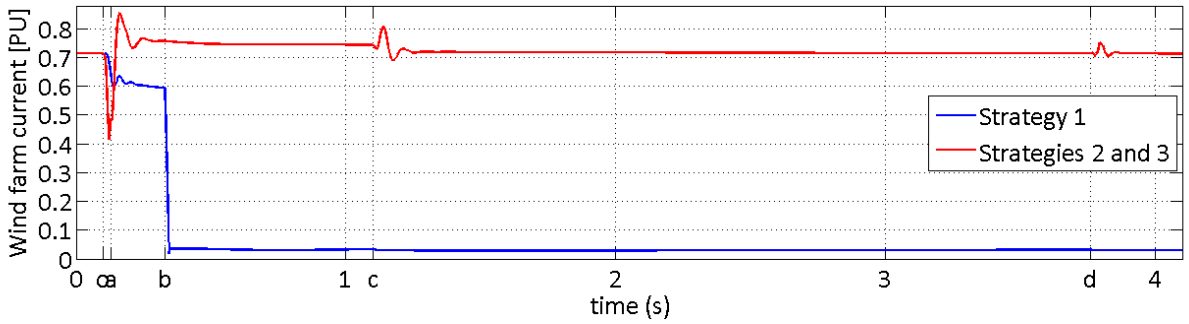

In case of strategy 1 the wind farm current reduces its value when swell begins, maintaining the power balance. In point *b* (after 100 ms) the wind farm cuts itself out of the system and the wind farm current falls to 0. For strategies 2 and 3 the reactive power absorption by the generator during the swell represents a brief current increase of the wind farm current. After swell clearance the wind farm current recovers its pre-swell value. Wind farm active power response is presented in Figure 6.5.

Figure 6.5 – Wind farm active power response to a 35% swell at bus 1.

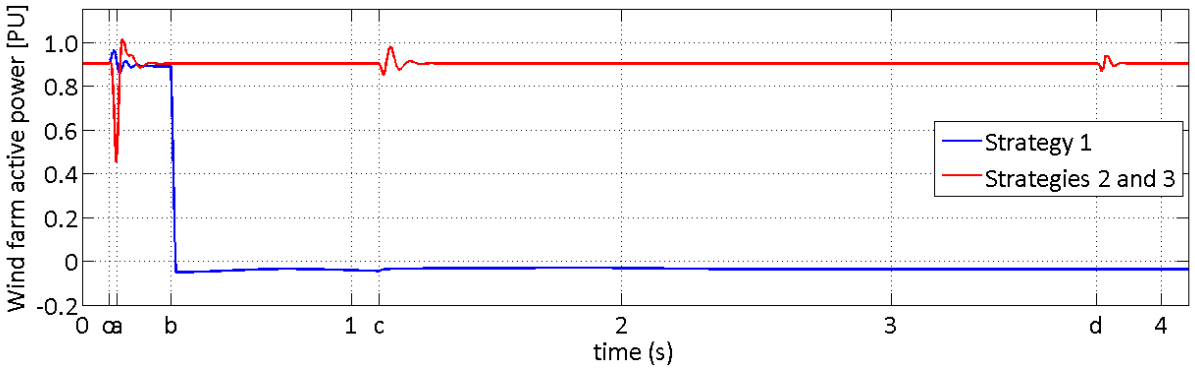

In case of strategy 1 the active power generated by the wind farm keeps its value during 100 ms after swell beginning. In point *b* the wind farm cuts itself out of the system and the wind farm active power is reduced to 0. For strategies 2 and 3 the active power keeps its value constant and just presents some transient disturbances at the beginning and in the end of the swell, as well as the control mode change done in the DFIG. Wind farm reactive power response is showed in Figure 6.6.

Figure 6.6 – Wind farm reactive power response to a 35% swell at bus 1.

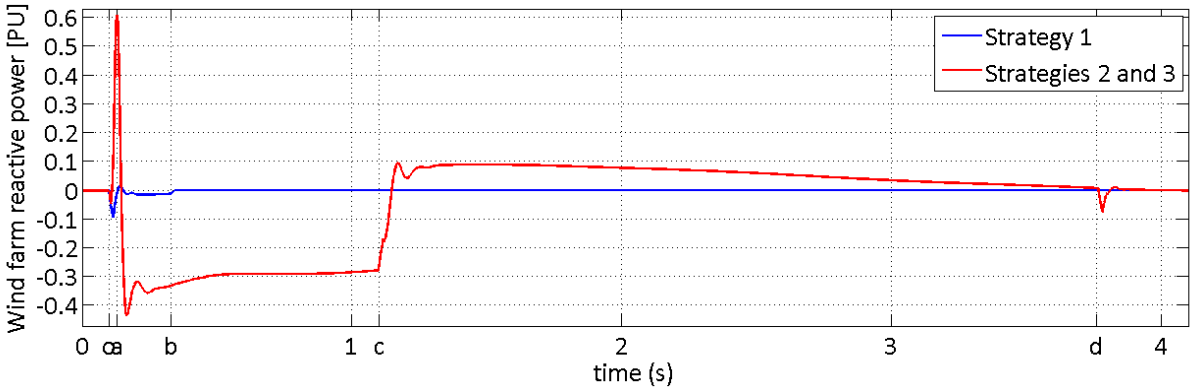

For strategy 1 case the reactive power is always 0 because the control is determined to maintain unity power factor during the wind farm operation. In cases of strategies 2 and 3 there is reactive power absorption to keep the wind farm voltage close to the set voltage (1,0253 PU) during the swell. After swell clearance a part of the reactive power absorbed during the swell is delivered to the system after the disturbance and when wind farm reactive power is close to 0 PU the switch to reactive power control mode is done in point *d* causing a little transient disturbance in the electrical parameters.

6.1.2 **Voltage sag**

A voltage sag with 50% of magnitude (in this work, voltage sag magnitude refers to the voltage reduction respect to the nominal one) and duration of 250 ms at bus 1 is considered for this analysis. Wind farm voltage response is presented in Figure 6.7.

Figure 6.7 – Wind farm voltage response to a 50% sag at bus 1.

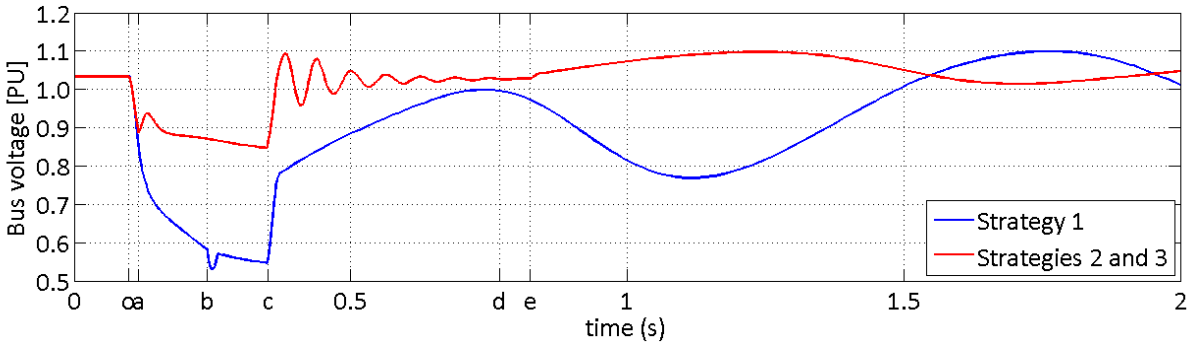

Voltage sag begins in point *o* and wind farm voltage reaches a value lower than 0,9 PU that is the safe operation limit and is also lower than 0,7 PU that is the set voltage for undervoltage protection trip. For strategy 1 the voltage reaches a value below the set voltage in the protection and wind farm trips out 100 ms (delay protection) after the disturbance beginning (point *b*). In point *c* the voltage sag finishes and voltage value returns to its pre-fault value after a transient period with marked oscillations, during and after the sag following the dynamic imposed by the hydraulic generator. In cases of strategies 2 and 3 the wind farm voltage response is equal for this kind of disturbance. In point *a* the control switch is done to voltage control mode trying to increase the bus voltage to the pre-fault value, through the reactive power injection. In point *c* the voltage sag finishes and voltage value returns to its pre-fault value after a transient period with some oscillations after the sag. In Figure 6.8 the wind farm current response is showed.

Figure 6.8 – Wind farm current response to a 50% sag at bus 1.

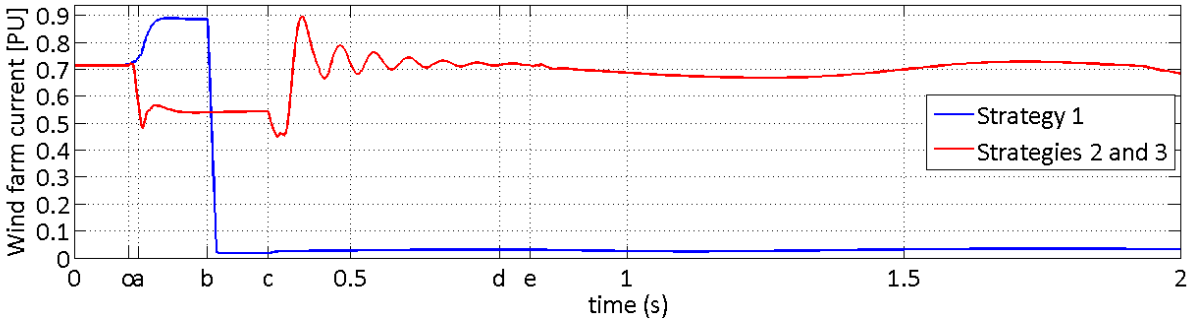

In case of strategy 1 the wind farm current increases its value during 100 ms after sag begins. In point *b* (after 100 ms) the wind farm cuts itself out of the system and the wind farm current is reduced to 0. For strategies 2 and 3 the wind farm current decreases its value during the voltage sag because voltage reduction. After sag clearance the current value recovers its pre-sag value after some oscillations because the power exchange and they could be more or less pronounced depending of the controller's constants. Wind farm active power response is presented in Figure 6.9.

Figure 6.9 – Wind farm active power response to a 50% sag at bus 1.

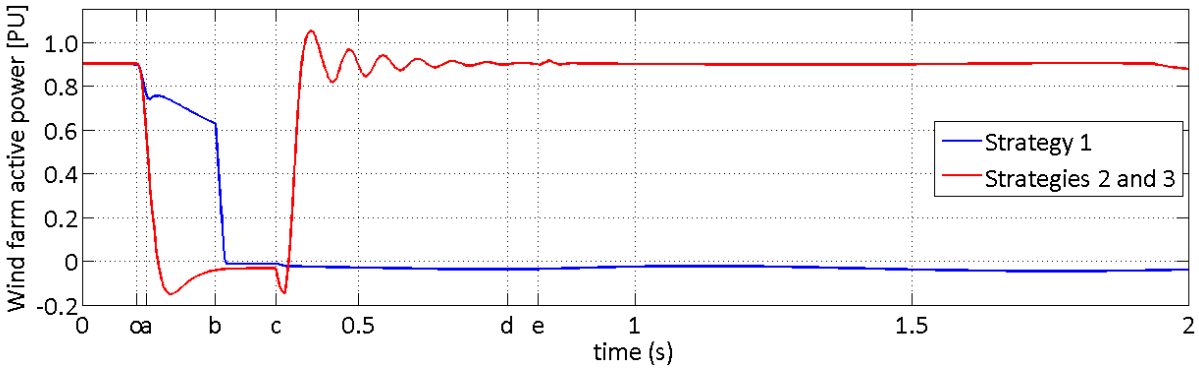

For the strategy 1 the active power delivered by the wind farm is reduced slowly, but by the wind farm trip out the active power falls to 0. In strategies 2 and 3 the active power is reduced to 0 by the current reactive current priority established in the converser's control. After sag clearance (point *c*), the wind farm active power is reestablished to the pre-sag value after some oscillations. Wind farm reactive power response is presented in Figure 6.10.

Figure 6.10 – Wind farm reactive power response to a 50% sag at bus 1.

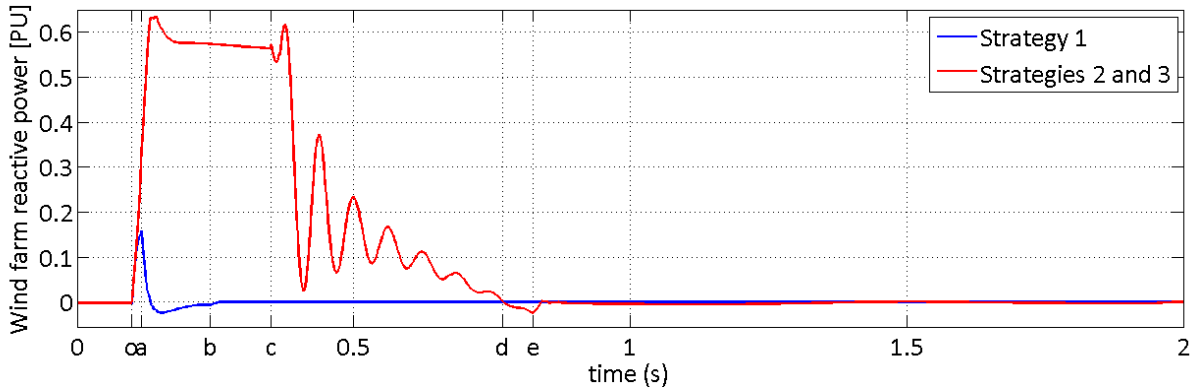

In case of strategy 1 the reactive power injected by the wind farm is equal to 0 all the time, there is a transient disturbance when voltage sag occurs. For strategies 2 and 3 there is a control mode change from unity power factor to voltage control because the voltage reduction. For this reason the DFIG can inject reactive power to maintain constant the wind farm terminal voltage. During the voltage sag and while the voltage is recovered there is reactive power injection by the generators. After sag clearance the injected reactive power reduces its value progressively while wind farm voltage is reestablished. When injected reactive power is close to 0 PU the switch to reactive power control mode is done in point *e* causing a little transient disturbance in the electrical parameters.

6.1.3 **Solid short circuit in load B**

A solid three phase short circuit of 150 ms duration at bus 8 (load b) is considered within this analysis. Wind farm voltage, current, active power and reactive power responses are presented in

Figure 6.11, Figure 6.12, Figure 6.13, and Figure 6.14 respectively. The short circuit begins at the point *o* and wind farm voltage falls down close to 0 PU that is below of the set voltage for undervoltage protection trip. For strategy 1 the voltage is below the set voltage in the protection which trip and let out the wind farm 100 ms (delay protection) after the disturbance occurs (point *c*). Wind farm current, active and reactive power fall down to 0 because the trip, the bus voltage follows the system dynamic imposed by the other generators. In point *d* the short circuit is tripped and system voltages increase instantaneously following the hydraulic generator dynamic.

Figure 6.11 – Wind farm voltage response to a solid short circuit at bus 8.

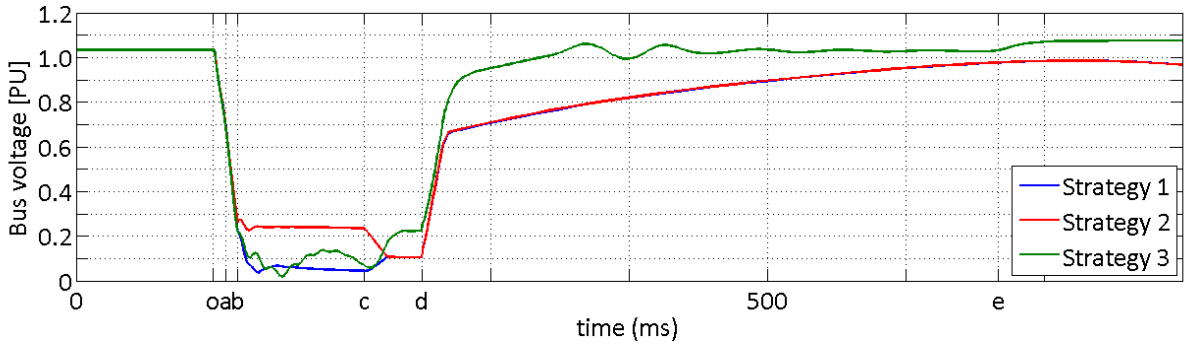

Figure 6.12 – Wind farm current response to a solid short circuit at bus 8.

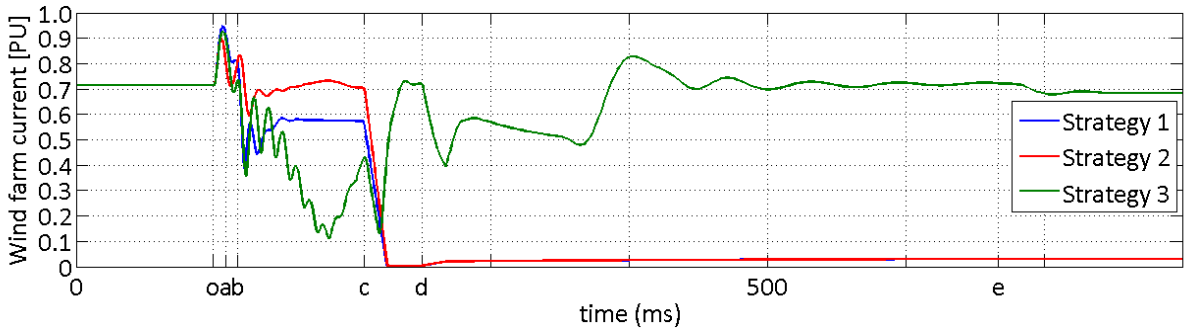

For the strategy 2 the control change to voltage control mode is done in point *b* in an attempt to increase the bus voltage to the pre-fault value, but bus voltage remains in 0,25 PU (Figure 6.11) through the reactive power injection during the disturbance as shown in Figure 6.14. Bus voltage is down of the set voltage in the protection which trip and let out the wind farm 100 ms (delay protection) after the disturbance occurs (point *c*) similarly to the strategy 1. Wind farm current, active and reactive power fall down to 0 because the trip, the bus voltage follows the system dynamic imposed by the other generators. In point *d* the short circuit is tripped out the system and system voltages increase instantaneously following the hydraulic generator dynamic. Because DFIG converters inject active and reactive power during the fault until the wind farm trip out all the electrical values are higher than in the strategy 1 case.

The last strategy start with the rotor side converter (RSC) disconnection from the rotor while the crowbar resistance is connected to the rotor winding in point *a* during 100 ms (until point *c*) limiting rotor current during this time interval. Control switch to voltage control mode is done in point *a* saturating the PI controller in the RSC and inject more reactive power when RSC is reconnected to the rotor. In point *c* the crowbar resistance is disconnected and RSC is reconnected to the rotor to supply reactive power to the system. Bus voltage increase to 0,23 PU, fault clearance occurs in point *d* and wind farm voltage increase quickly above 0,9 PU and become stable until point *e* when the control operation mode is switching back to reactive power control as shown in Figure 6.11.

Figure 6.13 – Wind farm active power response to a solid short circuit at bus 8.

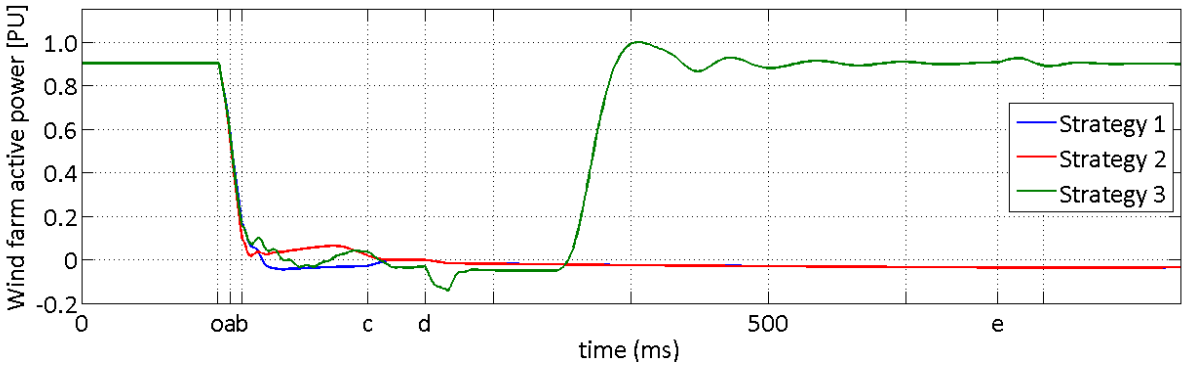

Figure 6.14 – Wind farm reactive power response to a solid short circuit at bus 8.

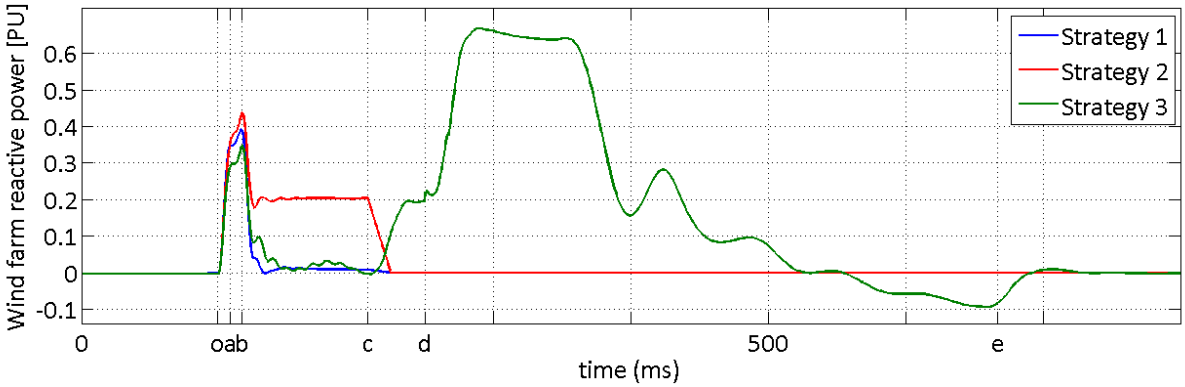

Wind farm current decreases when the crowbar resistance is connected, the opposite is also saw the increases when it is disconnected because the reactive power injection. After the fault clearance the wind farm current oscillates, suffering a decrease followed by a suddenly increase to re-establish the supplied active power (Figure 6.12). Wind farm active power diminishes to almost 0 PU when crowbar is operating and it re-establishes itself when reactive power injection decreases after fault clearance (Figure 6.13). Reactive power injection by wind farm begins after crowbar operation as shown in Figure 6.14, this injection is necessary to reestablish the bus voltage during and after the fault to fulfill the grid codes (see chapter 4). In point e the electrical values return to their pre-fault

values after a transient period with soft oscillations, during and after the fault, when wind farm reactive power is close to 0 PU the switch to reactive power control mode is done causing a transient disturbance in the wind farm electrical parameters.

Figure 6.15 summarizes the response of the three strategies of the DFIG with unity power factor to some electrical disturbances on the network. It seems that the control mode change to voltage control improves the generator performance to large voltage disturbance, such voltage sag and swell. To improve the DFIG performance in presence of severe faults on the systems, the use of crowbar resistance and DC chopper is mandatory.

Figure 6.15 – Response of DFIG with unity power factor in presence of different disturbances on the grid.

Control strategy		Strategy 1	Strategy 2	Strategy 3
Disturbances in the network	Voltage swell	●	○	○
	Voltage sag	●	○	○
	Short-circuit	●	●	○

● Base ○ Improve

6.2 VOLTAGE SAGS

Unbalanced short-circuits on transmission systems, motors starting, lightning, sudden load changes and transformers energizing could be reasons for happening voltage sags. So voltage sags can appear with relative frequency. Wind farms presence may affect the system behavior when there are voltage sags on the grid [49]. For this reason, the system behavior during a voltage sag to 50% residual voltage and duration of 250 ms in the IEEE 9 bus system (the voltage sag amplitude considered is the voltage fallen value) was studied in this work. Same wind penetration levels used in section 5.2 are considered in this section. Wind farms in the bus 2 with following features are used:

- DFIG with reactive power control using generators with unity power factor (strategy 1);
- DFIG with voltage control using generators with output voltage 1,0253 PU;
- and SCIG with capacitor banks of one third of rated value.

6.2.1 **30% of wind power penetration**

Simulations were performed and transient disturbances occur in presence of any type of generator. The dynamic responses of wind farm voltage, current, active and reactive powers are presented in Figure 6.16, Figure 6.17, Figure 6.18 and Figure 6.19 respectively, for the three generator technologies. The active power generated by the DFIG with unity power factor reduces its value slowly while the bus voltage is above 0,7 PU, below this value the active power falls to 0 because the wind farm trip. In case of DFIG with voltage control the wind farm active power falls to 0 during the sag because the reactive power priority in the control system. Active power supplied by the SCIG decreases slowly during the sag as well as the voltage. When voltage sag ends the wind farm active power is recovery with oscillatory transient following the hydraulic generator behavior.

Figure 6.16 – Wind farm voltage response to 50% sag applied at bus 1 for 30% of wind power penetration.

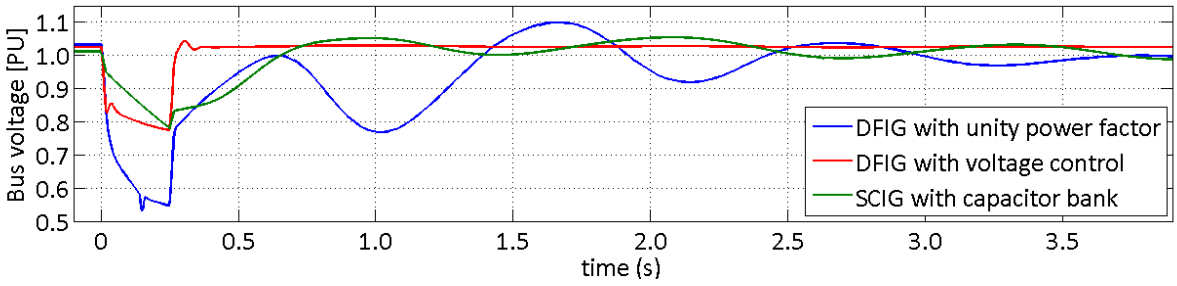

Wind farm installation benefits the bus voltage during the sag; it occurs because the wind farm supplies power, reducing the power flow from swing bar. DFIG with unity power factor is tripped out by the undervoltage protection when voltage is below 0,7 PU, the minimum value during the sag is 0,55 PU and then the wind farm voltage is reestablished following the dynamic imposed by hydraulic generator in around 5 s. For the DFIG with voltage control the wind farm voltage is reestablished in 200 ms to its set value (1,0253 PU) when the sag ends; the minimum value during the disturbance is 0,775 PU. SCIG with capacitor bank presents a slow voltage drop during the sag because capacitors do not allow instantaneous voltage changes, as the same way when the sag ends the voltage recovery is slow too.

Wind farm current for the DIFG with unity power factor case increases its value until the wind farm is tripped out and wind farm current fall down 0. For the case of DFIG with voltage control the current is lower during the sag than before the disturbance because wind turbines do not generate active power but inject reactive power to maintain the highest possible voltage value in this time interval. SCIG with capacitor bank presents a high increase in current at the beginning of the sag and then the current value decreases until sag ends. After disturbance clearance the wind farm current have a peak value again and returns to the pre-sag value in around 8 seconds.

Figure 6.17 – Wind farm current response to 50% sag applied at bus 1 for 30% of wind power penetration.

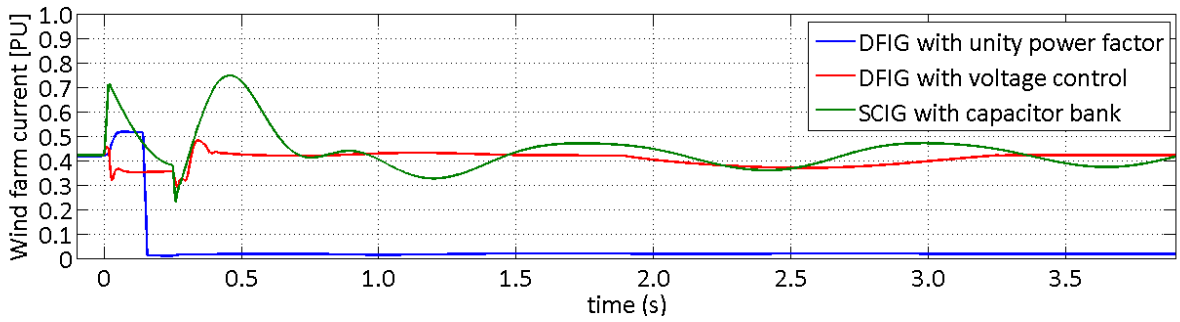

Figure 6.18 – Wind farm active power response to 50% sag applied at bus 1 for 30% of wind power penetration.

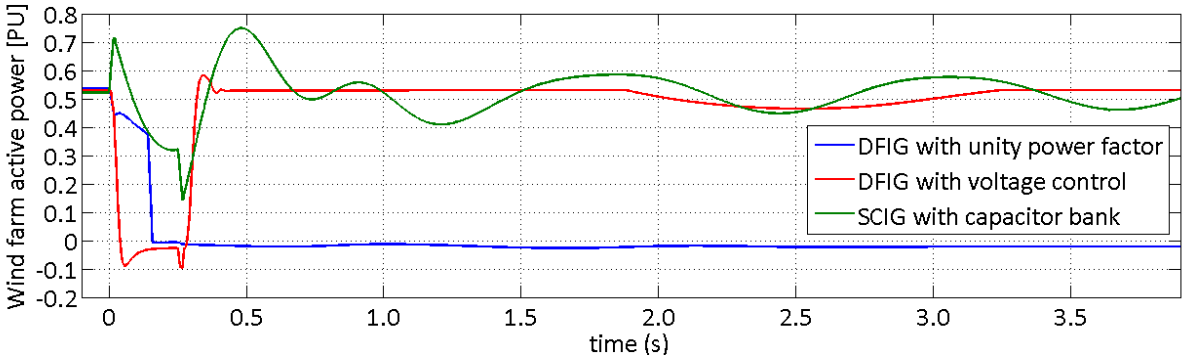

The active power generated by the DFIG with unity power factor reduces its value slowly while the bus voltage is above 0,7 PU, below this value the active power falls to 0 because the wind farm trip. In case of DFIG with voltage control the wind farm active power falls to 0 during the sag because the reactive power priority in the control system. Active power supplied by the SCIG decreases slowly during the sag as well as the voltage. When voltage sag ends the wind farm active power is recovery with oscillatory transient following the hydraulic generator behavior.

DFIG with unity power factor is unable to inject reactive power and therefore during sag voltages this parameter just has transient disturbances at the beginning of the sag and in the end, particularly in this situation the generator is tripped out and there is the transient effect at the beginning only. In case of DFIG with voltage control, the generator injects reactive power trying to maintain the voltage value the higher than possible during the disturbance. When voltage sag ends there is a transient effect and the reactive power value returns to its pre-sag value in around 5 seconds. The capacitor bank of the SCIG injects reactive power during the sag but at the same time the generator consumes reactive power reducing the injected reactive power to the system. After the sag the SCIG consumes reactive power and slowly return to its pre-sag value.

Figure 6.19 – Wind farm reactive power response to 50% sag at bus 1 for 30% of wind power penetration.

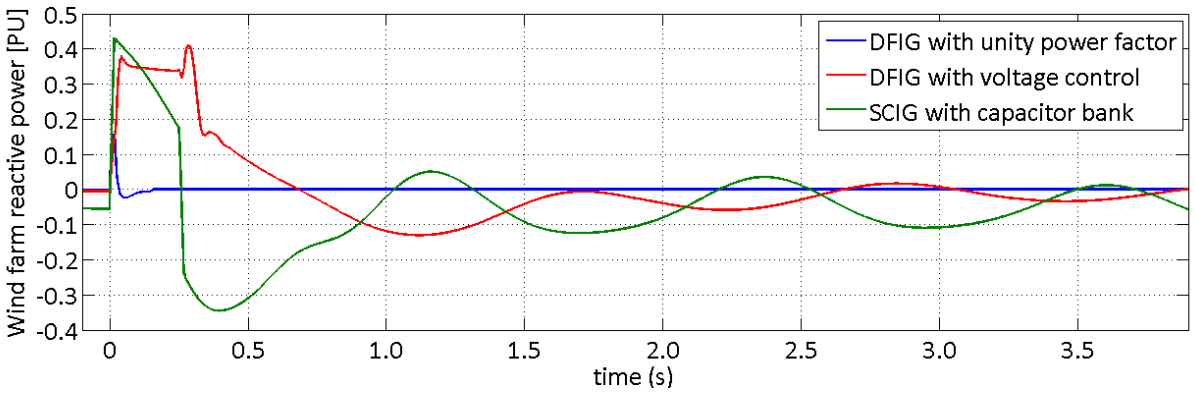

6.2.2 **Wind power penetration level influence**

Simulations were performed considering a 50% voltage sag at swing bus with 50%, 70% and 90% of wind power penetration in the system with the three generator technologies. The dynamic responses of the wind farm electrical parameters (bus 2) have similar behavior that in the 30% case for the three technologies. The wind farm voltage response to the disturbance for all the wind penetration levels by the DFIGs with unity power factor are showed in Figure 6.20.

Figure 6.20 – Wind farm voltage response to 50% sag at bus 1 in presence of DFIG with unity power factor.

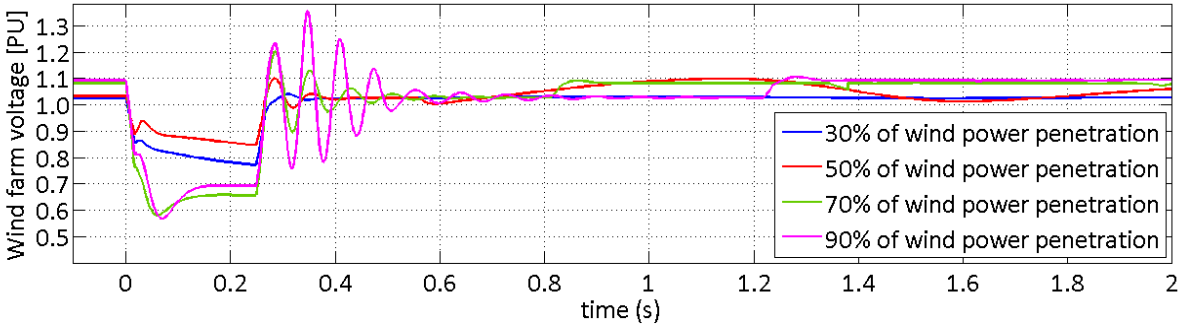

Considering the wind farm disconnection when DFIG with unity power factor presents terminal voltages below 0,7 PU for all the wind penetration levels, the strategy 2 of DFIG with unity power factor (see section 6.1) was used for this study. DFIG switches from unity power factor to voltage control when wind farm voltage is below 0,9 PU. For 30% and 50% of wind penetration, the wind farm voltage reduces its value above 0.8 PU and the response pos-sag has underdamped behavior returning to the unity power factor control mode when the reactive power injected by the DFIG is close to 0. In cases of 70% and 90% of wind penetration the wind farm voltage gets values below 0,7 PU because the generation deficit additional to wind power. When sag ends the voltage recovers its pre-sag value after oscillatory behavior. When higher penetration levels are presented into the system there are higher amplitude values in the oscillatory response of the generators and requires long time to DFIGs switch back to the unity power factor control.

The wind farm voltage response to the disturbance for all the wind penetration levels by the DFIGs with voltage control are showed in Figure 6.21. For all wind penetration levels there are an underdamped oscillatory response in wind farm voltage. The higher the wind penetration level, the longer the time to stabilize and the greater the oscillations amplitude of the bus voltage are. The voltage behavior is the same of the previous case during the sag because both wind farms have DFIGs with voltage control during the disturbance.

Figure 6.21 – Wind farm voltage response to 50% sag at bus 1 in presence of DFIG with voltage control.

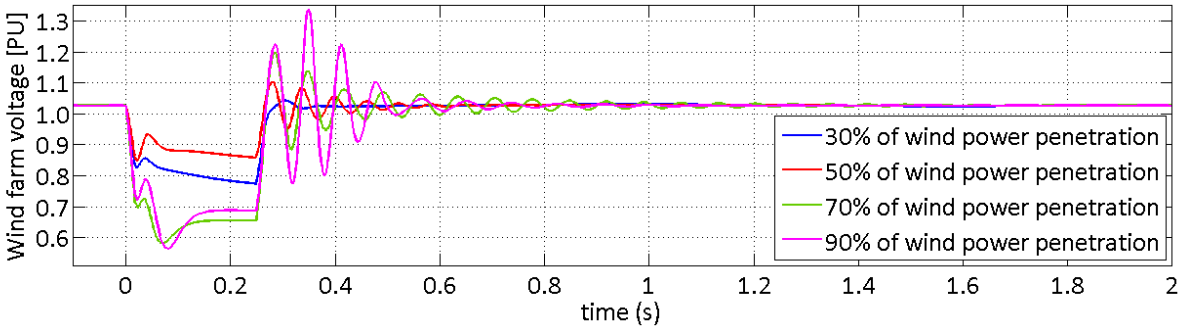

The wind farm voltage response to the disturbance for all the wind penetration levels by the SCIGs with capacitor banks are showed in Figure 6.22.

Figure 6.22 – Wind farm voltage response to 50% sag applied at bus 1 in presence of SCIG with capacitor bank.

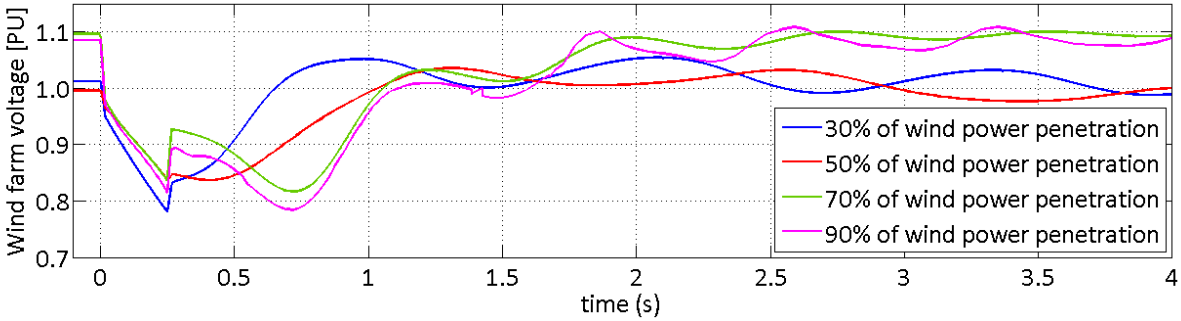

During the voltage sag the terminal voltage of the wind farm is reduced slowly above 0,8 PU for all the wind penetration levels, it because the bank capacitor does not allow fast changes in voltages and inject reactive power to the system. After the sag ends there are transient disturbances for the four penetration levels stabilizing in around 8 seconds. For all the penetration levels the wind farm voltage recovers its pre-sag value. The higher the wind penetration level, the longer the time to stabilize the bus voltage is.

6.3 SHORT-CIRCUIT

Installation of alternating current generators can increase the values of the short-circuit currents, making necessary the adjustment of system protections. Furthermore, the relay settings must be readjusted to detect faults adequately. As wind turbines use generally induction generators, these increase the short-circuit level on the power systems. Wind farms presence will affect the system behavior when short-circuits happen in the network [49]. Also, several grid codes around the world demands low voltage ride through from wind farms [46]. For this reason, system behavior in presence of solid short-circuit at load B (bus 8) with duration of 150 ms in the IEEE 9 bus system was studied. Same wind penetration levels used in section 6.2 are considered. Wind farms in the bus 2 with the same features of section 6.2 are used.

6.3.1 **30% of wind power penetration**

Simulations were performed and transient disturbances occur in presence of any type of generator. The dynamic responses of wind farm voltage, current, active and reactive powers are presented in Figure 6.23, Figure 6.24, Figure 6.25 and Figure 6.26 respectively, for the three generator technologies.

Figure 6.23 – Wind farm voltage response to a short-circuit at bus 8 for 30% of wind power penetration.

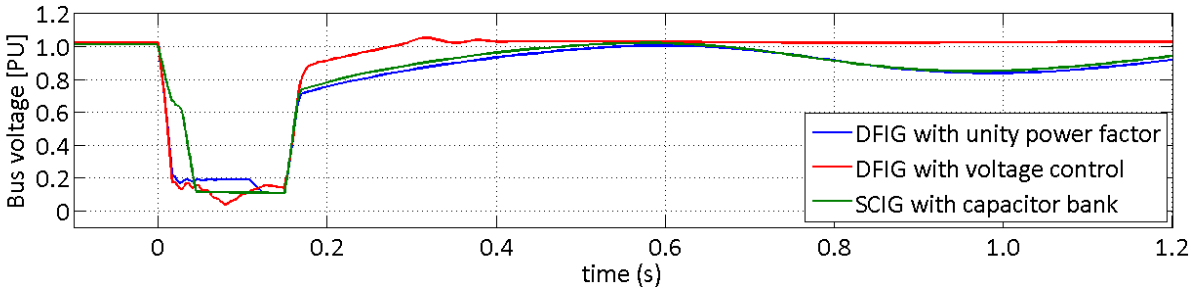

DFIG with unity power factor and SCIG with capacitor bank are tripped out the system by undervoltage and instantaneous over-current protection respectively. Bus 2 voltage follows the dynamic imposed by the hydraulic generator and is also reestablished a few seconds later because the other generators can provide enough apparent power to the system. In case of DFIG with voltage control the RSC is disconnected from the rotor circuit and the crowbar resistance is connected instead during 100 ms when the fault is detected. After this time crowbar resistance is disconnected and RSC is connected again to inject the maximum possible reactive power. The wind farm voltage is reestablished in about 250 ms to pre-fault value after fault clearance.

Figure 6.24 – Wind farm current response to a short-circuit at bus 8 for 30% of wind power penetration.

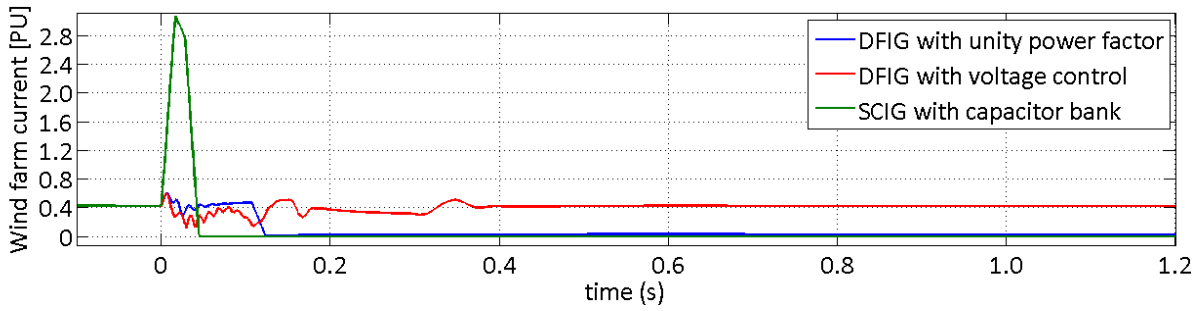

In cases of DFIG with unity power factor and SCIG with capacitor bank the wind farm current falls to 0 after the trip out of the generators, but in case of DFIG the current does not increase its value during the fault before the protection action while in the SCIG case the current increase dramatically its value due to the fast change in terminal voltage of the capacitor bank. For DFIG with voltage control the wind farm current (Figure 6.24) is limited by crowbar resistance presence first and then by the DC-chopper.

Figure 6.25 – Wind farm active power response to a short-circuit at bus 8 for 30% of wind power penetration.

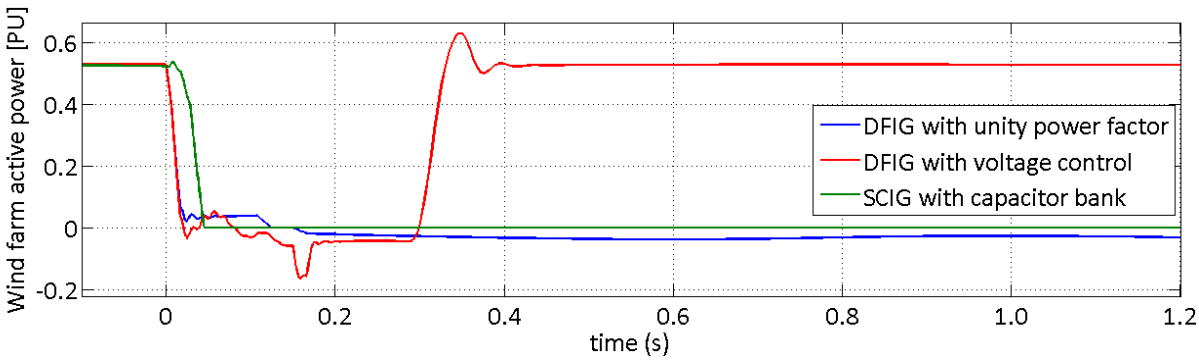

Figure 6.26 – Wind farm reactive power response to a short-circuit at bus 8 for 30% of wind power penetration.

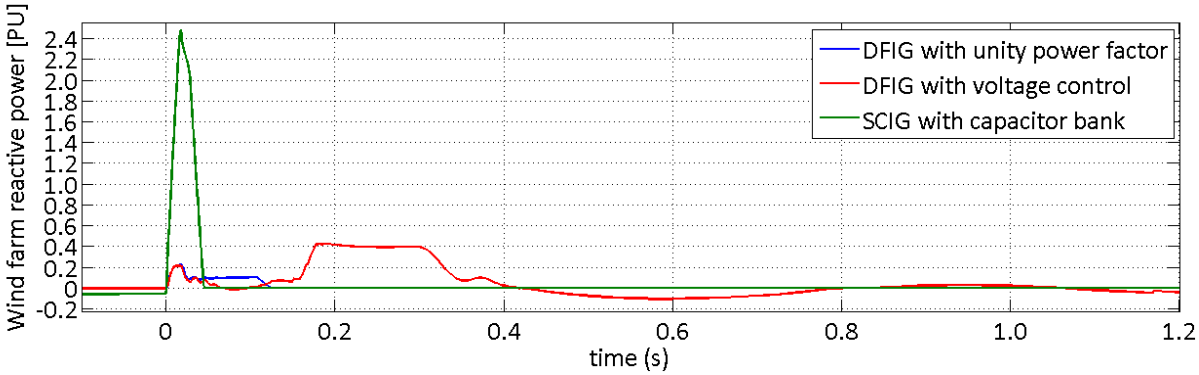

The active power supplied by the DFIG with unity power factor during the fault is reduced to 5% during the fault before this device is tripped out, then after fault clearance the shunt resistance of the wind farm consumes 5% of the rated active power. For DFIG with voltage control no active power is produced by the DFIG during the fault because the q axis current priority (operation mode) and even

there is active power consumption by the generator while the voltage is reestablished. When wind farm voltage is reestablished DFIG supplies active power again, recovering its pre-fault value with underdamped response. In case of SCIG with capacitor bank, the active power decreases its value together to the voltage before the wind farm is tripped out, after the trip the active power falls to 0.

DFIG with unity power factor injects 0,1 PU of reactive power during the fault despite its operation mode, when wind farm is tripped out the reactive power injected fall to 0. DFIG with voltage control does not inject reactive power during crowbar operation because the RSC is disconnected. After crowbar disconnection the generator injects reactive power to recover the voltage the fastest possible. When wind farm voltage is reestablished the wind farm reactive power recovers its pre-fault value. In case of SCIG with capacitor bank, the reactive power increases its injected value by the capacitor bank in response to the voltage before the wind farm is tripped out, after the trip reactive power falls to 0.

6.3.2 **Wind power penetration level influence**

Simulations were performed considering a solid short-circuit at load B (bus 8) with duration of 150 ms and with 50%, 70% and 90% of wind power penetration in the system with the three generator technologies. The dynamic responses of the wind farm electrical parameters (bus 2) have similar behavior that in the 30% case for the three technologies. The wind farm voltage response to the disturbance for all the wind penetration levels by the DFIGs with voltage control are showed in Figure 6.27.

Figure 6.27 – Wind farm voltage response to short-circuit at bus 8 in presence of DFIG with voltage control.

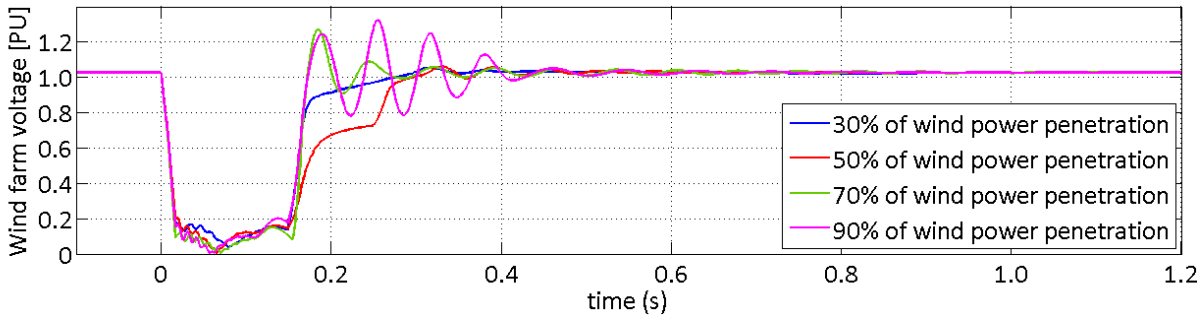

Considering the wind farm disconnection when DFIG with unity power factor presents terminal voltages below 0.7 PU for all the wind penetration levels, therefore, DFIG with unity power factor switches to DFIG with voltage control (see section 6.1) when a fault appears in the system and just this analysis is presented. During the fault wind farm voltage have the same behavior for all the penetration levels, it reduces its value below 0,2 PU. The difference in wind farm behavior for different wind penetration levels occurs after fault clearance. For 30% and 50% of wind penetration,

the wind farm voltage pos-fault has behavior similar to an overdamped response, recovering the pre-fault value in less than 270 ms for both penetration levels. In these cases the influence of the other generator devices is important, and for this reason the wind farm voltage increases its value after fault clearance faster in the case of 30% than in the case of 50% of penetration level.

In cases of 70% and 90% of wind penetration the wind farm voltage, after fault clearance, recovers its pre-fault value after oscillatory behavior of duration 450 ms. This behavior is presented because the exchange in active power and reactive power between the wind farm and the grid after fault clearance to get the steady-state. When higher penetration levels are presented into the system there are higher amplitude values in the oscillatory response of the generators. It due to the higher wind penetration level is, the stronger the impact in the system is. For SCIGs the wind farm is tripped out by overcurrent protection and with higher wind penetration level the tripping time is lower.

Figure 6.28 summarizes the response of the three wind turbines presented in sections 6.2 and 6.3 to some electrical disturbances on the network. It seems that DFIG with voltage control is able to maintain itself connected to the grid for all the electrical disturbances. Also it shows that the three generators keep connected to the grid in case of a large load connection on the grid. To improve the DFIG with unity power factor (strategy 1) the control mode change to voltage control improves the generator performance to large voltage disturbance, such voltage sag and swell. The increase of wind power penetration level led the SCIG with capacitor bank to the disconnection of the system.

Figure 6.28 – Response of the three generators in presence of different disturbances on the grid.

Technology		DFIG with p.f=1	DFIG with V cst	SCIG with capacitor bank
Disturbances in the network	Load shedding	disconnect	connected	disconnect
	Load connection	connected	connected	connected
	Voltage sag	disconnect	connected	connected
	Short circuit	disconnect	connected	disconnect
	Wind power penetration influence	> WP level need control mode switch	>WP level >transients	> WP level led to disconnection

6.4 SMALL-DISTURBANCE VOLTAGE STABILITY (PV AND VQ CURVES)

This is concerned with a system ability to control voltages following small disturbances as incremental changes in system loads. This form of stability is determined by the characteristics of load, continuous controls and discrete controls. This concept is useful to know the response to small system changes. The basic processes contributing to small-disturbance voltage instability are the steady-state nature. Therefore, static analysis may be used to determine stability margins, identify factors that influence the stability and examine several conditions and large number of scenarios [28].

The criterion for small-disturbance voltage stability is that bus voltage magnitude increases as the reactive power injection at the same bus increased. The system is unstable when one of the system bus voltage decreases as the reactive power injection at the bus increases. With generators installation into power system, especially near to the loads is expected to obtain a major voltage stability margin [73]. Nevertheless, the impact over this margin depends mainly of reactive power exchange between the grid and the generators [8], which can change depending of the technology and the generator control mode. Wind farms integration can improve the voltage stability increasing the stability margin with active and reactive power injection in different points.

Figure 6.29 shows the PV curves of the PCC for modified IEEE 9 bus system considering a 180 MVA wind farm at bus 2 with different wind power technologies. These curves were obtained by varying the active and reactive power of the loads and maintaining constant the control parameters in wind farms and neglecting the protections action.

Figure 6.29 – PV curves of a 180 MVA wind farm located at bus 2.

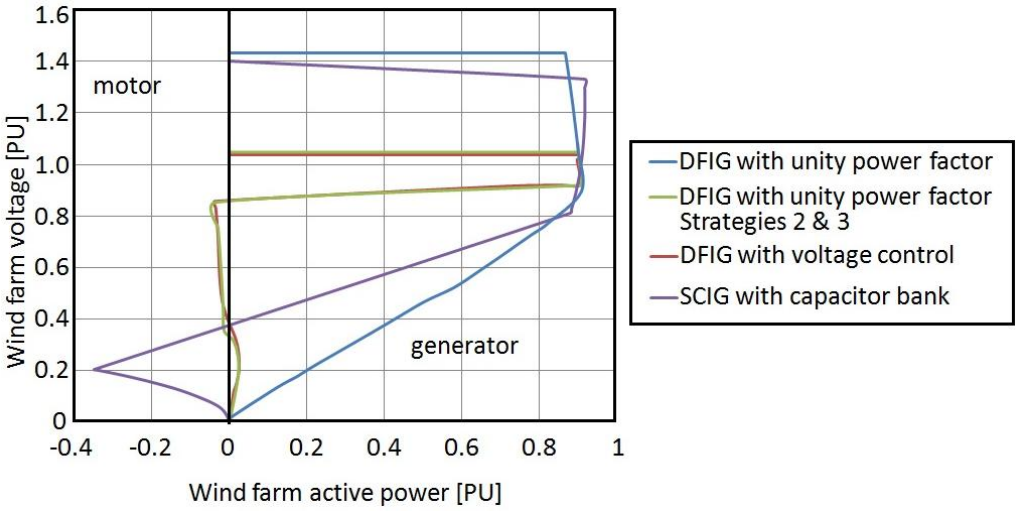

DFIG with unity power factor presents high voltages above 1,4 PU with active power generated lesser than 0,87 PU. It happens because the transmission lines are highly capacitive and

inject reactive power to the system. When these generators are supplying active power in values between 0,87 and 0,92 PU the PCC voltage reduces its value linearly from 1,43 to 0,9 PU. At this last point there is a knee point where the voltage collapse happens and the system turns unstable. DFIG with voltage control and strategies 2 and 3 of DFIG with unity power factor (see section 6.1) have the same PV curve. The PCC bus voltage takes a value of 1,025 PU (set value) while the wind farm active power is less than 0,9 PU. After the active power value exceeds 0,9 PU until 0,91 PU, the voltage reduces its value to 0,92 PU. These generators have the ability to maintain the voltage value high by reactive power injection and without active power supply. When PCC voltage is below 0,85 PU the knee point appears and the voltage collapse happens and the system turns unstable.

In case of wind farm based on SCIGs with capacitor banks the PCC voltage is above 1,32 PU with low load while supplies less power than 0,93 PU. Because the PCC voltage value this operation point is not desired in electrical power systems. Since this point, the PCC voltage and the active power generated reduce their value to 0,81 and 0,88 PU respectively, with the increase of the load. At this last point there is a knee point where the voltage collapse happens and the system turns unstable.

Considering that reactive power injection by the generators to the network influences the voltage stability of the system, the Figure 6.30 shows the QV curves to assess their influences in this topic. These curves were obtained by varying the active and reactive power of the loads and maintaining constant the control parameters in wind farms and neglecting the protections action.

Figure 6.30 – QV curves of a 180 MVA wind farm located at bus 2.

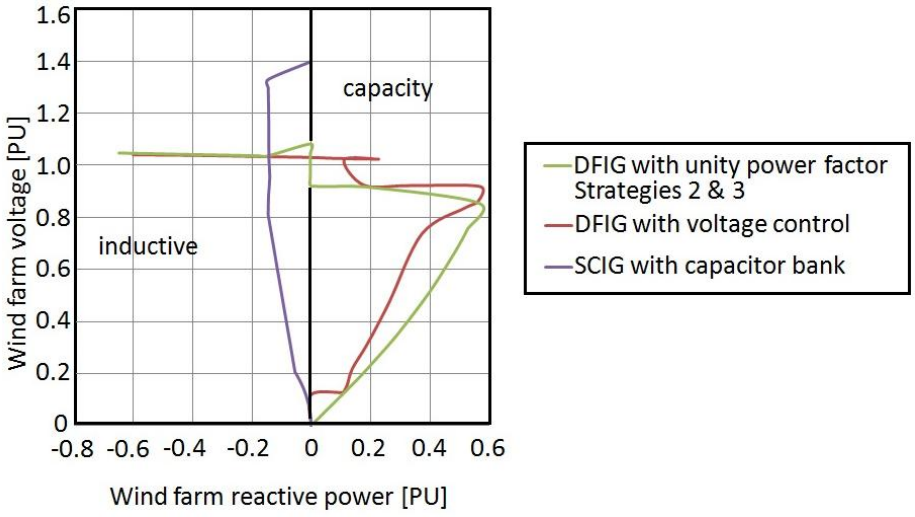

DFIG with unity power factor does not inject reactive power in any situation and for this reason is not appearing its curve on the figure. DFIG with unity power factor using the strategies 2 and 3 absorb reactive power to maintain the PCC voltage in the set value (1,025 PU). When no reactive

power absorption is necessary to establish a PCC voltage between 0,9 and 1,1 PU the reactive power of the wind turbines is 0. When PCC voltage is below 0,92 PU the wind farm injects reactive power with a nose curve which reaches a maximum value of 0,58 PU of reactive power and a voltage value of 0,84 PU. At this last point there is a knee point where the voltage collapse happens and the system turns unstable.

For DFIG with voltage control the PCC voltage maintains almost constant its value with the increase of the load demanded. In case of load is low the generators absorb reactive power to maintain the voltage close to set value (1,025 PU). With the increasing load the DFIG injects reactive power until the point where the DFIG just generates reactive power and reduces the PCC voltage below 0,92 PU. After the previous point the turbine injects reactive power keeping PCC voltage constant in 0,91 PU until reach a maximum value of 0,58 PU. At this last point there is a knee point where the voltage collapse happens and the system turns unstable. Wind farm with SCIGs presents the worst performance in this analysis because it consumes reactive power for all PCC voltage value. The voltage collapse happens when PCC voltage is below 0,8 PU and consuming more than 0,13 PU of reactive power.

The load demanded and PCC voltage curves for is presented in Figure 6.31. In this figure can be seen that DFIGs with voltage control can supply greater loads without loose the voltage stability. Loads close to 350% of the rated value represent PCC voltage above 0,8 PU. DFIGs with unity power factor and using the strategies 2 and 3 are the second best technology because can support the PCC voltage above 0,8 with a few more than twice the rated load. For the other two technologies the PCC voltage is below 0,8 PU with 190% and 150% for DFIG with unity power factor and SCIG with capacitor bank respectively.

Figure 6.31 – Load demanded vs. PCC voltages curves of a 180 MVA wind farm located at bus 2.

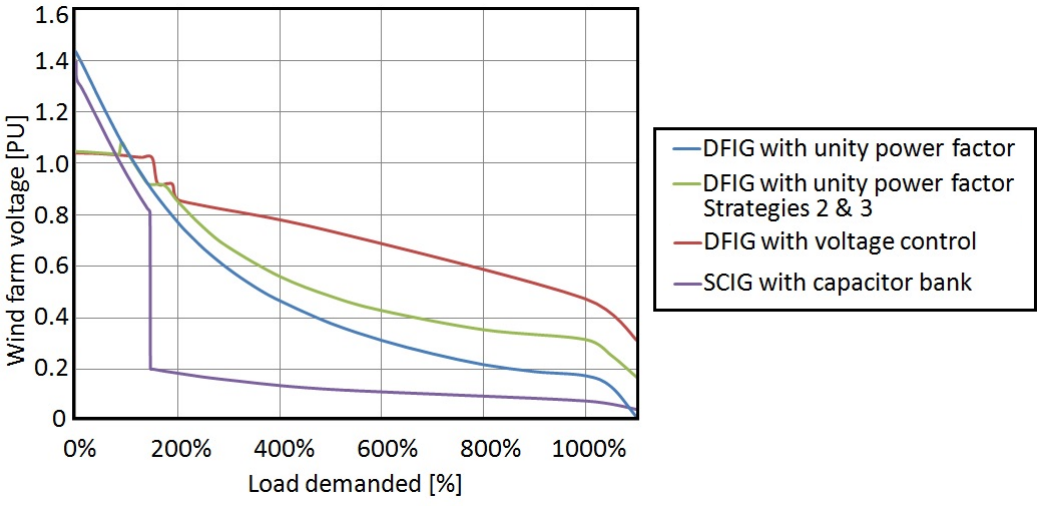

6.5 CONCLUSIONS

Voltage sags and swells in IEEE 9 bus system

The different wind penetration levels in this analysis were found by variations of load percentage and the power delivered by the wind farm. For large disturbances the SCIGs are no able to keep connected to the grid, it may happen because overcurrents or undervoltages that endangering the turbine integrity. For this reason the utilization of SCIGs for large scale wind farms is not convenient because their disconnection from the grid will affect the voltage stability.

DFIGs with unity power factor are not able to inject or absorb reactive power during disturbances in the electrical system. Those unities may be disconnected from the grid depending on the disturbance size. The proposal of changing the control mode to voltage control in cases of large disturbances may improve the voltage stability during disturbances as voltage sags and swells.

In the analysis performed of voltage sags was verified that, for wind penetration levels lower than 30% the SCIGs are able to keep connected during voltage sags (maximum amplitude of 50%) following the dynamics imposed for other generating devices (hydraulic generator in this case). For higher penetration levels the SCIGs are disconnected by the overcurrent protection and they are not able to give voltage support during the disturbance.

DFIGs with unity power factor are not able to keep connected during the sag for any wind penetration level because the low voltages. DFIGs with voltage control are able to give voltage support, injecting or absorbing reactive power during voltage sags and swells. In general, for higher wind power penetration levels, the variations of voltage levels and the reactive power exchanges are higher.

Short-circuits in IEEE 9 bus system

In short circuit analysis just the DFIG with crowbar resistance and DC-chopper are able to keep operating and ride-through the low voltage without endangering the turbine safety. In this work, just the case of DFIG with voltage control has this ability and, by consequence, only this technology is able to stay connected during severe short circuits.

SCIG unities are tripped out of the system by the overcurrent protection. The current value at the PCC increases dramatically during instantaneous changes in voltage when the capacitor banks also inject reactive power at the beginning of the disturbance.

DIFGs with unity power factor are disconnected by the undervoltage protection in case of this disturbance. For DFIGs with voltage control, the difference in terminal voltage is related to the

penetration levels after the fault clearance. Higher wind penetration levels increase the peak values of voltages and currents.

Small-disturbance voltage stability (PV and VQ curves)

The assessment of voltage stability margins were performed in this work for the IEEE 9 bus transmission system. The capability of injection or absorption of reactive power by the wind turbines determines the voltage stability margins. DFIGs with voltage control present higher voltage stability margins than SCIGs with capacitor banks and DFIGs with unity power factor. It is due to the reactive power absorption when the load is low of the rated value and the reactive power injection when the load has higher values than the nominal ones.

DFIGs with unity power factor can be switched to voltage control to supply reactive power when voltages values are out of the allowed limits and, therefore to increase the voltage stability margins.

7 WIND POWER INTEGRATION IN IEEE 9 BUS SYSTEM

Wind power supply are only a small fraction of the total power demand (≈3% of the worldwide demand), but it can reach significant penetration values in some regions. Countries such as Denmark, Ireland, Northern Germany, Portugal, Spain and Texas, the wind power has a significant share in electricity demand. In 2009, wind energy had a 35% of penetration in the German province of Schleswig-Holstein [44], [74]. Denmark presented a 30% of wind penetration in 2012, and Portugal and Spain a wind power penetration nearby to 20% [3]. For further details, see also Table 7.1.

Table 7.1 – Examples of wind power penetration levels.

Country or region	Installed wind capacity (MW)	Total installed power capacity (MW)	Average annual penetration level (%)	Peak penetration level (%)
Western Denmark:	2.720	7.000	~22,5	>120
Thy Mors	~40	--	>50	~300
Germany:	26.000	115.000	~7,5	--
Schleswig Holstein	2.858	--	~35	>100
Spain:	19.390	94.600	~14	>50
Navarra	961	--	~70	>120
Island systems:				
Ireland	1.425	8.500	~10,5	>50
Denham, Australia	0,69	2,41	~50	~70

Source: Wind Power in power Systems [44]

Wind power will introduce more uncertainties in power system operation because it is variable and partially unpredictable. In this sense, the integration of high wind power penetration levels within power systems, specially designed to work with large-scale synchronous generators, will require new approaches and solutions. To meet this challenge, more flexibility in power systems is mandatory. That flexibility is dependent either on the amount of wind power in the system and also the flexibility of the electrical system itself [6]. The examples mentioned above, show that the integration of significant penetration levels of wind power is possible, and could not require an extensive redesign of the existing power system. Nevertheless, systems with very high penetration levels in Denmark, Germany, Portugal and Spain are connected to a large and strongly interconnected power system.

Considering the consequences entailed by a high wind power penetration in power systems, studies have been conducted in several countries both in academic and industrial ambit. For example, the IEA countries are coordinating research activities for wind power implementation in these countries. One of the tasks in development is the number 25: "Power Systems with Large Amounts of

Wind Power". The main objective of this task is to provide information to facilitate the highest economically feasible wind energy penetration within the power systems worldwide [3], [6], [44].

7.1 METHODOLOGY PROPOSED

In this work a different strategy for wind farm connection in power systems is proposed. The aim is to integrate a determined wind power quantity in a specific bus (assuming that the assessment of wind resources in the area is adequate) and just is necessary fulfill the grid code, thus determining the most convenient option to install (may be a mix of technologies). Initially, in grid codes, wind turbines disconnection was allowed/forced in case of disturbances on the grid; no contribution to power system stability was required. However, with the increase of wind power penetration levels in power systems, different problems have been experienced in some countries such as China, Denmark, and USA.

In the first half of 2011, there were four cases of massive wind farm disconnection in Gansu province and Hebei's city of Zhangjiakou (China), which resulted in electricity output loss of 4.195 MW [6], [75]-[77]. Another example, happened in Denmark, on January 8, 2005 where a severe storm with high wind speeds caused the loss of around 3.000 MW in the wind power production over a period of 6 hours, which was 60-80% of the Danish total demand at that time [9], [48]. Moreover, the opposite situation happened in Texas in February 2008 when a cold front moved over Texas causing wind power reduction from 1.700 MW to 300 MW for three hours. Although no power outages were reported, the customers needed to be disconnected on a rotating basis, leading to lost revenues for the operators and customer inconvenience [48], [78].

By disturbances of these kinds the grid codes have reevaluated their requirements and the immediate disconnection of wind generators is no more admitted and therefore voltage stability support is in some cases required (see chapter 4). Currently, grid codes include several technical requirements to guarantee the system security and, although the modern wind turbines can fulfill these requirements, sometimes, they are not even necessary to the system stability, just resulting in additional costs in manufacture. Wind turbines with DFIGs to ride through a fault increases their total costs by up to 5% [44]. Similarly, stringent requirements do not allow the integration of low cost technologies based on SCIG without additional investments in dynamic reactive power support devices like static reactive power compensators (SVC) or static synchronous compensators (STATCOM) [34], [79].

By this reason a methodology to decide the technologies to be installed in a certain wind farm fulfilling the necessary requirements could be interesting. In this work some requirements to be

fulfilled at point of common coupling (PCC) by new wind turbines to be installed are established. Those requirements are the following for transmission systems:

- PCC voltage limits ($0{,}9\ PU \leq V_{PCC} \leq 1{,}1$);
- reactive power control and voltage regulation (Danish system);
- low voltage ride through (Danish system);
- high voltage ride through (Danish system);
- and reactive power support during voltage disturbances.

for the distribution systems there are:

- PCC voltage limits ($0{,}95\ PU \leq V_{PCC} \leq 1{,}05$);
- low voltage ride through ($V_{PCC} = 0{,}7\ PU$ during 250 ms);
- and reactive power support during minor voltage disturbances.

The strategy proposed in this work is based on the adaptive strategy presented in [79] to obtain technically justified fault ride-through requirements for wind turbines. The proposed strategy considers a determined turbine number and installed capacity. It is also assumed that studies of wind, location and resources already were performed and validated. A certain number of wind turbine technologies is regarded and ranked by complexity of the technology or control, e.g. SCIGs are less complex and cheaper than DFIGs and for these reason SCIGs are lower rank than DFIGs.

The main idea in the proposed strategy is to connect one turbine in each iteration of the algorithm iteration until complete the total capacity to be installed, *i.e*. one turbine is connected on the system in one iteration and there are so many algorithm iterations as total turbines to be installed. For each iteration, the grid performance and the compliance of the grid code requirements are assessed by simulating. Simulations with each generator technology are performed to choose the generator to be connected, for each iteration, from lowest to highest rank of hierarchy. It means that the first simulations with SCIG are performed and then, if necessary, the simulations with DFIGs are after that further performed.

The step to the next iteration is done when the technology assessment meets the grid codes, choosing this technology for the turbine. If the grid code requirements are fulfilled by a wind turbine technology, this one is selected to be connected in the wind farm and the step to the next iteration is done. If none of the technologies meet the grid code requirements, the most ranked technology (the most complex) is chosen to form a basis to ensure that, at least, with increasing number of turbines the grid codes are met. It is clear that simulations of the most severe contingencies on the system are those ones that must be evaluated. The algorithm finishes when the installed capacity is equal to the planned

capacity to be installed. Figure 7.1 shows the flow chart of the proposed methodology to select the generator for each turbine in a wind farm.

Figure 7.1 – Flow chart of wind farm installation in a determined bus.

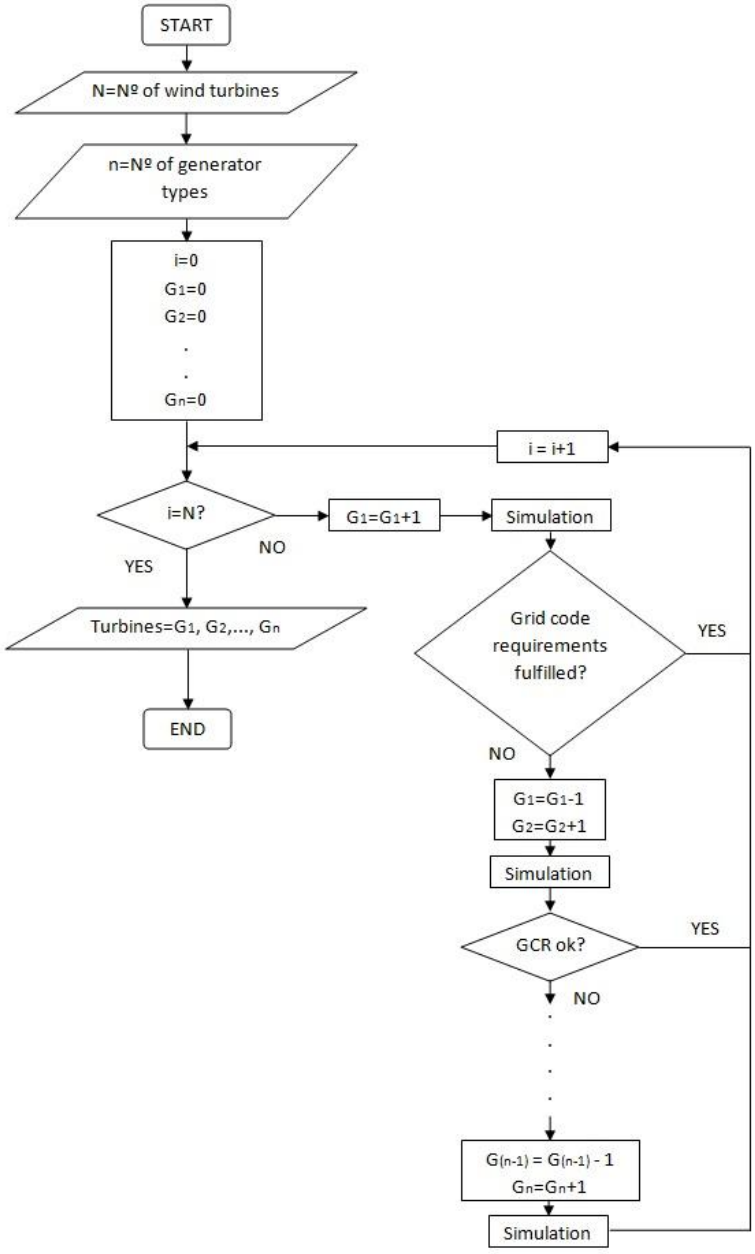

Source: Author

An example is presented below to better understand the methodology. A wind farm with three turbines is considered to be connected in a determined system. SCIG and DFIG are the technologies regarded to be installed in the wind farm; SCIGs are lower rank than DFIGs. As there are three turbines in the wind farm, three iterations are needed to determine the turbines connected in the farm.

In the **first iteration** there is no wind turbines selected and the grid codes requirements are not fulfilled. First the wind turbine with the lowest hierarchy, SCIG for this case, is considered to be connected in the wind farm and the grid code requirements assessment is performed with this. In this example is considered that the grid code requirements are not fulfilled and, therefore, the follow wind technology in the ranking (DFIG) is considered to perform the grid code requirements evaluation. For this technology the requirements are not fulfilled neither, and as DFIG has the highest hierarchy, this is selected to the wind turbine to be connected in the first iteration and the step to the second iteration is done.

For the **second iteration** the wind turbine with the lowest hierarchy (SCIG) is considered to be connected in the wind farm in first place. The grid code requirements assessment is performed for this mixture and, for this example is considered that the grid code requirements are fulfilled. This technology is selected for the wind turbine to be connected in the second iteration and the step to the third iteration is done.

For the **third iteration** (the last one) the wind turbine with the lowest hierarchy (SCIG) is considered to be connected in the wind farm. The grid code requirements assessment is performed for this mixture and, for this example is considered that the grid code requirements are fulfilled. This technology is selected for the last wind turbine to be connected the algorithm is concluded.

7.2 WIND FARM INTEGRATION IN TRANSMISSION SYSTEM

In this analysis the modified IEEE 9 bus system presented in Figure 5.1 is used and, wherefore it is a transmission system just those grid code criteria will be considered in the study. To assess the grid code requirements some simulation studies are carried out: a solid short-circuit at synchronous generator (bus 3) with duration of 300 ms is simulated to evaluate LVRT and reactive power support requirements (the most critical fault); a 40% voltage swell at bus 1 with one second of duration to assess the HVRT requirement; steady-state analysis to evaluate voltage and power factor criteria. In this study five generator types are used to implement the proposed integration strategy, from highest to lowest hierarchy as follow:

1. DFIG with voltage control, crowbar and DC chopper;
2. DFIG with unity power factor, change to voltage control mode, crowbar and DC chopper;
3. DFIG with unity power factor and change to voltage control mode;
4. DFIG with unity power factor;
5. and SCIG with capacitor bank.

Analyses of the transmission system in absence of wind farms in steady-state and dynamic analysis are necessary to determine the benefits of installing a wind farm on the system. For this system in absence of wind farms the other generators are able to supply the active and reactive power needed to keep all the buses voltages within the limits and to recover the system voltages in case of disturbances. Table 7.2 presents the voltages of all buses in absence of wind farms in steady-state before and after a solid short-circuit at bus 8 (load B) without generation trip out.

Table 7.2 – System voltages in absence of wind farms.

Bus number	1	3	4	5	6	7	8	9
Bus voltage	0,9673	1,0246	0,9671	0,9488	0,9736	0,9873	0,9898	1,024

The output power values of the system generator devices are found in Table 7.3. The generator located at swing bar supplies more than 70% of the active power demanded by the system, therefore the system is very vulnerable to the output of this generator and it might be exposed to blackout in case of swing bus failure.

Table 7.3 – Output power values of the system generator devices in absence of wind farms.

Power generated			
Swing bar		Hydraulic generator	
Active power (MW)	Reactive power (MVAr)	Active power (MW)	Reactive power (MVAr)
212,65	7,28	85,06	28,68

There are faults in the system that leads to a tripping out of the hydraulic generator. In order to avoid these problems, the analysis of those disturbances is relevant. While the hydraulic generator and the swing bus are supplying energy to the system, the bus voltages will work within the allowed limits. But in case of hydraulic generator disconnection all the bus will be below the limit value of 0,9 PU and system will be in risk of blackout. Table 7.4 shows the buses voltages in absence of wind farms in steady-state before and after a solid fault at bus 8 (load B) considering the trip out of the hydraulic generator.

Table 7.4 – System voltages in absence of wind farms.

Bus number		1	3	4	5	6	7	8	9
Bus voltage	Before the fault	0,9673	1,0246	0,9671	0,9488	0,9736	0,9873	0,9898	1,024
	After the fault	0,8245	0,7784	0,7951	0,7649	0,7761	0,7706	0,7644	0,7784

The buses voltages reduce their values drastically and swing bar generation is reduced too because the generation loss. The swing bar cannot supply enough power to the system and to keep the buses voltages above 0,9 PU, despite this generator increases the reactive power injected and reduces the active power supplied. The output power values of the generator devices are found in Table 7.5.

Table 7.5 – Output power values of the system generator devices in absence of wind farms.

	Power generated			
	Swing bar		Hydraulic generator	
	Active power (MW)	Reactive power (MVAr)	Active power (MW)	Reactive power (MVAr)
Before the fault	212,65	7,28	85,06	28,68
After the fault	289,72	51,54	0	0

When a fault occurs on the system and the hydraulic generator is not tripped out, the voltages at all the buses recover their pre-fault (see Table 7.2) in less than 4 seconds with underdamped responses. In the opposite case, the hydraulic generator is tripped out and the buses voltages are below the limit values of the system and active and reactive power of the loads are lower too. When the fault is cleared the active power generated in the swing bus falls by more than 20 MW and reactive power injected increases its value over 40 MVAr (see Table 7.5). Voltage at the connection point of a future wind farm for that two scenarios represented above is shown in Figure 7.2. When hydraulic generator is disconnected, the PCC voltage is below the limit required by the Danish operator for generating plants. In the other case the requirements demanded are reached and no additional generation would be required.

Figure 7.2 – PCC voltage response to a solid fault at bus 8 in absence of wind farms.

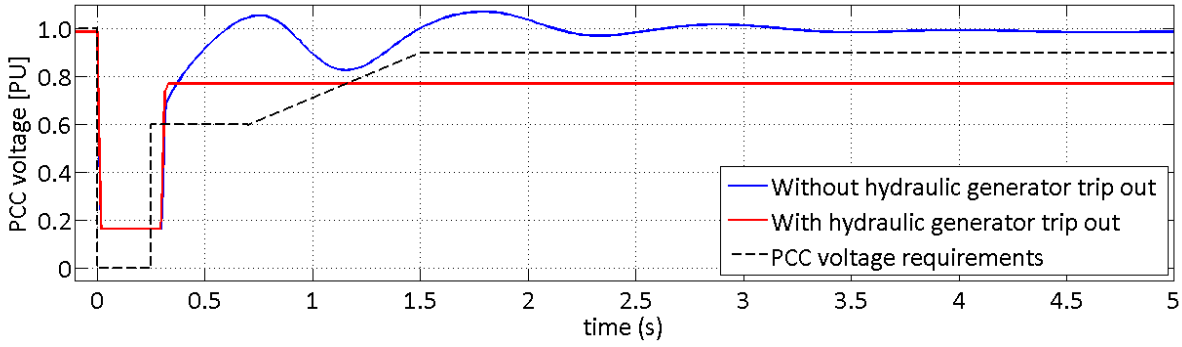

Solely wind turbines with 1,5 MW of capacity are considered in this work. Furthermore, the total installed capacity of wind power is 165 MW (110 turbines). The most severe disturbance contemplated was a solid fault in hydraulic generator terminals leading to its disconnection. Applying the proposed methodology in this work, the minimum wind turbines number to guarantee the

compliance of LVRT criteria was found, being 65 with 64 DFIG with voltage control and the other is DFIG with unity power factor and switch to voltage control during disturbances. However, in this case the other buses voltages are below the system limit (0,9 PU) endangering the system elements security as shown in Table 7.6.

Table 7.6 – System voltages with minimum wind turbines number.

Bus number		1	2	3	4	5	6	7	8	9
Bus voltage	Before the fault	1,0372	1,0252	1,0261	1,0242	0,998	1,011	1,0247	1,0128	1,0263
	After the fault	0,8141	0,9011	0,8511	0,8109	0,8119	0,8097	0,8865	0,861	0,8512

The wind farm gives reactive power support after the fault as observed in Table 7.7. The wind farm active power falls after the disturbance close to 0 and this inject reactive power to raise the PCC voltage to 0,9 PU. The generator located at the swing bar supplies the total active power to the system, but it is not enough to maintain the buses voltages in the secure limits of operation. Figure 7.3 shows wind farm voltage at PCC with the minimum number of wind turbines.

Table 7.7 – Output power values of the system generator devices with minimum wind turbines number.

Generator	Power generated					
	Swing bar		Wind farm		Hydraulic generator	
	Active power (MW)	Reactive power (MVAr)	Active power (MW)	Reactive power (MVAr)	Active power (MW)	Reactive power (MVAr)
Before the fault	145,30	24,20	87,99	0,26	85,02	-17,96
After the fault	299,53	19,97	-6,40	63,49	0	0

Figure 7.3 – Wind farm voltage response to a solid short-circuit at bus 3 with minimum wind turbines.

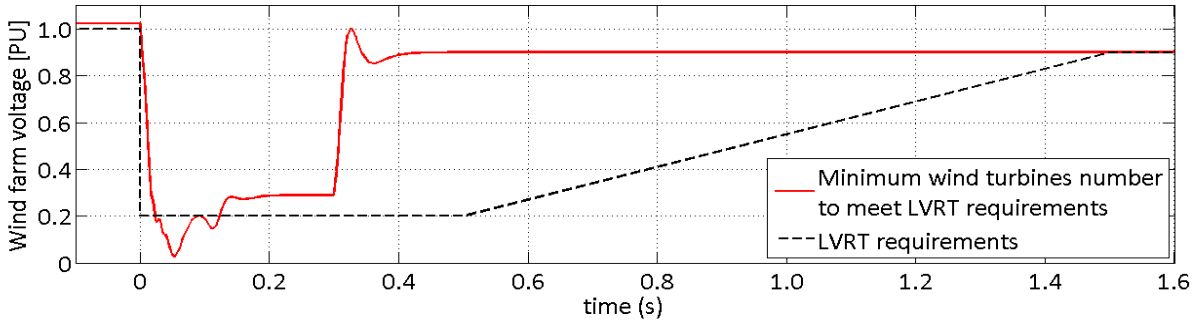

Since the bus voltages are below the allowed limits, introduction of more wind turbines with capability of "ride through" the low voltage during the fault are needed. Nine additional wind turbines equipped with DFIG with unity power factor and switching to voltage control during disturbances are necessary to meet the grid code requirements for all system buses. Finally, the installed wind turbines number in the wind farm according the proposed methodology is: 64 with DFIG with voltage control,

10 with DFIG with unity power factor and switch to voltage control during disturbances, and 36 with SCIG with capacitor bank. Simulations were performed to verify the performance of the combination determined by the method proposed here and check the compliance of the grid code requirements. This performance was compared with the behavior of a wind farm based on DFIGs with voltage control. Simulations of solid short-circuits on hydraulic generator terminals (bus 2) and load B (bus 8), voltage sag and swell at bus 1 (swing bar) were considered to asses grid code compliance.

7.2.1 **Short-circuit on hydraulic generator terminals**

A three-phase solid short circuit at hydraulic generator terminals with 300 ms of duration was simulated to assess the LVRT capability of the wind farm with the proposed methodology. The voltage response is presented in Figure 7.4.

Figure 7.4 – Wind farm voltage response to a solid short-circuit at bus 3.

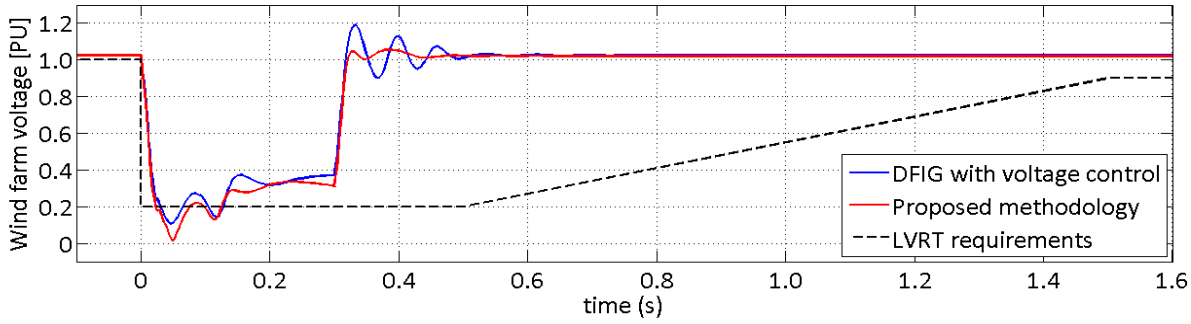

The bus voltage falls below 0,2 PU during the fault, but for less than 100 ms avoiding the DFIGs trip in both cases (delay of protection settings). Then the voltage rises with reactive power injection above 0,3 PU, and after fault clearance the voltage recovers its pre-fault value in less than 500 ms for both cases. The transient disturbance is more pronounced for wind farm based on DFIG with voltage control than in the other model, because in this last one the 36 wind turbines with SCIGs are tripped out of the system, therefore the change in power flux is lower than the first case. The wind farm current response for both cases is presented in Figure 7.5.

Wind farm currents in both studied cases have similar response to the fault limiting the current magnitude during the fault thanks to the crowbar resistance in DFIGs and SCIGs disconnection. Current magnitude in the DFIGs case is greater than the other one because there are more generators injecting reactive power during the fault, and after fault clearance the apparent power is higher too. The reactive power delivered by the wind farm for the both conditions is shown in Figure 7.6.

Figure 7.5 – Wind farm current response to a solid short-circuit at bus 3.

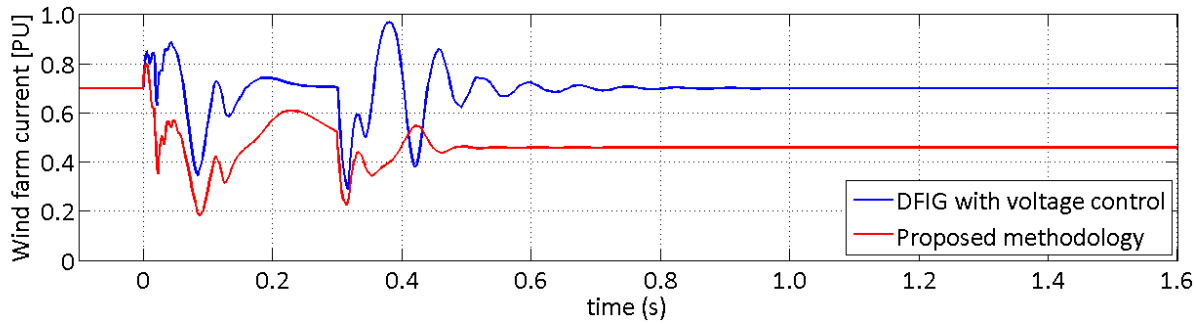

Figure 7.6 – Wind farm active power response to a solid short-circuit at bus 3.

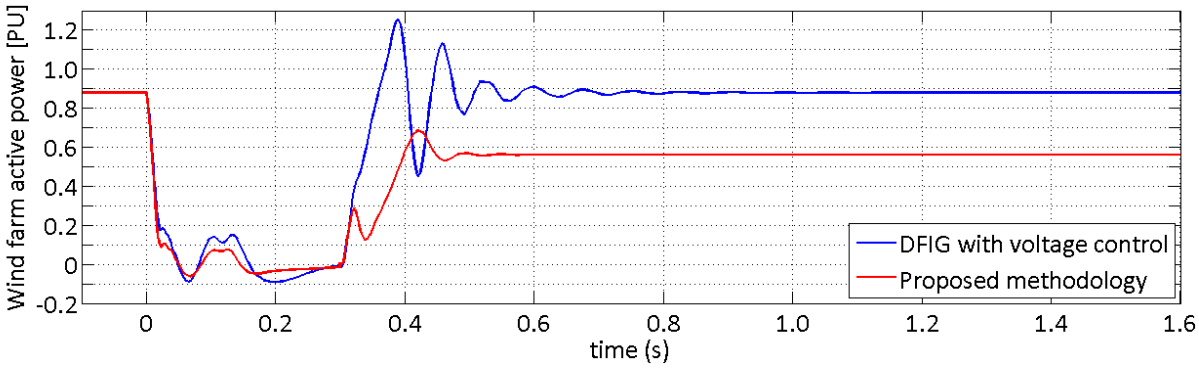

The generated active power falls close to 0 during the fault (reactive current priority to recovery the voltage) in both cases and after fault clearance the wind farm based with just DFIGs with voltage control recovers its pre-fault value, generating more active power than the wind farm with the proposed method. The reactive power injected by the wind farm for the both cases is presented in Figure 7.7.

Figure 7.7 – Wind farm reactive power response to a solid short-circuit at bus 3.

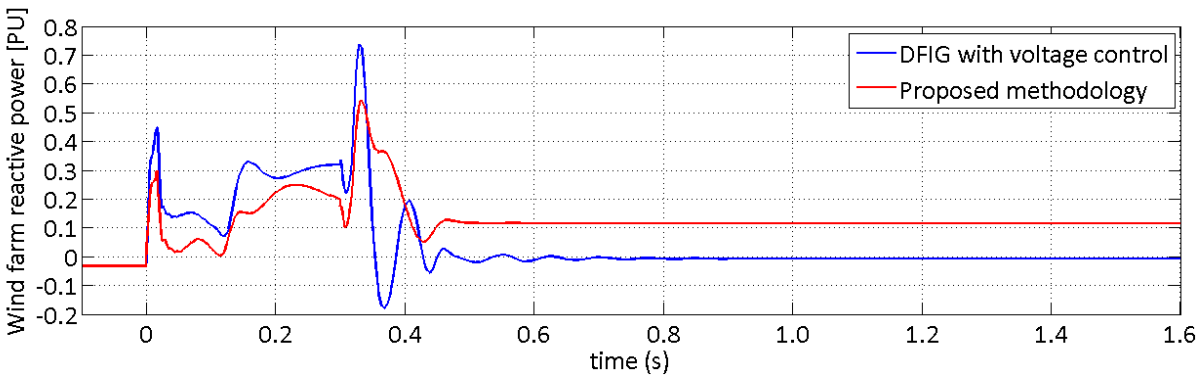

Both wind farms presented reactive power injection after the fault, but then again after the fault clearance the wind farm with the proposed method requires an additional reactive power injection to reach the set voltage value at PCC, while the wind farm based only in DFIGs does not. To prevent the output of the entire farm and the respective power loss in the system, wind farm remains connected

even with lower voltages at 0,2 PU if these have duration lower than 100 ms. In both wind farm cases the buses voltages are within the system limits after the fault as shown in Table 7.8.

Table 7.8 – System voltages including wind farm at bus 2.

Bus number		1	2	3	4	5	6	7	8	9
Bus voltage	Before the fault	1,061	1,026	1,026	1,039	1,005	1,02	1,026	1,014	1,027
	After the fault with DFIG with voltage control	1,03	1,025	1,032	1,02	0,9952	1,011	1,025	1,014	1,032
	After the fault with proposed methodology	0,9845	1,021	1,009	0,9828	0,9693	0,978	1,017	1,001	1,009

When our proposal is applied, all buses show voltage values lower if compared with the system using solely DFIGs with voltage control. This happens because there are less wind turbines delivering power to the system and because the generator in the swing bar supplies the power of the generators that were disconnected (hydraulic generators and SCIGs). In Table 7.9 the output power values for the system generators can be observed. For this disturbance kind, the compliance of voltage limits, LVRT and reactive power support during voltage disturbances requirements are checked for both wind farm cases.

Table 7.9 – Output power values of the system generator devices including wind farm at bus 2

Generator	Power generated					
	Swing bar		Wind farm		Hydraulic generator	
	Active power (MW)	Reactive power (MVAr)	Active power (MW)	Reactive power (MVAr)	Active power (MW)	Reactive power (MVAr)
Before the fault	80,32	39,7	158,3	-5,49	85	-25,44
After the fault with DFIG with voltage control	160,7	19,24	158,3	-1,278	0	0
After the fault with proposed methodology	203,9	8,623	101,1	20,87	0	0

7.2.2 **Voltage swell at swing bus**

A 40% voltage swell at swing bus with a second of duration was simulated to assess the HVRT capability of the wind farm with the method proposed here and for a wind farm based on DFIGs with voltage control. The voltage response for the both cases is presented in Figure 7.8, demonstrating that, during the swell, the bus voltage maintains its value between 0,9 and 1,1 PU and just there is a peak of 1,14 PU for DFIG with voltage control case; after fault clearance voltage recovers its pre-fault value in less than 400 ms for both cases. The transient disturbance is more

pronounced for wind farm based with DFIG with voltage control than in the case of the wind farm with the technology mix because in the last one the 36 wind turbines with SCIGs are tripped out by overcurrent.

Figure 7.8 – Wind farm voltage response to a 40% voltage swell at swing bus.

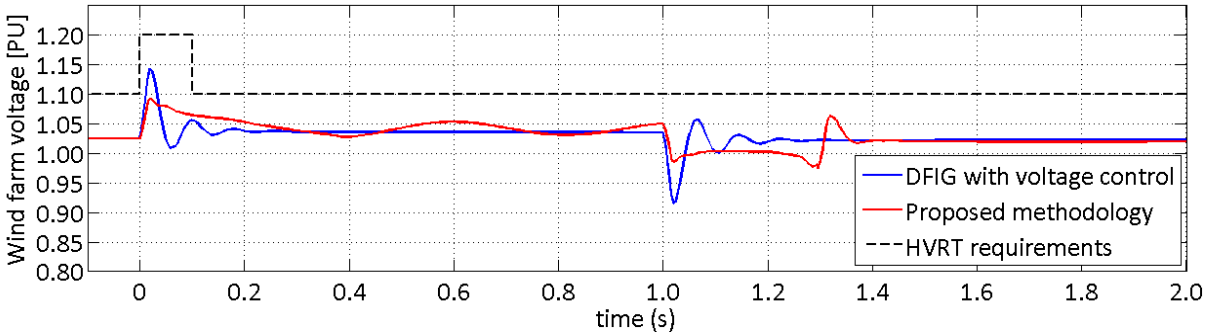

Wind farm currents in both studied cases have different response to the disturbance as shown in Figure 7.9. Both the proposed method and the DFIG case (with voltage control) have an increase in the current magnitude during the swell, due to the reactive power absorption of the DFIGs. Specifically, for DFIGs, the current during the disturbance is constant, presenting transients at the beginning and in the end of the swell and, then returning to its pre-swell value. In the other hand the mixed case, shows an oscillatory behavior for the current during the swell, the SCIGs are disconnected by overcurrent protection after the swell, it due the power exchanging with the grid. Current magnitude is greater in the DFIGs case than the mix case after the disturbance because there are more generators connected to the network.

Figure 7.9 – Wind farm current response to a 40% voltage swell at swing bus.

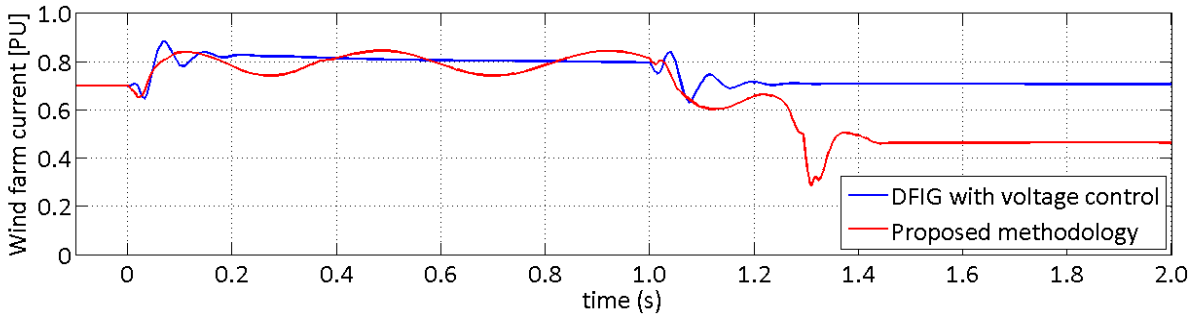

The active power delivered by the wind farm during the swell for the both analyzed cases is presented in Figure 7.10

.

Figure 7.10 – Wind farm active power response to a 40% voltage swell at swing bus.

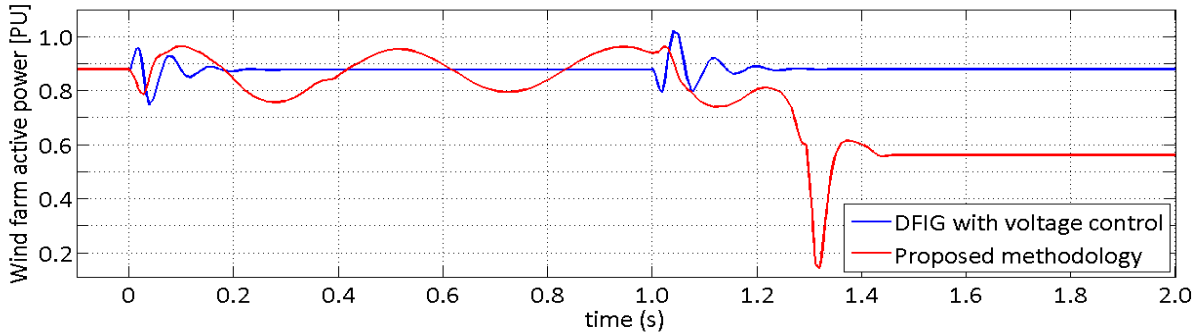

The generated active power maintains almost constant its value in the DFIG case and has an oscillatory behavior for the other case during the swell. After the swell the wind farm based on DFIGs with voltage control generates more active power than the wind farm with the proposed methodology because there are more wind turbines connected to the network. During the swell both wind farm cases absorb reactive power as seen in Figure 7.11.

Figure 7.11 – Wind farm reactive power response to a 40% voltage swell at swing bus.

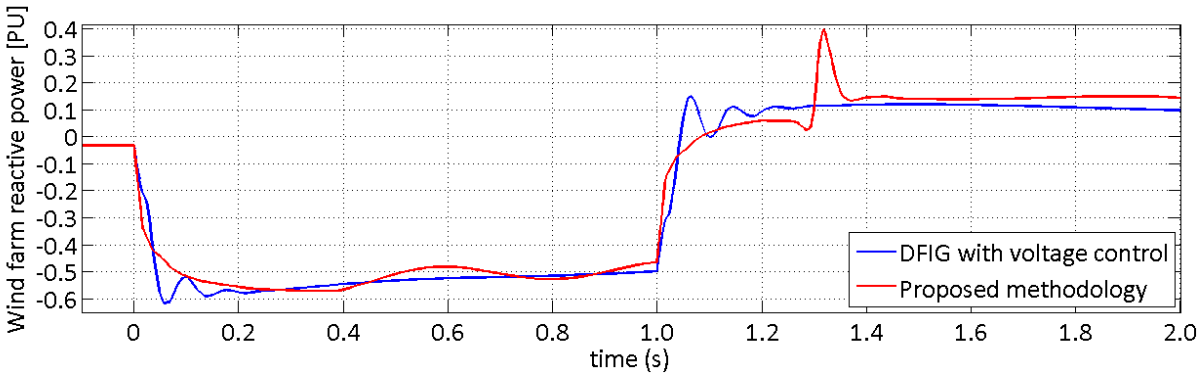

After swell clearance the wind farm with the proposed method requires to inject more reactive power to reach the set voltage value at PCC than in the case of wind farm based on DFIGs. The principal difference in the two cases is given by the presence of condensers in turbines with SCIG, the reactive power exchange is different for the both case, causing a different response. With this disturbance the compliance of requirements of voltage limits, HVRT and reactive power support during voltage disturbances requirements are checked for both wind farm cases. Furthermore, the reactive power control and voltage regulation are met because in both cases the DFIGs with voltage control can operate with different power factors to inject or absorb reactive power depending of the need on the system.

In this section, an adaptive strategy to obtain the "cheapest" option of a new wind farm to be installed on a transmission system was presented. This strategy is proposed to find this option fulfilling the grid code requirements previously established and considering different wind turbines

technologies that could be present in the electrical power systems. The strategy is based on technical and economical assumptions, *i.e*. there is not an economical evaluation with real values.

Dynamic simulations have shown that the system performance by adopting the proposed strategy does not differ significantly considering the same installed capacity of wind power of just DFIGs with voltage control. The DFIGs considered are able to "ride through" grid faults and to support voltage stability when larger disturbances occurs in electrical power systems.

7.3 EFFECT OF WIND POWER PENETRATION

Simulations of voltage swell and three-phase solid fault at load B (bus 8) are performed to assess the influence of different wind penetration levels on the system regarding the wind farm resulted from the proposed method (technology mix found in the previous section). Three levels of the active power demanded by the system: 10%, 30% and 50% are considered in this analysis. To obtain each penetration level a wind speed variation is carried out maintaining constant the capacity of the turbines used in the wind farm. Wind speeds regarded are 8 m/s for 10%, 11,5 m/s for 30% and 14 m/s for 50% respectively.

7.3.1 **Voltage swell**

A voltage swell with magnitude of 40% (swell magnitude refers to the magnitude above the nominal value) and duration of one second at swing bus was considered to assess the effect of different wind penetration levels and wind speeds when there is a short duration augmentation in the PCC voltage. Figure 7.12 presents the voltage response at PCC for the described disturbance for three wind penetration levels (10%, 30% and 50%).

Figure 7.12 – Wind farm voltage response to a 40% voltage swell at swing bus.

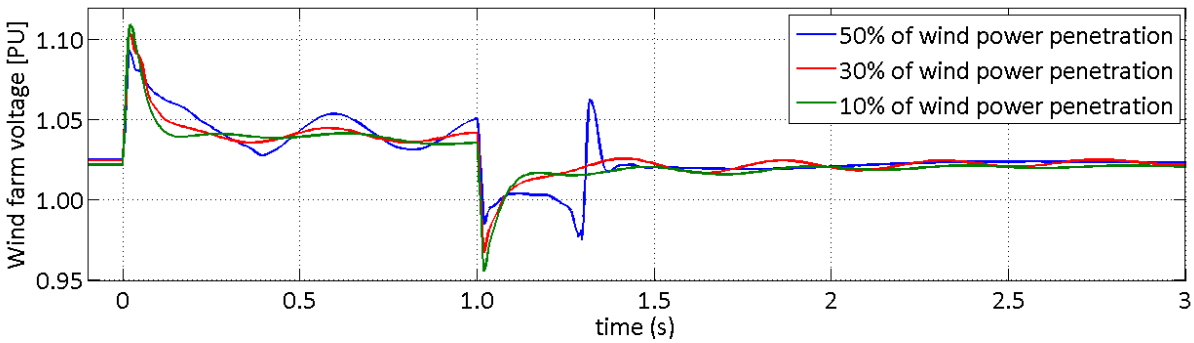

During the disturbance the PCC voltages for the three wind penetration levels are very similar and when the larger the wind power penetration, the greater the oscillations in voltage value are. Although the peaks values are higher with the penetration level reduction. The PCC voltage for the

three levels presents a peak value when voltage swell begins and decreases its value below 1,05 PU. After voltage swell ends there is a sudden voltage drop near to 0,95 PU and then the voltage increases to the pre-swell value for the penetration levels of 10% and 30%. In case of 50% of wind penetration 200 ms after the swell end the SCIGs are tripped out by the overcurrent protection and the voltage drop slowly and 100 ms later suddenly is recovered to the pre-swell value by reactive power injection from DFIGs. Figure 7.13 shows the wind farm current for the 40% voltage swell at the swing bar for the three penetration levels.

Figure 7.13 – Wind farm current response to a 40% voltage swell at swing bus.

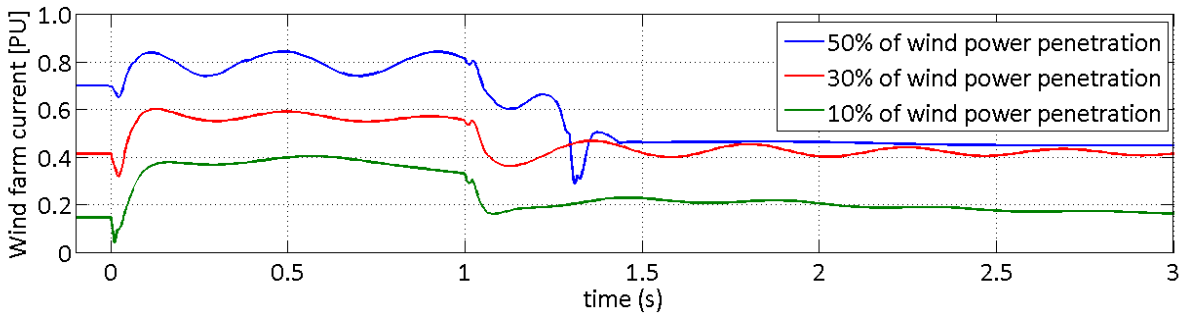

As already seen in the PCC voltage, the current behavior for the three penetration levels is very similar during the swell. The larger the wind power penetration, the greater the current value is. During the swell the current value increases because the reactive power absorption by the DFIGs. For 10% and 30% of wind penetration after the voltage swell, the current recovers its pre-swell value in less than 2 seconds. In case of 50% of wind penetration 200 ms after the swell end the SCIGs are tripped out by the overcurrent protection and the current value is lower than the pre-swell value. Figure 7.14 presents the wind farm active power response for the 40% voltage swell at swing bar for the three wind penetration levels.

Figure 7.14 – Wind farm active power response to a 40% voltage swell at swing bus.

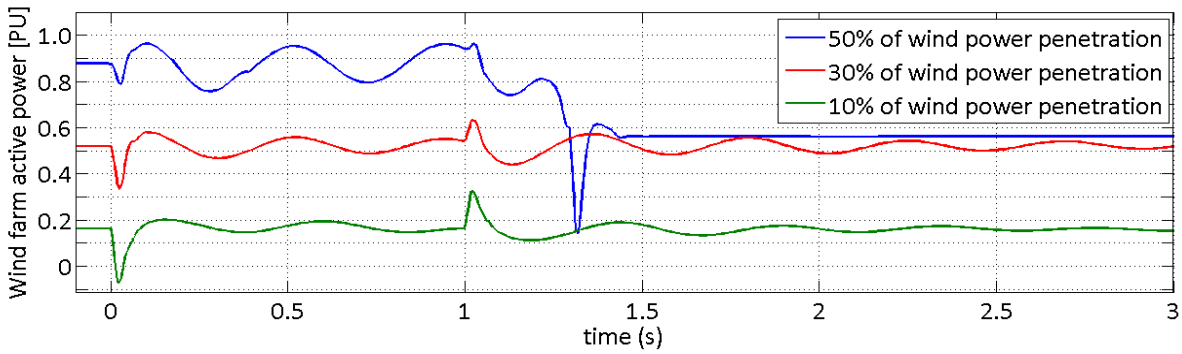

The active power delivered by the wind farm presents oscillatory behavior during the swell for the three wind penetration levels because the power exchanging between the grid and the generators. For the three penetration levels the active power has similar behavior waveform-shaped during the

swell. In cases of 10% and 30% of wind penetration the oscillatory behavior is kept after the swell end during few seconds and stabilizing in the pre-swell value. Because the SCIGs disconnection after the swell there are power loss and in case of 50% of wind penetration the active power are not able to recover its pre-swell value and it stabilizes in less than 200 ms after the disconnection.

Figure 7.15 presents the reactive power response for the three wind penetration levels. As well as in the other parameters, reactive power behavior for the three penetration levels is almost the same during the swell. The larger the wind power penetration, the greater the reactive power absorbed values are. During the voltage swell the reactive power absorbed values increase close to 50% for the three wind penetration levels. For 10% and 30% of wind penetration after the voltage swell the reactive power recovers its pre-swell values in less than 5 seconds. In case of 50% of wind penetration 200 ms after the swell end the SCIGs are tripped out by the overcurrent protection presenting transient effect and the reactive power absorbed drop to 0 a few seconds later.

Figure 7.15 – Wind farm reactive power response to a 40% voltage swell at swing bus.

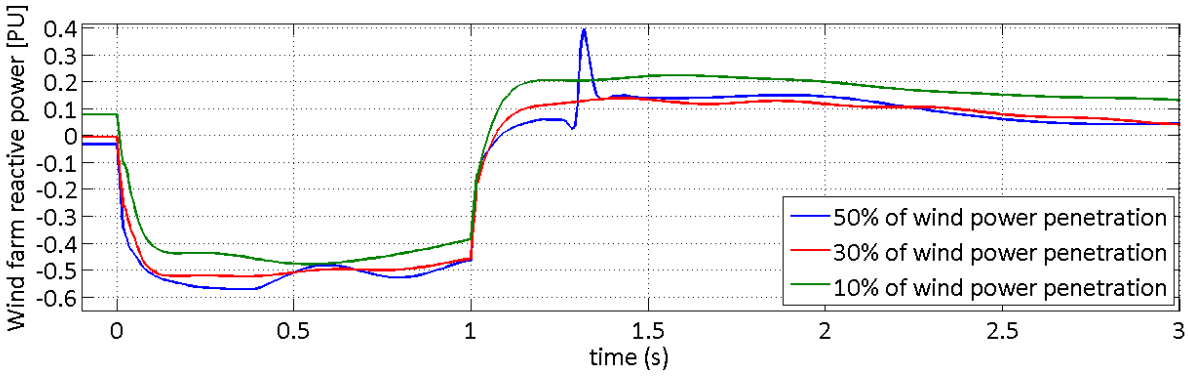

7.3.2 **Short-circuit in a nearby load (bus 8)**

A solid fault with 150 ms of duration at load B (bus 8) was regarded to assess the effect of different wind penetration levels and wind speeds when there are large disturbances on transmission system. Figure 7.16 presents the voltage response at PCC for the described disturbance for the three wind penetration levels (10%, 30% and 50%).

During the fault the voltage at the PCC for the three wind penetration levels has almost the same behavior and the larger the wind power penetration, the longer the voltage stabilization time is. It due to the wind farm needs to do a greater effort injecting reactive power and generating more active power. The PCC voltage for the three levels drops below 0,2 PU during the fault. After fault clearance the PCC voltage recovers its pre-fault value in 150 ms for 10%, 180 ms for 30% and 210 ms for 50% of wind penetration.

Figure 7.16 – Wind farm voltage response to a solid fault at load B.

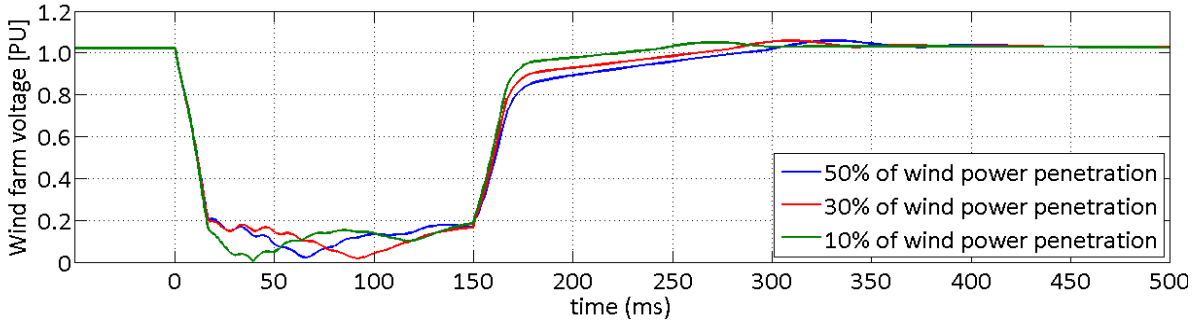

Figure 7.17 shows the wind farm current response to a solid fault at bus 8 for the three wind penetration levels.

Figure 7.17 – Wind farm current response to a solid fault at load B.

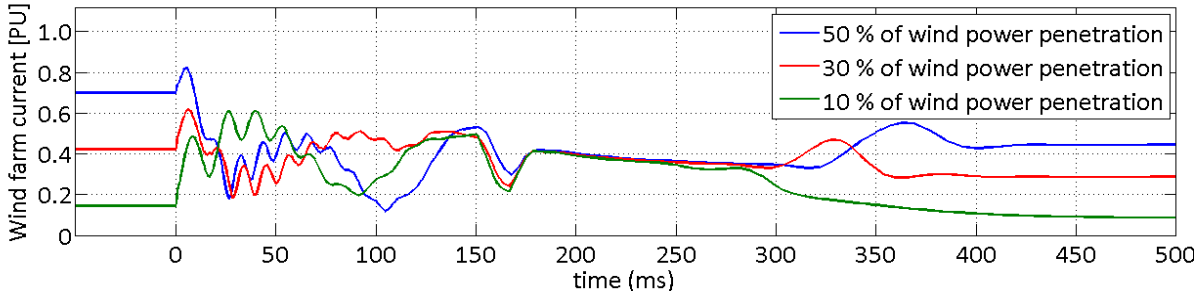

The SCIGs are trip out by the undervoltage protection when the fault occurs. During the fault the wind farm current is limited by the crowbar resistance on DFIGs, the crowbar is connected to the rotor during 100 ms operating like a SCIG. When crowbar is disconnected from the rotor circuit the RSC is reconnected to the rotor for voltage stability support by reactive power injection. When voltage is recovered to the pre-fault value the current increase its value for all wind penetration levels. Figure 7.18 presents the wind farm active power response for the fault at bus 8 for the three wind penetration levels.

Figure 7.18 – Wind farm active power response to a solid fault at load B.

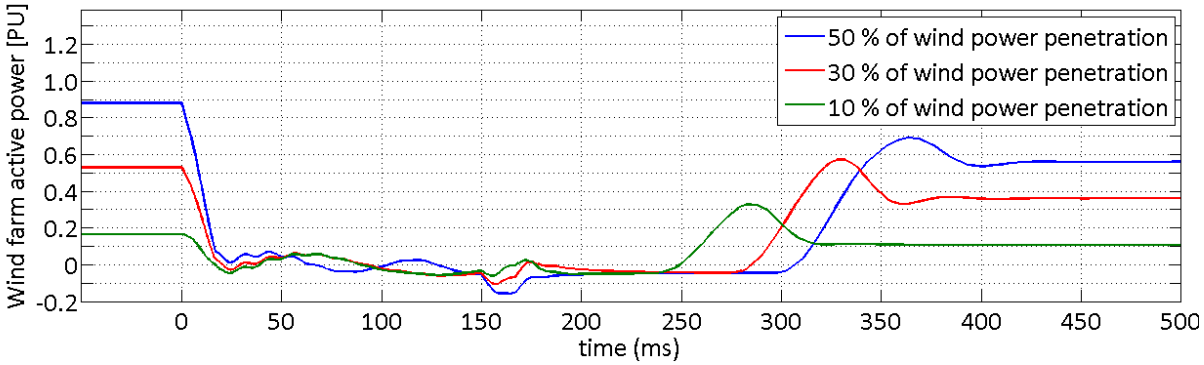

Figure 7.19 shows the wind farm reactive power response for the fault at bus 8 for the three wind penetration levels. During the fault the crowbar resistance in connected instead the rotor side converter and the reactive power injection is below 0,1 PU. In the three cases the reactive power increases its value close to 0,5 PU after crowbar disconnection to recovers the PCC voltage the faster than possible. After the PCC voltage recovery the reactive power drops to 0. In the three wind penetration levels the behavior is almost the same and the larger the wind power penetration, the longer the reactive power injection time is.

Figure 7.19 – Wind farm reactive power response to a solid fault at load B.

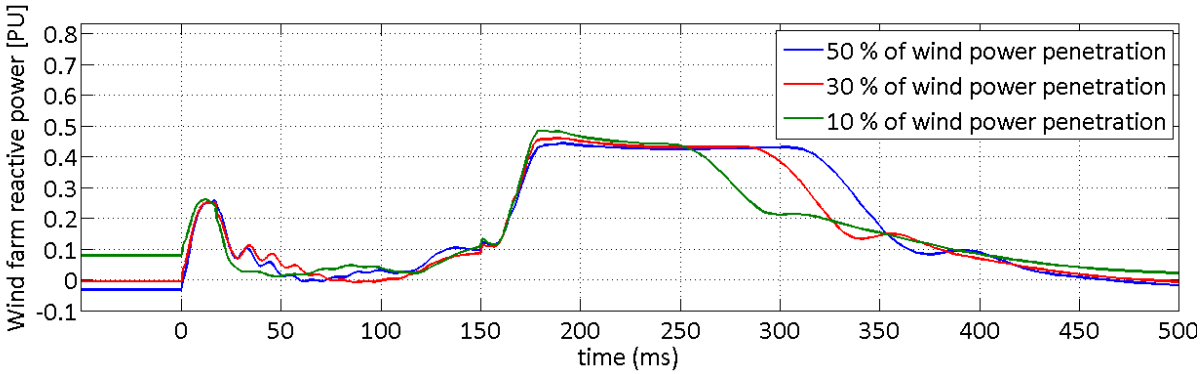

Despite the generation loss presented in the wind farm composed with the technology mix, the system is not exposed to blackout in case of solid faults on the system. The voltage restoration to the nominal value is smoother when the wind farm founded by the proposed methodology is considered; the differences are not significant enough to justify the utilization of more DFIGs with LVRT fulfillment. With different wind penetration levels the response following large-disturbances is good enough to fulfill the grid code requirements with all wind penetration levels considered. With the highest penetration level considered (50%) in the medium disturbances (sags and swells) the SCIGs within the wind farm are tripped out by overcurrent protection.

Although SCIG devices are not common in new wind farms, within this work the SCIGs are considered to show the performance of the proposed method as an option to select the "cheapest" alternative of wind turbines to connect in the system. A complementary economic study is mandatory to apply the methodology but their results showed that the technical requirements imposed by grid codes could be met.

7.4 CONCLUSIONS

The technology combination determined by the proposed methodology is based on technical and economical considerations for LVRT capability and voltage support (more strict for the connection in the Transmission Systems).

Dynamic simulations showed that the system performance by adopting the proposed strategy does not differ significantly when the same installed capacity of wind turbines with only DFIGs able to ride-through the low voltage (DFIGs with voltage control) are used. Although the voltage restoration to its nominal value is slower by considering the proposed strategy, the differences are not significant and the use of SCIG can be justified.

The proposed methodology may be used in new wind farms considering different technologies available in the market, even the ones that were not studied in this project. The existing wind farms would be repowered using the main idea described above, where a technology mix could be benefic to get the cheapest option, while promoting the network integration without threatening the system security.

8 WIND POWER CONNECTED TO IEEE 30 BUS SYSTEM

The proposed methodology is applied in the IEEE 30 bus system with some modifications, including wind farms and hydraulic generators. This grid consists of two areas: the first one with voltage 132 kV (transmission network) and the other one with voltage 33 kV (distribution network). In the transmission network are located the swing bar at bus 1, two hydraulic generators: one of 40 MW at bus 2 and the other of 30 MW at bus 5, a wind farm with 90 MW at bus 8, and six inductive-resistive loads at buses 2, 3, 4, 5, 7 and 8. In the distribution network are located two 30 MW wind farms (buses 26 and 30), two synchronous condensers (buses 11 and 13), two capacitor banks (buses 10 and 24), and fourteen inductive resistive loads at buses 10, 12, 14, 15, 16, 17, 18, 19, 20, 21, 23, 26, 29 and 30. Furthermore, there are three substations at buses 4, 6 and 28 for perform the voltage level change to buses 12, 10 and 27 respectively. Figure 8.1 presents the system described and used in this analysis.

Figure 8.1 – Modified IEEE 30 bus system with wind power generators.

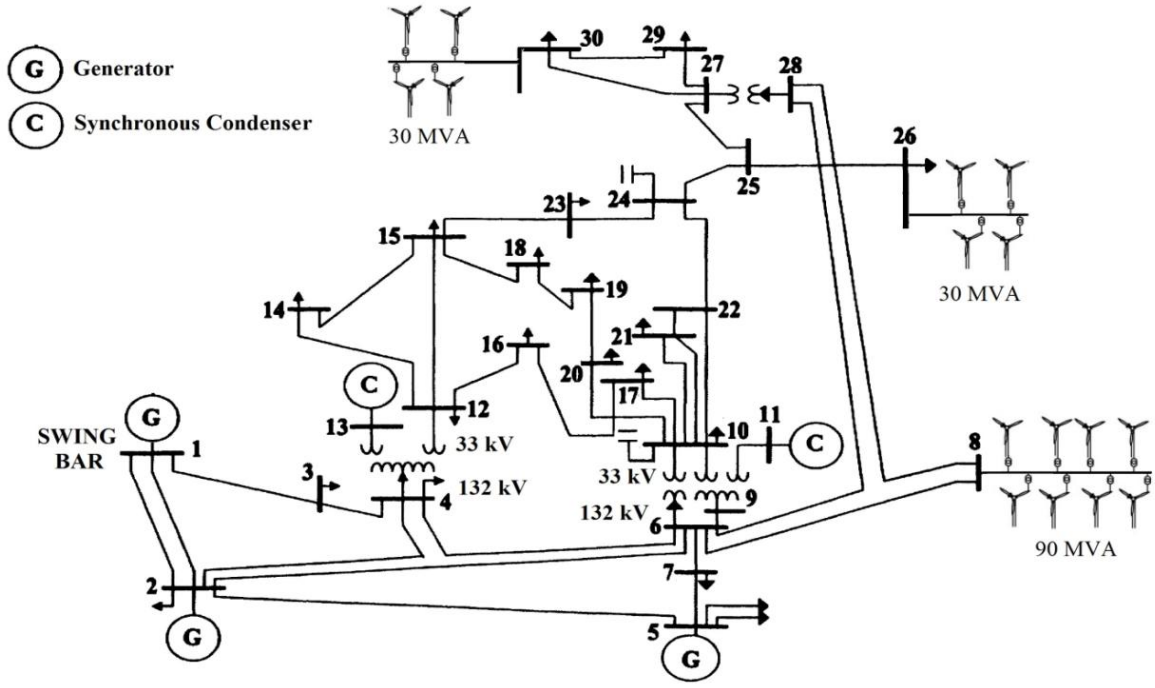

Author

To assess the grid code requirements some simulation studies are carried out: solid short-circuit at bus 2 with duration of 300 ms is simulated to evaluate the LVRT and reactive power support requirements; a 40% voltage swell at bus 1 with one second of duration to assess the HVRT requirement in transmission system, a 50% voltage sag at bus 1 with 250 ms of duration to assess the LVRT requirement in distribution system, and steady-state analysis to evaluate voltage and factor power criteria. In this study five generator types are used to implement the proposed integration strategy, from highest to lowest hierarchy as follow:

1. DFIG with voltage control, crowbar and DC chopper;
2. DFIG with unity power factor, control mode change, crowbar and DC chopper;
3. DFIG with unity power factor and control mode change;
4. DFIG with unity power factor;
5. and SCIG with capacitor bank.

In transmission network the five turbine types are used to implement the methodology and the last three types of turbines are used in the distribution grid. Analyses of the electrical system in absence of wind farms in steady-state and also dynamic analysis are necessary to determine the benefits of the wind farms installation. The other generators cannot supply the active and reactive power needed to keep all bus voltages within the limits and to recover the voltages system in case of disturbances. Figure 8.2 presents the buses voltages in absence of wind farms in steady-state before and after disturbances without trips out in the system equipments.

Figure 8.2 – System voltages in absence of wind farms.

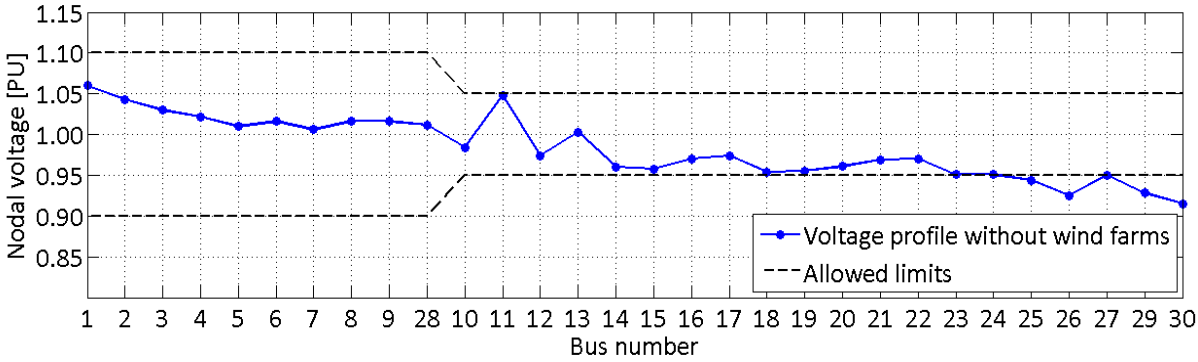

The output power values of the system generator devices in absence of wind farms are found in Table 8.1.

Table 8.1 – Output power values of the system generator devices in absence of wind farms.

Power generated					
Swing bar		Hydraulic generator (bus 2)		Hydraulic generator (bus 5)	
Active power (MW)	Reactive power (MVAr)	Active power (MW)	Reactive power (MVAr)	Active power (MW)	Reactive power (MVAr)
228,8	-18,5	38,3	35,5	28, 9	22,9
	Synchronous condenser (bus 11)		Synchronous condenser (bus 13)		
	Active power (MW)	Reactive power (MVAr)	Active power (MW)	Reactive power (MVAr)	
	0	23,88	0	23,87	

In absence of wind farms in this system there are some violations in nodal voltages in distribution grid (buses 25, 26, 29 and 30). For this reason there is the need to connect more generators to guarantee the

system safety and do not be dependent, on the possibility of a fault, in the tripping out of other generator from the grid. Besides all these facts, the maintenance operations are scheduled in generation plants doing mandatory the installation of power plants on the system.

To simplify the application of the proposed method in this system a DFIG based wind farm of 30 MW (unity power factor) was considered as existent within the system at bus 30. A fault on the distribution grid was simulated to assess the impact of the wind farm trip out over the system. Figure 8.3 shows the steady-state voltages for the grid before and after the fault. The wind farm trip out causes the decrease of some nodal voltage, this happens due to the redistribution of the active and reactive power generated or absorbed by the other generation plants.

Figure 8.3 – System voltages in presence of wind farm at bus 30.

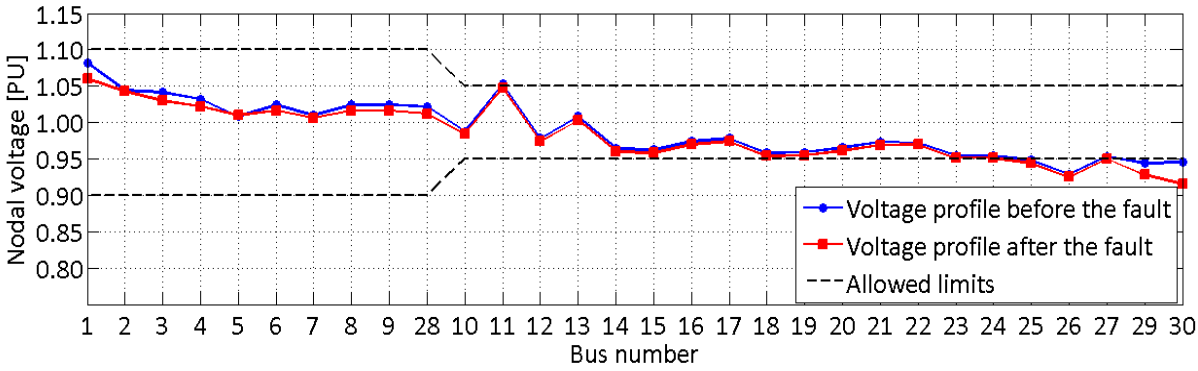

Table 8.2 presents the output power values of the system generator devices before and after the fault for the system. Swing bus supply more than 65% of the power demanded by the system exposing the system to blackout in case of bus 1 fault.

Table 8.2 – Output power values of the system generator devices in presence of wind farm at bus 30.

	Power generated					
	Swing bar		Hydraulic generator (bus 2)		Hydraulic generator (bus 5)	
	Active power (MW)	Reactive power (MVAr)	Active power (MW)	Reactive power (MVAr)	Active power (MW)	Reactive power (MVAr)
Before the fault	205,4	34,27	38,46	-14,95	29,99	16,36
After the fault	228,8	-18,5	38,3	35,5	28,9	22,9
	Synchronous condenser (bus 11)		Synchronous condenser (bus 13)		Wind farm (bus 30)	
	Active power (MW)	Reactive power (MVAr)	Active power (MW)	Reactive power (MVAr)	Active power (MW)	Reactive power (MVAr)
Before the fault	0	24,26	0	24,23	25,66	-0,61
After the fault	0	23,88	0	23,87	0	0

For the reasons previously exposed, the installation of more generation is needed. Assuming that the results of all wind studies are suitable and the wind farms installation is profitable, two of them will be integrated to this system. Wind turbines with 1,5 MW of capacity are considered in this work. The total capacity of wind power to be installed is 90 MW (60 turbines) at bus 8 and 30 MW (20 turbines) at bus 26. The integration of the wind farms is performed by connecting first one on the distribution grid (bus 26), and the other one on the transmission network (bus 8) later.

8.1 DISTRIBUTION NETWORK

8.1.1 **Voltage sag at swing bus**

In order to assess the grid code requirements in this network a voltage sag with magnitude of 50% and duration of 250 ms at swing bar was considered. The number of wind turbines installed in the wind farm (bus 26) according the proposed methodology is: 18 with DFIG with unity power factor and switch to voltage control during minor disturbances, and 2 with SCIG with capacitor bank. The voltage responses of the wind farms located at buses 26 and 30 are presented in Figure 8.4.

Figure 8.4 – Wind farm voltage response to a 50% voltage sag at swing bus.

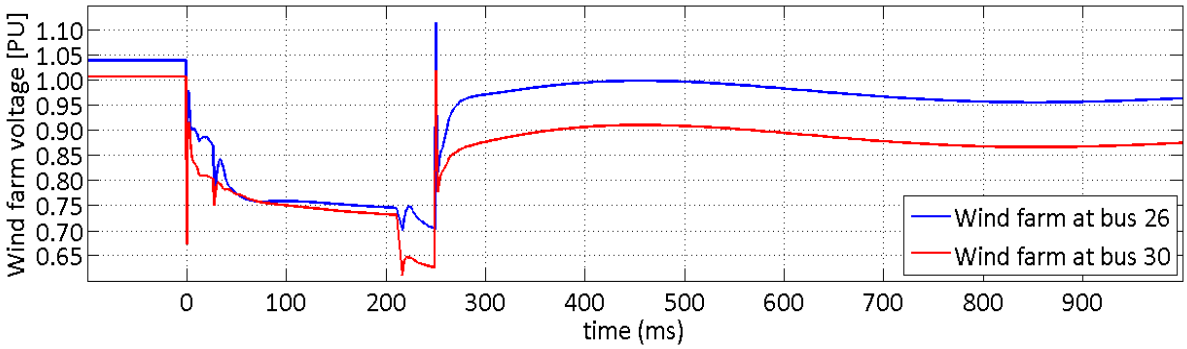

This result demonstrated that during the sag the bus voltage at bus 26 reduces its value above 0,7 PU, approximately 200 ms after sag beginning the voltage reduces its value again because wind farm at bus 30 is tripped out by undervoltage protection. SCIGs in wind farm at bus 26 are tripped out by the overcurrent protection when sag begins. After sag clearance the wind farm voltage increase above 0,95 PU. The voltage of wind farm at bus 30 has similar behavior that the bus 26 voltage but with lower values than the other bus. Because the wind farm trip the post-sag bus voltage is below 0,9 PU. The current responses of the wind farms at buses 26 and 30 are showed in Figure 8.5.

.

Figure 8.5 – Wind farm current response to a 50% voltage sag at swing bus.

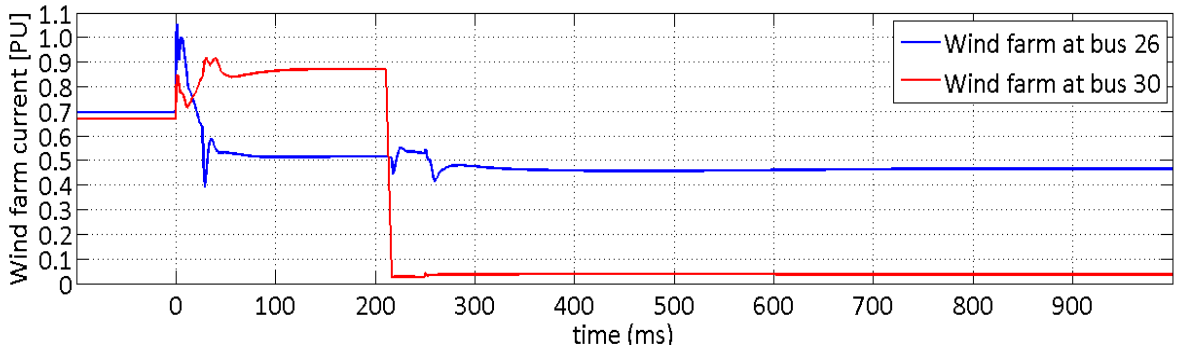

The current response of the wind farm located at bus 26 increases its value above 1,0 PU when the sag begins. During the voltage dip the wind farm current also decreases its value to 0,5 PU and after the sag clearance the current is established in 0,47 PU. There are transient phenomena when sag begins and ends, and when wind turbines are tripped out. For the wind farm at bus 30, the current increases its value to 0,88 PU during the sag, 220 ms after sag beginning the wind farm is tripped and current falls to 0. The active power responses of the wind farms at buses 26 and 30 are illustrated in Figure 8.6.

Figure 8.6 – Wind farm active power response to a 50% voltage sag at swing bus.

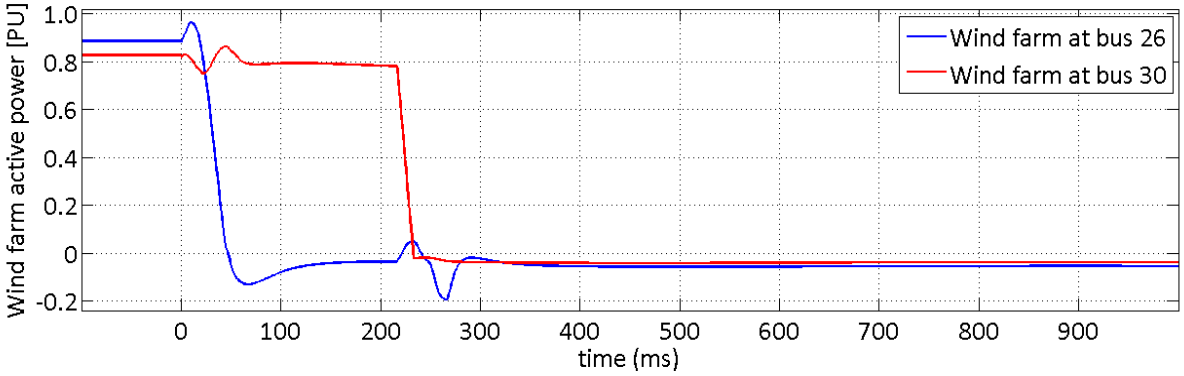

The active power generated by the wind farm at bus 26 falls to 0 during and after the sag because the reactive current priority imposed in the DFIG converters. Some disturbances occur at the beginning and in the end of the dip. In the wind farm located in bus 30 the active power generated remains constant during the sag before the wind farm trip and this value falls to 0. The reactive power responses of the wind farms at buses 26 and 30 are illustrated in Figure 8.7.

The reactive power injected by the wind farm located at bus 30 is 0 all the time; and it just presents some disturbances at the beginning and in the end of the sag. The reactive power injected by the wind farm in the bar 26 increases its value to 0,48 PU during the sag and to 0,55 PU after the sag.

Figure 8.7 – Wind farm reactive power response to a 50% voltage sag at swing bus.

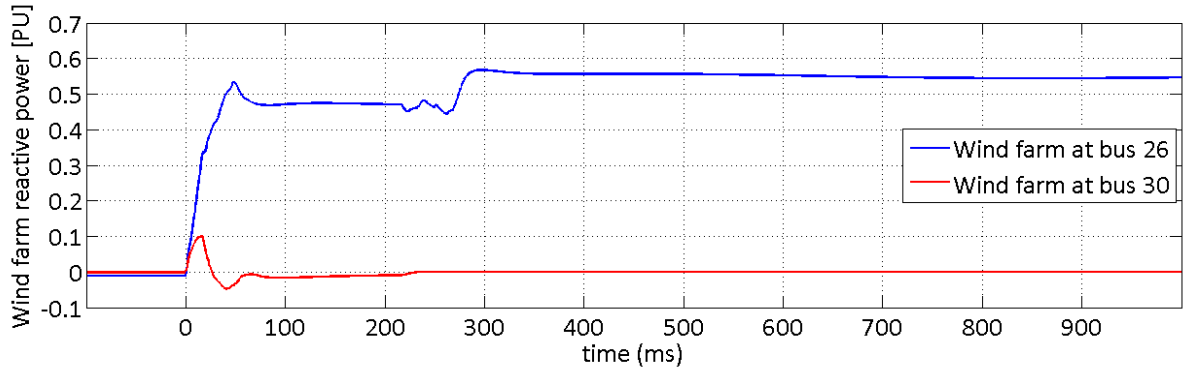

The bus voltage values before and after the sag are presented in the system voltage profiles in Figure 8.8. Before the disturbance all bus voltages are within the allowed operation limits, an exception is the bus 11 due to be a generation point. Wind farm connection at bus 26 helps to supply active power locally in the distribution network demanding less power from the swing bus as shown in Table 8.3.

Figure 8.8 – System voltages in presence of wind farms at buses 26 and 30.

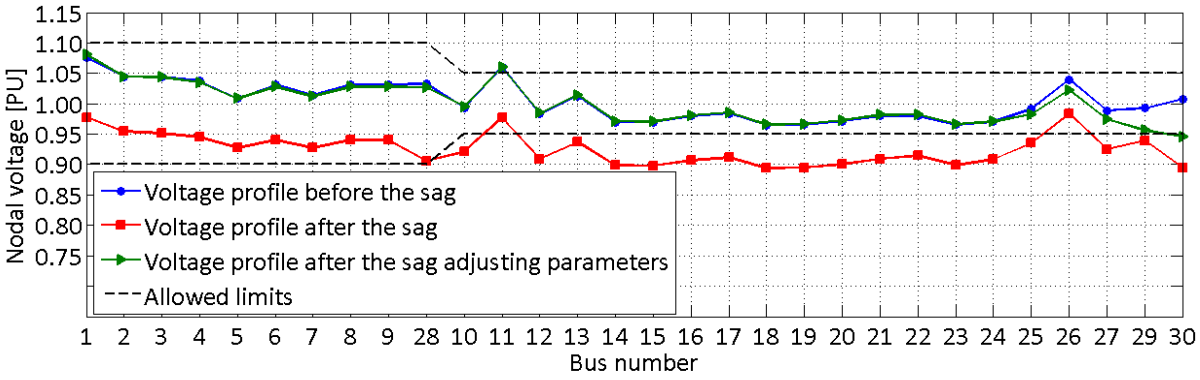

After the disturbance clearance all bus voltages reduce considerably their values because the trips out of some wind turbines and the respective apparent power loss. Almost all bus voltages in the distribution network are below the minimum allowed value (0,95 PU). But adjusting the generator parameters and importing more apparent power all bus voltages increase their value (green line) and just the bus 30 is not fulfilling the allowed value. After the adjusting of generator parameters the power flow changes and the turbines in wind farm at bus 26 just generate active power. With the wind farm connection at bus 26, the grid code requirements established for the distribution network in section 7.1 are fulfilled. However, still there is a great dependence of the swing bus for power supply and for this reason integration of more generation plant is mandatory.

Table 8.3 – Output power values of the system generator devices in presence of wind farms at buses 26 and 30.

	Power generated					
	Swing bar		Hydraulic generator (bus 2)		Hydraulic generator (bus 5)	
	Active power (MW)	Reactive power (MVAr)	Active power (MW)	Reactive power (MVAr)	Active power (MW)	Reactive power (MVAr)
Before the fault	172.55	23.94	38.46	-14.05	28.99	13.1
After the fault	178.1	3.61	41.73	-3.05	36	12.97
After the fault adjusting parameters	203.75	31.07	38,57	-17.42	29.1	14.55

	Synchronous condenser (bus 11)		Synchronous condenser (bus 13)	
	Active power (MW)	Reactive power (MVAr)	Active power (MW)	Reactive power (MVAr)
Before the fault	0	24.59	0	24.46
After the fault	0	20.9	0	20.93
After the fault adjusting parameters	0	24.56	0	24.54

	Wind farm (bus 26)		Wind farm (bus 30)	
	Active power (MW)	Reactive power (MVAr)	Active power (MW)	Reactive power (MVAr)
Before the fault	29.55	-0.36	27.54	-0.065
After the fault	-1.5	18.4	-1.36	0
After the fault adjusting parameters	24.57	-0.05	0	0

8.2 TRANSMISSION NETWORK

60 wind turbines of 1.5 MW of capacity (90 MW) are considered for this wind farm. The most severe disturbance contemplated was a solid short-circuit in terminals of the hydraulic generator located at bus 5 leading to the disconnection of the hydraulic generator located at bus 2, wind farms located in distribution network, and its own disconnection. Applying the method proposed in this work, the minimum wind turbines number to guarantee the compliance of LVRT criteria was found, being 19 with 18 DFIG with voltage control and the other is DFIG with unity power factor and switch to voltage control during disturbances. Nevertheless, as in the IEEE 9 transmission system, the voltages on the other buses are out of the allowed limits exposing the system loads operation.

As bus voltages are below the allowed limits, introduction of more wind turbines with capability of "ride through" the low voltage during the fault and they are not disconnected from the grid. Thirty four additional wind turbines equipped with DFIG with unity power factor and switch to voltage control during disturbances were necessary to meet the grid code requirements for all system buses. Finally, the wind turbines number installed in the wind farm according the proposed methodology is: 18 with DFIG with voltage control, 35 with DFIG with unity power factor and switch

to voltage control during disturbances, and 7 with SCIG with capacitor bank. Simulations were performed to verify the performance and compliance with the grid code requirements of the combination determined by our method against the wind farm based on DFIGs with voltage control. Simulations of solid short-circuits on hydraulics generator terminals (bus 2 and 5) and the transformer in bus 28, voltage sag and swell at bus 1 (swing bar) were considered to asses grid code compliance.

8.2.1 **Short-circuit at terminals of the hydraulic generator located in bus 5**

A three-phase solid fault at terminals of hydraulic generator at bus 5, with 300 ms of duration was simulated to assess the LVRT capability of the wind farm with the proposed methodology. Figure 8.9 shows the voltage response to the described fault in terminals for the wind farm composed by different technologies, which was determined within this work, and for the one based on DFIGs with voltage control.

Figure 8.9 – Voltage response of the wind farm in bus 8 to a solid fault at bus 5.

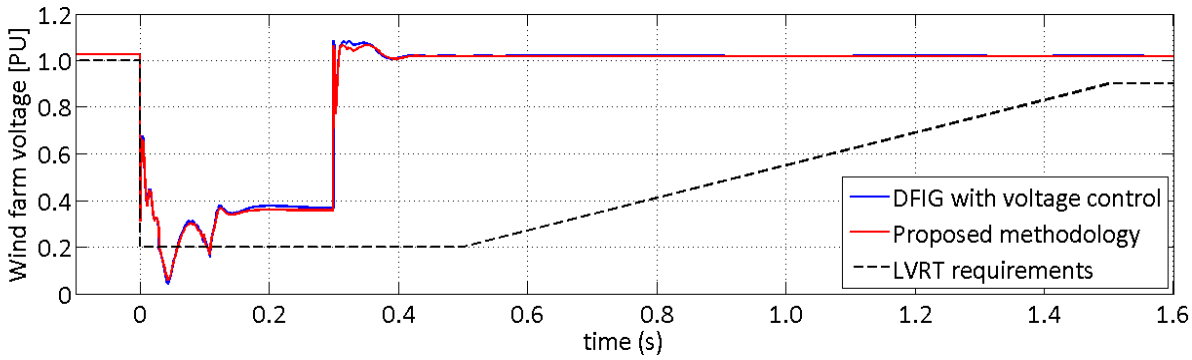

Voltage response shows that during the fault the bus voltage falls below 0,2 PU for approximately 30 ms, avoiding the DFIGs trip in both cases (delay of protection settings), then the voltage rises by reactive power injection close to 0,4 PU, and after fault clearance voltage recovers its pre-fault value in less than 200 ms for both cases. The transient disturbance is slightly more pronounced for wind farm based with DFIG with voltage control than the other case, because in the last one the 7 wind turbines with SCIGs are tripped out of the system and the active power generated, as well the current take lower values than in the DFIG case. To prevent the output of the entire farm and the respective power loss in the system, wind farm remains connected even with lower voltages at 0,2 PU if these have duration lower than 100 ms. During the fault the two hydraulic generators and the tow wind farms located in the distribution grid are tripped out by the undervoltage protection.

The current response to the fault in the hydraulic generator at the bus 5 is presented in Figure 8.10 for both wind farm kinds the responses have similar behavior when the fault happens. At the beginning of the fault the current increases its value above 1,4 PU when voltage close to 0, and with

the crowbar connection the wind farm current is limited. After crowbar resistance disconnection the current is limited by the DC chopper maintaining the wind farm current below 0,9 PU until fault clearance. After the fault clearance the current pre-fault value (0,7 PU) is recovered in the DFIG case and reach 0,6 PU of value in the proposed method.

Figure 8.10 – Current response of the wind farm in bus 8 to a solid fault at bus 5.

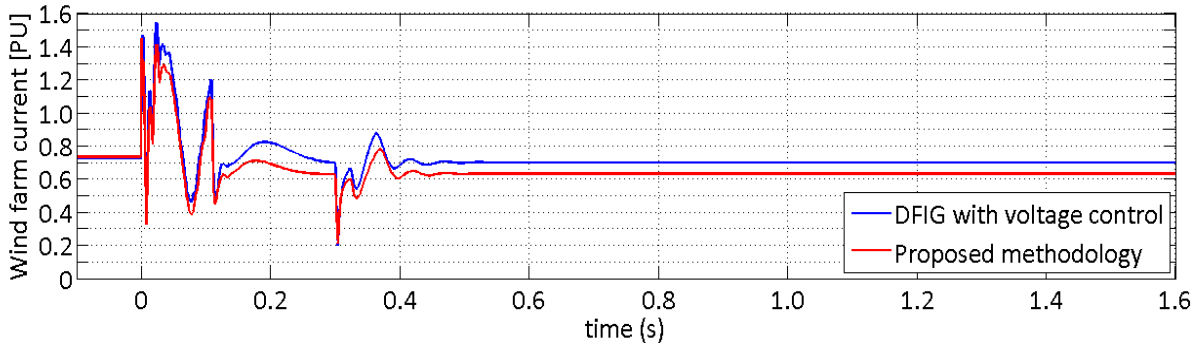

Figure 8.11 shows the response of the active power to the fault in the bus 5 for the two cases analyzed. The active power generated by the wind farm located at bus 8 decreases its value close to 0 during the fault because the current priorities established in DFIG converters. After fault clearance the active power recovers its pre-fault value (0,88 PU) for the DFIG with voltage control and reach 0,77 PU with the wind farm based on the proposed methodology. The active power of the wind farm stabilizes in less than 200 ms with underdamped behavior.

Figure 8.11 – Active power response of the wind farm in bus 8 to a solid fault at bus 5.

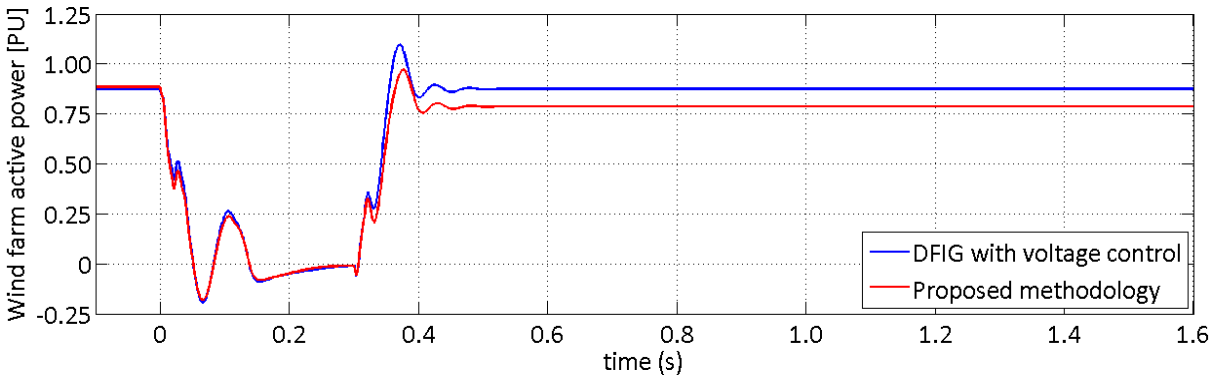

Figure 8.12 illustrates the reactive power injected by the wind farm located at bus 8 during the fault for the wind farm based on DFIG with voltage control and for the wind farm based on the proposed methodology. In both cases the wind turbines absorb reactive power from the grid before the fault, then after the crowbar disconnection the turbines injects reactive power to increase the wind farm voltage. After fault clearance the maximum reactive power is reached to recover the wind farm voltage quickly. When the wind farm voltage is recovered, the turbines inject less reactive power and supply active power to the grid. For the DFIG with voltage control there is no reactive power after

voltage recovery. For the wind farm based on the proposed method, the wind farm injects 0,06 PU of reactive power to maintain high the bus voltage.

Figure 8.12 – Reactive power response of the wind farm in bus 8 to a solid fault at bus 5.

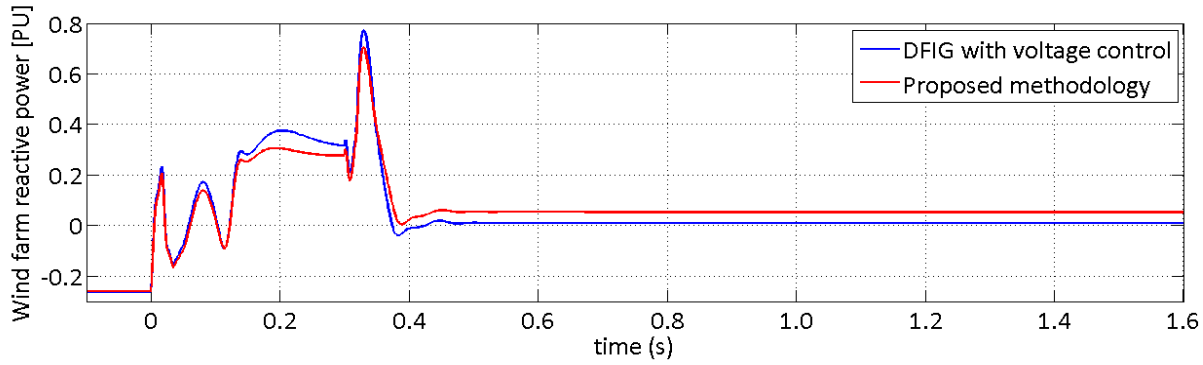

The steady-state voltages before and after the fault are showed in Figure 8.13. It can be seen that with the integration of this wind farm, all the buses voltages are within the allowed operation limits before and even after the fault.

Figure 8.13 – System voltages in presence of wind farms at buses 8, 26 and 30.

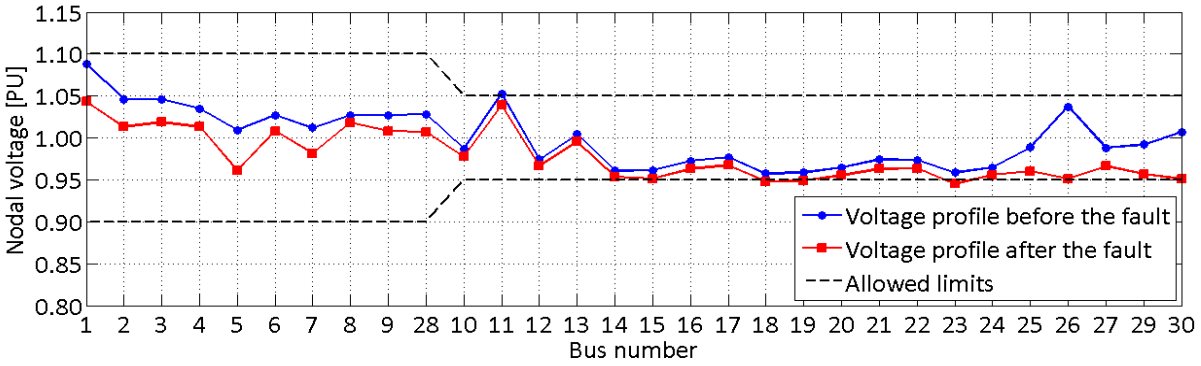

The wind farm connection at bus 8 helps to supply active power to the distribution network, demanding less power from the swing bar as shown in Table 8.4. After fault clearance all bus voltages considerably reduce their values, because the trip out of the hydraulic plants and the wind farms in the distribution network. With this disturbance kind the compliance of voltage limits, LVRT and reactive power support during voltage disturbances requirements established for the transmission network in section 7.1 are fulfilled in both cases. Within the Table 8.4 can be observed that just in case of the most severe disturbance the swing bar needs to supply a huge quantity of apparent power (more than 50%) to the system to keep the voltage stability and to avoid the voltage collapse, blackouts or undesirable load shedding.

Table 8.4 – Output power values of the system generators in presence of wind farms at buses 8, 26 and 30.

	Power generated					
	Swing bar		Hydraulic generator (bus 2)		Hydraulic generator (bus 5)	
	Active power (MW)	Reactive power (MVAr)	Active power (MW)	Reactive power (MVAr)	Active power (MW)	Reactive power (MVAr)
Before the fault	81,19	66,97	38,38	-34,03	29	14,81
After the fault	199,78	14,91	0	0	0	0
	Wind farm (bus 8)		Wind farm (bus 26)		Wind farm (bus 30)	
	Active power (MW)	Reactive power (MVAr)	Active power (MW)	Reactive power (MVAr)	Active power (MW)	Reactive power (MVAr)
Before the fault	88,61	-26,04	29,35	0	27,54	-0,06
After the fault	78,67	31,02	0	0	0	0
	Synchronous condenser (bus 11)		Synchronous condenser (bus 13)			
	Active power (MW)	Reactive power (MVAr)	Active power (MW)	Reactive power (MVAr)		
Before the fault	0	23,16	0	22,83		
After the fault	0	24,92	0	24,9		

8.2.2 **Voltage swell at swing bus**

A 40% voltage swell at swing bus with a second of duration was simulated to assess the HVRT capability of the wind farms with the proposed methodology. Voltage response (Figure 8.14) shows that during the swell the bus voltage maintains its value between 0,9 and 1,1 PU with just a peak of 1,14 PU for DFIG with voltage control case; after fault clearance voltage recovers its pre-fault value in less than 400 ms for both cases. The transient disturbance is more pronounced for wind farm based with DFIG with voltage control than in the other case because in the last one the seven wind turbines with SCIGs do not perform the voltage control through reactive power.

Figure 8.14 – Wind farm voltage response to a 40% voltage swell at swing bus.

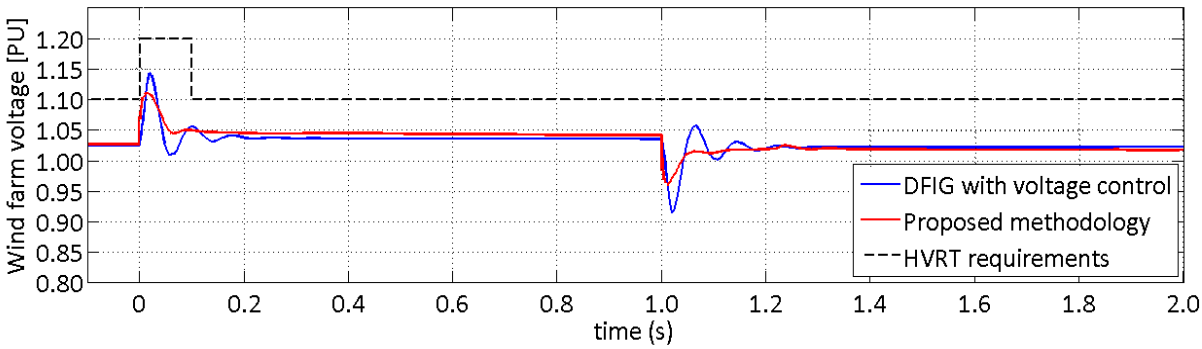

The wind farm current response to the voltage swell is presented in Figure 8.15. For both cases the wind farm current has almost the same behavior. When the swell begins the current value increase above 0,9 PU because the reactive power absorption of DFIGs to maintain the terminal voltage

constant. After the swell the wind farm current reduces its value close to 0,7 PU, this value is lower than before the swell because the change on power flow by the voltage disturbance.

Figure 8.15 – Wind farm current response to a 40% voltage swell at swing bus.

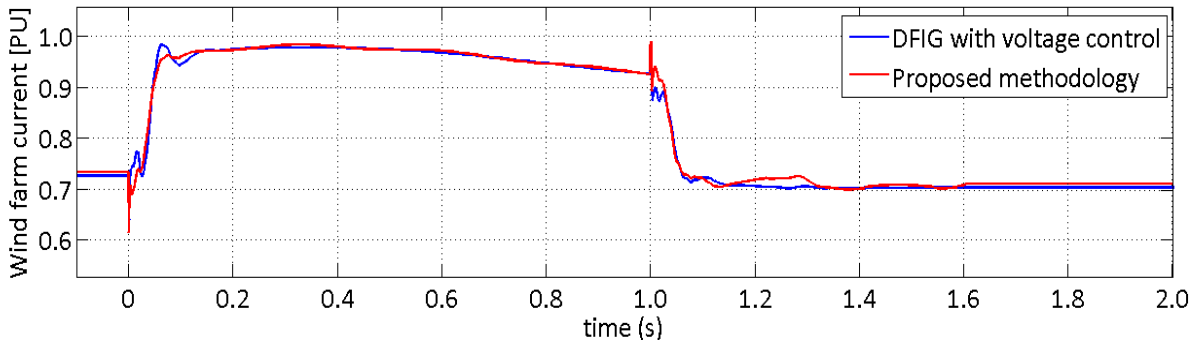

The active power generated by the wind farm in the both cases is very similar. It keeps almost constant its value and presents disturbances at the beginning and in the end of the voltage swell as shown in Figure 8.16.

Figure 8.16 – Wind farm active power response to a 40% voltage swell at swing bus.

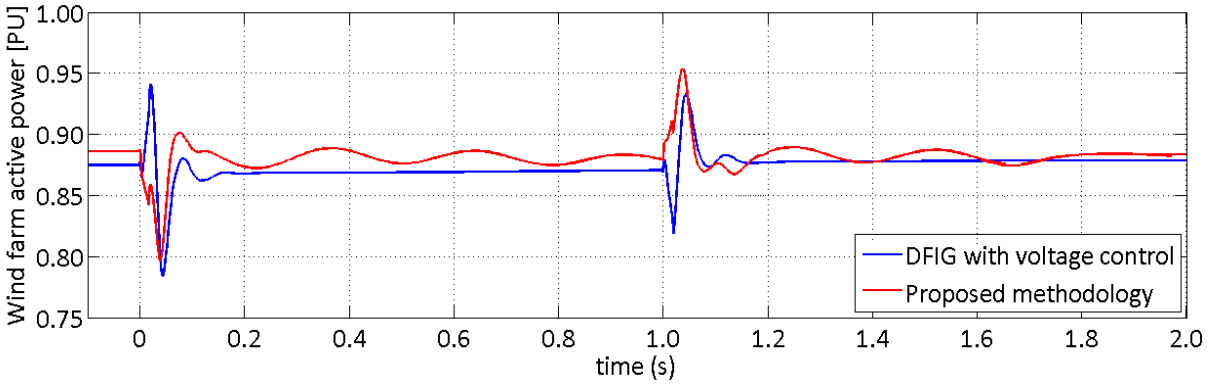

Figure 8.17 – Wind farm reactive power response to a 50% voltage swell at swing bus.

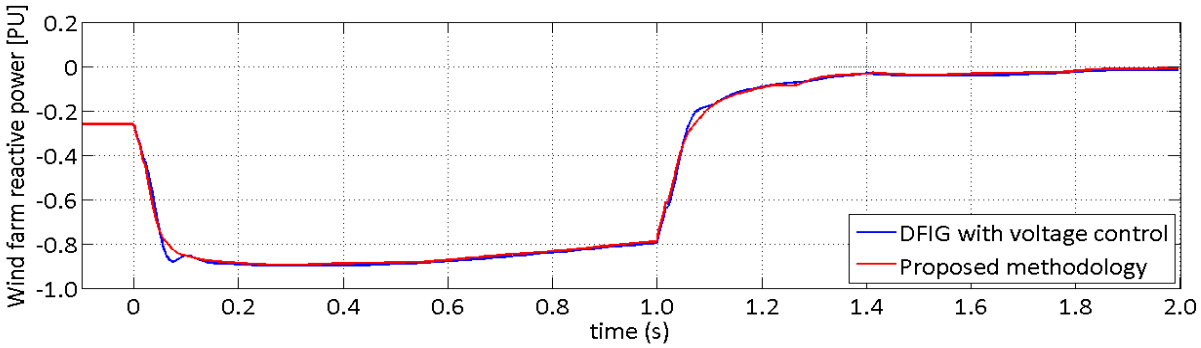

During the swell both wind farm cases there is reactive power absorption by the wind turbines (see Figure 8.17) to maintain the terminal voltage constant. After the swell end the reactive absorption

is reduces close to 0 because the redistribution in the power flow (it is represented in the wind farm current too).

With this disturbance kind the compliance of voltage limits, HVRT and reactive power support during voltage disturbances requirements are checked for both wind farm cases. Furthermore the reactive power control and voltage regulation are met, because for both cases DFIGs with voltage control can operate with different power factors to inject or absorb reactive power depending of the necessity on the system.

In this chapter can be observed that the proposed method is able to fulfill the grid code requirements imposed for this work in this system, in the distribution as well as the transmission network. For the system analyzed it was proved that the wind farms connection could be progressive, in the developed example, three wind farms were considered and their connections were independent of the connection of the others.

Table 8.5 presents a comparison of the results of the proposed methodology in the IEEE 9 bus and IEEE 30 bus systems. The table shows that when all the wind power is connected in the transmission system only, the number of generator fulfilling the grid code requirements are lower than the case when they are connected in both transmission and distribution systems. In case of IEEE 30 bus system the percentage of generators fulfilling the grid codes are similar in transmission and in distribution network.

Table 8.5 – Comparison of the proposed methodology in both electrical systems.

System	Network	Generator in the turbines	% technology	% fullfill
9 bus	***Transmission***	64 DFIG with voltage control	**58**	**67**
		10 DFIG with p.f=1 strategy 3	**9**	
		36 SCIG with capacitor bank	33	
30 bus	***Distribution***	18 DFIG with p.f=1 strategy 2	**90**	**90**
		2 SCIG with capacitor bank	10	
	Transmission	18 DFIG com controle de tensão	**30**	**88**
		35 DFIG with p.f=1 strategy 3	**58**	
		7 SCIG with capacitor bank	12	

9 FINAL CONCLUSIONS

The connection of wind turbines in electrical power systems and their effects in the system general performance when electrical perturbations occur were presented in this work. Also, steady state analyses were considered to assess the impact of high penetration levels in electrical power systems.

Steady state voltage profile

The performances of the hydraulic generator and the DFIG are similar at all wind power penetration levels. SCIG unities consume reactive power in their operation, so the voltages at terminals are smaller and the use of auxiliary equipment is necessary. With higher penetration levels, the variations in voltage and reactive power exchange are greater. SCIGs without reactive compensation represent high currents and low voltages in the system.

Large disturbances in IEEE 9 bus system

Large disturbances can disconnect SCIGs of the system; therefore its use is not convenient for large wind farms. The DFIG control mode change from unity power factor to voltage control in case of large disturbances can improve the voltage stability in electrical systems. DFIGs with voltage control showed the ability to remain connected during voltage sags and swells. Higher wind penetration levels represent major exchanges in reactive power and larger variations in voltages

The use of crowbar resistance and DC-chopper is needed for DFIGs keep connected to the network without being at risk. SCIGs with capacitor bank are disconnected when faults happen due to high currents presented. DFIGs with unity power factor are disconnected because low voltages. In case of DFIGs with voltage control, the higher levels of wind power represent higher peak values of voltage and current.

Small-disturbance voltage stability (PV and VQ curves)

The ability to inject or absorb reactive power is related to voltage stability margins. DFIGs with tension control have the highest margins.

Mix of technology of Wind turbines in wind farm

The wind farm found with the proposed method does not present significant differences with the wind farm composed by DFIGs with tension control. The proposed method could be used in new wind farms with the technologies available in the market. It could be used on existing wind farms too, by repowering of wind turbines looking for the most economical option.

10 PAPERS PUBLISHED DURING THE MASTER AND FUTURE WORKS

10.1 PUBLICATIONS DURING THE MASTER

During the development of this master, some papers were published in a national and an international conference, being both selected for oral presentation in the conferences. Both papers are available in the IEEE database. The papers are the following:

- "Analysis of transmission Systems with High Penetration of Wind Power using DFIG based Wind Farms during Voltage Sags" in International Conference on Clean Electrical Power Renewable Energy Resources Impact (Alghero, Sardinia – Italy, June 2013)
- "Voltage Sags and Short Circuit Analysis in Power Systems with High Wind Power Penetration based on Doubly Fed Induction Generator" em "Innovative Smart Grid Technologies" – IEEE ISGT Latin America (São Paulo – Brasil, Abril 2013)

10.2 SUGGESTIONS FOR FUTURE WORKS

Some proposals to follow up the work developed in this dissertation are given below:

- Studies of the impact of high penetration levels of wind power on the Voltage Stability of power systems using other technologies of wind turbines, such as Electrically Excited Synchronous generator (EESG) and Permanent Magnet Synchronous Generator (PMSG).
- Studies of the impact of high penetration levels of wind power on the Angle Stability of power systems using all the technologies of wind turbines, Double fed induction generator (DFIG), Squirrel cage induction generator (SCIG), Electrically Excited Synchronous generator (EESG) and Permanent Magnet Synchronous Generator (PMSG).
- Economic assessment of the method proposed in this work, considering the maintenances costs, operation costs, turbines prices, etc.

11 REFERENCES

[1] Mohanty, K.; Barik, A. K. "Power System Stability Improvement Using FACTS Devices." International Journal of Modern Engineering Research (IJMER), v. 1, n. 2, p. 666-672.

[2] World Wind Energy Association. "World Wind Energy Report 2012." Available: www.wwindea.org. Accessed: 19 July 2013.

[3] International Energy Agency. "IEA Wind 2012 Annual Report." Available: www.ieawind.org. Accessed: 19 July 2013.

[4] Global Wind Energy Council. "Global Wind Report Annual Market Update 2012." Available: www.gwec.net. Accessed: 19 July 2013.

[5] Index mundi. "Historical Data Graphs per Year." Available: http://www.indexmundi.com Accessed: 19 July 2013.

[6] International Energy Agency, "IEA Wind 2011 Annual Report." Available: www.ieawind.org. Accessed: 19 July 2013.

[7] World Wind Energy Association, "World Wind Energy Report 2011." Available: www.wwindea.org. Accessed: 19 July 2013.

[8] Freitas, W.; Vieira, J. C. M.; Morelato, A.; Silva, L. C. P.; Costa, V. F.; Lemos, F. A. "Comparative Analysis Between Synchronous and Induction Machines for Distributed Generation Applications." IEEE Transactions on Power Systems, v. 21, n. 1, p. 301-311, 2006.

[9] Abildgaard, H. "Experience of the Danish Transmission System Operator." In: IEA Technology Experts Meeting - grid integration of electricity from renewables, Paris, 2007.

[10] Barrera F., A. "El viento generó casi el 25% de la electricidad en Australia del Sur el año pasado." Energías renovables. October 7, 2012. Available: http://www.energias-renovables.com. Accessed: 17 October 2013.

[11] Associação Brasileira de Energia Eólica, "Boletim de dados ABEEolica Junho 2014." Available: http://www.portalabeeolica.org.br. Accessed: 28 Juy 2014.

[12] The guardian. "Japan to scrap nuclear power in favour of renewable." 10 May 2011. Available: http://www.theguardian.com. Accessed 31: October 2013.

[13] Castano, I. "Nuclear Woes Boost Japanese Wind but Supply Remains Limited." 12 April 2011. Available: http://www.renewableenergyworld.com. Accessed 31: October 2013.

[14] Elcacho, J. "Fukushima estrena un parque eólico marino y Catalunya aparca el suyo." 31 October 2013. Available: http://www.lavanguardia.com. Accessed: 31 October 2013.

[15] Weyndling, R. "Portugal slices 23% off 2020 wind target." Wind Power Monthly, 25 April 2012. Available: http://www.windpowermonthly.com. Accessed: 06 November 2013.

[16] Petersen, A. "Wind power hits peak to cover half of all electricity production." The Portugal News Online, 19 December 2012. Available: http://theportugalnews.com. Accessed: 05 November 2013.

[17] Lenz, K. F. "Portugal Hit 70% Renewable Electricity In Q1 2013." Clean Technical, 09 April 2013. Available: http://cleantechnica.com. Accessed: 05 November 2013.

[18] Koronowski, R. "Is 70 Percent Renewable Power Possible? Portugal Just Did It for 3 Months." Climate Progress, 14 April 2013. Available: http://thinkprogress.org. Accessed: 05 November 2013.

[19] Kennedy, C. "Portugal Generated 70% of Energy from Renewable Sources in First Quarter." Oilprice.com, 11 April 2013. Available: http://oilprice.com. Accessed: 05 November 2013.

[20] algarvedailynews.com. "Portugal's wind power record." algarvedailynews.com, 01 November 2013. Available: http://algarvedailynews.com. Accessed: 05 November 2013.

[21] Abo Wind. "La energía eólica en España." ABOWIND. Available: http://www.abowind.com. Accessed: 11 November 2013.

[22] Asociación Empresarial Eólica. "Eólica '13." 2013. Available: www.aeeolica.org. Accessed: 11 March 2014.

[23] Lainformacion.com. "La eólica bate récord al producir el 60% de la electricidad." Lainformacion.com, 16 April 2012. Available: http://noticias.lainformacion.com. Accessed: 11 November 2013.

[24] lainformacion.com. "6 de febrero, 15.50 horas: nuevo récord nacional de producción de energía eólica." lainformacion.com, 06 February 2013. Available: http://noticias.lainformacion.com. Accessed: 11 November 2013.

[25] Tleis, N. D. "Power Systems Modelling and Fault Analysis Theory and Practice." Elsevier, 2008. Available: https://www.elsevier.com. Accessed: 11 November 2013.

[26] Andersson, G. “Modelling and Analysis of Electric Power Systems, Power Flow Analysis Fault Analysis.” In: Zürich: Eidgenössische Technische Hochschule Zürich, 2008. Available: http://www.ebooksmagz.com. Accessed: 11 November 2013.

[27] Borges, C. L. T. “Análise de Sistemas de Potência.” Apostila. Rio de Janeiro: EE-UFRJ-Departamento de Eletrotécnica, 2005.

[28] Kundur, P. “Power System Stability and Control.” Palo Alto, California: McGraw-Hill, 2007.

[29] IEEE Task Force on Load Representation for Dynamic Performance. "Load Representation for Dynamic Performance Analysis." IEEE Transactions on Power Systems, v. 8, p. 472-482, 1993.

[30] Concordia, C.; Ihara, S. "Load Representation in Power System Stability Studies." IEEE Transaction on Power Apparatus and Systems, v. PAS-101, p. 969 - 977, 1982.

[31] Mathworks. “Matlab SimPowerSystems User's Guide”. s.l.: Hydro-Québec, 2012.

[32] Grainger, J. J.; Stevenson. W. D. “Power System Analysis.” Singapore: McGraw-Hill, 1994.

[33] Vittal, E.; O'Malley, M.; Keane, A. "A Steady-State Voltage Stability Analysis of Power Systems with High Penetrations of Wind." IEEE Transactions in power systems, v. 25, n. 1, p. 433-442, 2010.

[34] Salles, M. B. C. “Análise do Desempenho Dinâmico de Geradores Eólicos Conectados em Redes de Distribuição de Energia Elétrica”, n. p. 2004. Dissertação (Mestrado) – Departamento de Engenharia Elétrica, Unicamp, Campinas, 2004.

[35] Abad, G.; Lopez, J.; Rodríguez, M. A.; Marroyo, L.; Iwansky, G. “Doubly Fed Induction Machine: Modeling and Control for Wind Energy Generation.” v. 1, New York: JohnWiley&Sons, 2011.

[36] Wessels, C.; Fuchs, F. W. "LVRT of DFIG Wind Turbines - Crowbar vs. Stator Current Feedback Solution." In: EPE Wind Energy Chapter Symposium (2010), Stafford, UK, 2010.

[37] Akhmatov, V. “Analysis of dynamic behaviour of electric power systems with large amount of wind power PhD thesis.” Kongens Lyngby, Denmark: Electric Power Enginnering, Ørsted-DTU, 2003.

[38] Akhmatov, V.; Knudsen, H. "An aggregate model of a grid-connected, large-scale, offshore wind farm for power stability investigations—importance of windmill mechanical system." International Journal of Electrical Power & Energy Systems, v. 24, p. 709-717, 2002.

[39] Fernández, L. M.; García, C. A.; Saenz, J. R.; Jurado, F. "Reduced Model of DFIGs Wind Farms Using Aggregation of Wind Turbines and Equivalent Wind." In: IEEE MELECON, Benalmádena, Spain, 2006.

[40] Fernández, L. M.; García, C. A.; Saenz, J. R.; Jurado, F. "Equivalent models of wind farms by using aggregated wind turbines and equivalent winds." Energy Conversion and Management, v. 50, p. 691-704, 2009.

[41] Panumpabi, M. P. “Large wind farm aggregation and model validation Ms Thesis.” Urbana, Illinois: University of Illinois, 2011.

[42] Conroy, J.; Watson, R."Aggregate modeling of wind farms containing full-converter wind turbine generators with permanent magnet synchronous machines: transient stability studies." IET Renewable Power Generation, v. 3, n. 1, p. 39-52, 2007.

[43] Pöller, M.; Achilles, S. "Aggregated Wind Park Models for Analyzing Power System Dynamics." In: Fourth international workshop on large-scale integration of wind power and transmission networks, Billund, Denmark, 2003.

[44] Ackermann, T. “Wind Power in Power System, 2th ed”. Nioda, India: Wiley and Sons, 2012.

[45] Zou, Y.; Elbuluk, M.; Sozer, Y. "A Complete Modeling and Simulation of Induction Generator Wind Power Systems." In: Industry Applications Society Annual Meeting (IAS), IEEE, Houston, 2010.

[46] Salles, M. B. C.; Hameyer, K.; Cardoso, J. R.; Grilo, A. P.; Rahmann, C. "Crowbar System in Doubly Fed Induction Wind Generators." Energies, v. 3, p. 738-753, 2010.

[47] Hansen, A. D.; Michalke, G. "Fault ride-through capability of DFIG wind turbines." Renewable energy, v. 32, n. 9, p. 1594-1610, 2007.

[48] Franke, C.; Timbus, A.; Larsson, M. "Extension of contingency analysis to wind power." In: European Wind Energy Conference & Exhibition 2010, Warsaw, Poland, 2010.

[49] Meegahapola, L.; Flynn, D., Kennedy, J.; Littler, T. "Active use of DFIG based Wind Farms for Transient Stability Improvement during Grid Disturbances." In: Power & Energy Society General Meeting, 2009. PES '09. IEEE, Calgary, AB, 2009.

[50] Margaris, I. D.; Hansen, A. D.; Sørensen, P.; Hatziargyriou, N. D. "Dynamic security issues in autonomous power systems with increasing wind power penetration." Electric Power System Research, v. 81, p. 880-887, 2011.

[51] Weisser, D.; García, R. S. "Instantaneous wind energy penetration in isolated electricity grids: concepts and review." Renewable Energy, Elsevier, v. 30, p. 1299-1308, 2005.

[52] Larsen, E.; Chandrashekhara, D. K.; Østergård, J. "Electric Vehicles for Improved Operation of Power Systems with High Wind Power Penetration." In: IEEE Energy2030, Atlanta, 2008.

[53] Hossain, M. J.; Pota, H. R.; Mahmud, A.; Ramos, R. A. "Investigation of the Impacts of Large-Scale Wind Power Penetration on the Angle and Voltage Stability of Power Systems." IEEE Systems Journal, v. 6, n. 1, p. 76-84, 2012.

[54] Shi, L.; Dai, S.; Ni, Y.; Yao, L.; Bazargan, M. "Transient Stability of Power Systems with High Penetration of DFIG Based Wind Farms." In: Power & Energy Society General Meeting, 2009. PES '09. IEEE, Calgary, AB, 2009.

[55] Sauer, P. W.; Pai, M. A. "Power System Dynamics and Stability." New York: Prentice Hall, 1997.

[56] Demiray, T. H. "Simulation of Power System Dynamics using Dynamic Phasor Models, Ph.D. Thesis." Zurich, Sweden: Swiss Federal Institute of technology Zurich, 2008.

[57] Dommel, H. W. "Digital computer solution of electromagnetic transients in single and multiphase networks." Computer Applications in Power, IEEE, v. 3, n. 4, p. 31-36, 1990.

[58] Anaya-Lara, O.; Jenkins, N.; Ekanayake, J.; Cartwright, P.; Huges, M. "Wind Energy Generation: Modelling and Control." Nioda, India: Wiley and Sons, 2009.

[59] Union for the co-ordination of transmission of electricity. "Final Report System Disturbance on 4 November 2006." Available: https://www.entsoe.eu. Accessed: 13 November 2013.

[60] Mohseni, M.; Islam, S. M. "Review of international grid codes for wind power integration: Diversity, technology and a case for global standard." Elsevier, Renewable and Sustainable Energy Reviews, n. 16, p. 3876-3890, 2012.

[61] Martínez de Alegría, I.; Andreu, J.; Martín, J. L.; Ibañez, P.; Villate, J. L.; Camblong, H. "Connection requirements for wind farms: A survey on technical requierements and regulation." Elsevier, Renewable and Sustainable Energy Reviews, v. 11, p. 1858-1872, 2007.

[62] Sudrià, A.; Chindris, M.; Sumper, A.; Gross, G.; Ferrer, F. "Wind Turbine Operation in Power Systems and Grid Connection Requirements." IEEE Power and Energy Magazine, v. 5, n. 6, p. 47-51, 2007.

[63] Operador Nacional do Sistema Elétrico. "Requisitos técnicos mínimos para a conexão às instalações de transmissão." 16 September 2010. Available: http://www.ons.org.br. Accessed 28 February 2014.

[64] Fuentes, J. A.; Cañas, M.; Molina, A.; Gómez, E.; Jiménez, F. "International Review of Grid Connection Requirements related with Voltage Dips for Wind Farms." In: International Conference on Renewable energies and power quality, Sevilla, 2007.

[65] Palomar Lozano, A. “Analysis, modelling and control of a doubly-fed induction generator for large wind turbines.” Madrid: Universidad Pontificia Comillas, Escuela Técnica superior de ingeniería, 2011.

[66] Hines, P.; Balasubramaniam, K.; Cotilla Sánchez, E."Cascading failures in power grids." IEEE, Potentials, v. 28, p. 24-30, 2009.

[67] Energinet. “Technical regulation 3.2.5 for wind power plants with a power output greater than 11 kW.” September 2010. Available: http://www.energinet.dk. Accessed: 15 April 2014.

[68] MEID. “Portaria n° 596/2010 - Anexo I: Regulamento da Rede de Transporte.” July 2010. Available: http://www.erse.pt. Accessed: 15 April 2014.

[69] Red Eléctrica de España. “Resolution-P.O.12.3-Response requirements against voltage dips in wind installations.” March 2006. Available: http://www.aeeolica.es/en. Accessed: 15 April 2014.

[70] Ullah N. R.; Thiringer, T; Karlsson, D. "Voltage and transient stability support by wind farms complying with the E.ON Netz code." IEEE Trans Power Syst, v. 22 p. 1647-1656, 2007.

[71] Masters, C. L. "Voltage rise: The big issue when connecting embedded generation to long 11 kV overhead lines." Power Eng. J., v. 16, n. 1, p. 5-12, 2002.

[72] Redes Energéticas Nacionais. "A energia eólica em Portugal 2011." 06 February 2011. Available: http://www.centrodeinformacao.ren.pt. Accessed: 03 January 2014.

[73] Naser, I. S.; Garba, A.; Anaya-Lara, O.; Lo, K. L. "Voltage Stability of Transmission Network with different penetration Levels of Wind Generation." In: IEEE/Universities Power Engineering Conference (UPEC), Cardiff, Wales, 2010.

[74] Ender, C. "Windenergienutzung in der Bundesrepublik Deutschland - Stand 31.12.2009 (Wind energy use in Germany - Status 31.12.2009)." DEWI Magazine, v. 36, p. 28-41, 2010.

[75] Xu, L.; Allene, J. "Embarrassments of China's Wind Power." SGT Research, 14 March 2012. Available: http://www.sgtresearch.com. Accessed: 13 March 2014.

[76] Kubota, H. "Current Status and Outlook of the Wind Energy in China." E-Journal of advanced maintenance EJAM, November 2011. Available: http://www.jsm.or.jp. Accessed: 13 March 2014.

[77] CNB Daily. "Chinese Wind Farm Power Grid Disconnection Accident." Deblock consulting Ltd., 15 April 2011. Available: http://deblockconsulting.com. Accessed: 13 March 2014.

[78] Fowler, T. "A near-miss on the Texas Grid." Chron, 27 February 2008 Available: http://blog.chron.com. Accessed: 13 March 2014.

[79] Rahmann, C.; Haubrich, H. J.; Moser, A.; Palma-Behnke, R.; Vargas, L.; Salles, M. B. C. "Justified Fault-Ride-Through Requirements for Wind Turbines in Power Systems," IEEE Transactions on Power Systems, v. 26, n. 3, p. 1555-1563, 2011.

[80] Vestergaard, J.; Brandstrup, L.; Goddard, R. D."A Brief History of the Wind Turbine Industries in Denmark and the United States." Academy of International Business Conference Proceedings, p. 322-327, 2004.

[81] Larsen, E.; Chandrashekhara, D. K.; Østergård, J. "Electric Vehicles for Improved Operation of Power Systems with High Wind Power Penetration." IEEE Energy 2030, 2008.

[82] Kaldellis, J. K.; Zafirakis, D."The wind energy (r)evolution: A short review of a long history." Elsevier, Renewable Energy, v. 36, p. 1887-1901, 2011.

[83] Brito, A. "Energia eólica já é mais barata que térmica a gás no Brasil." Folha de São Paulo, 19 August 2011. Available: http://www1.folha.uol.com.br. Accessed: 23 July 2013.

[84] The European Wind Energy Association. "Wind in power 2012 European statistics." 2013. Available: www.ewea.org. Accessed: 23 July 2003.

[85] Renewable Energy Policy Network for the 21st Century. "Renewables 2012 Global Status Report." 2013. Available: www.ren21.net. Accessed: 23 July 2003.

[86] BusinessGreen. "Denmark aims to get 50% of all electricity from wind power." theguardian.com, 26 March 2012. Available: http://www.theguardian.com. Accessed 23 October 2013.

[87] Energy Numbers. "Capacity factors at Danish offshore wind farms." Energy Numbers, 18 September 2013. Available: http://energynumbers.info. Accessed: 19 July 2013.

[88] Renewable Energy in the United Kingdom. "Burradale Wind Farm, Shetland Islands." reuk.co.uk, 19 January 2007. Available: http://www.reuk.co.uk. Accessed: 19 July 2013.

[89] IRENA-GWEC. "30 Years of policies for wind energy." 2013. Available: www.irena.org. Accessed: 23 July 2003.

[90] Rinaldi, S. M.; Peerenboom, J. P.; Kelly, T. K. "Identifying, understanding, and analyzing critical infrastructure interdependencies." Control Systems Magazine, v. 21, n. 6, p. 11-25, 2001.

APPENDIX A - IEEE 9 BUS SYSTEM

Figure A. 1 - Single line diagram of the IEEE 9 bus transmission system.

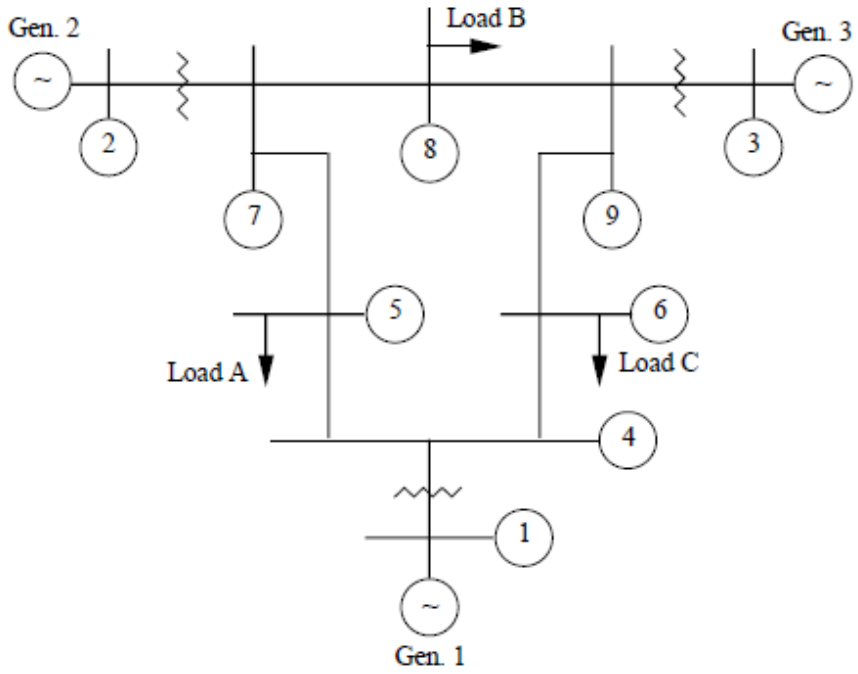

Table A. 1 – Transmission line data on 100 MVA base.

From Bus Number	To Bus Number	Series Resistance (Rs) PU	Series Reactance (Xs) PU	Shunt Susceptance (B) PU
1	4	0.0000	0.0576	0.0000
4	6	0.0170	0.0920	0.1580
6	9	0.0390	0.1700	0.3580
9	3	0.0000	0.0586	0.0000
9	8	0.0119	0.1004	0.2090
8	7	0.0085	0.0720	0.1490
7	2	0.0000	0.0625	0.0000
7	5	0.0320	0.1610	0.3060
5	4	0.0101	0.0850	0.1760

Table A. 2 – Bus data for the system.

Bus No.	Bus type	Generation (PU)		Load (PU)		Voltage Magnitude
		PG	QG	PL	QL	
1	Swing	--	--	0.00	0.00	1.04
2	PV	1.63	--	0.00	0.00	1.0253
3	PV	0.85	--	0.00	0.00	1.0253
4	PQ	0.00	0.00	0.00	0.00	--
5	PQ	0.00	0.00	1.25	0.50	--
6	PQ	0.00	0.00	0.90	0.30	--
7	PQ	0.00	0.00	0.00	0.00	--
8	PQ	0.00	0.00	1.00	0.35	--
9	PQ	0.00	0.00	0.00	0.00	--

APPENDIX B - IEEE 30 BUS SYSTEM

Figure A. 2 - Single line diagram of the IEEE 30 bus transmission system.

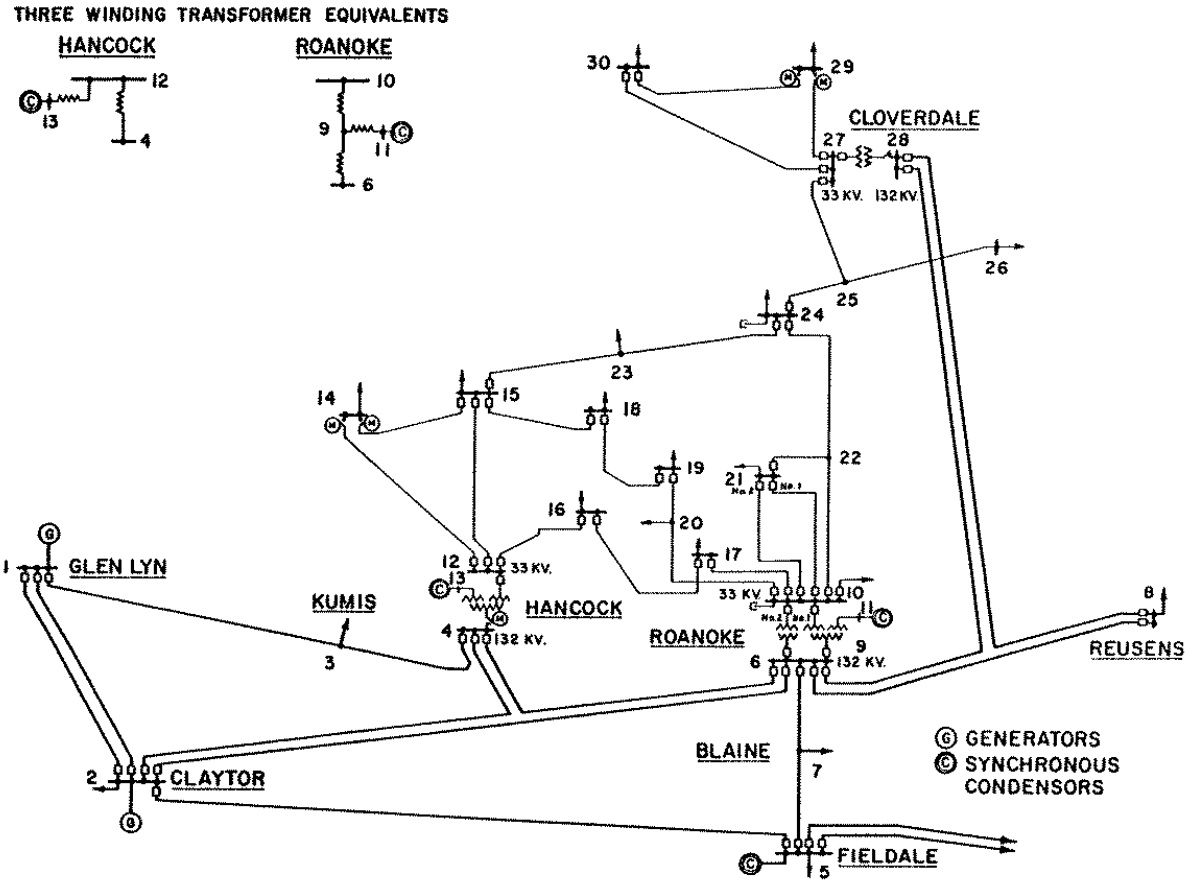

Table A. 3 – Transmission line data on 100 MVA base.

From Bus Number	To Bus Number	Series Resistance (Rs) PU	Series Reactance (Xs) PU	Shunt Susceptance (B) PU	Tap
1	2	0.0192	0.0575	0.0528	1.000
1	3	0.0452	0.1652	0.0408	1.000
2	4	0.0570	0.1737	0.0368	1.000
3	4	0.0132	0.0379	0.0084	1.000
2	5	0.0472	0.1983	0.0418	1.000
2	6	0.0581	0.1763	0.0374	1.000
4	6	0.0119	0.0414	0.0090	1.000
5	7	0.0460	0.1160	0.0204	1.000
6	7	0.0267	0.0820	0.0170	1.000
6	8	0.0120	0.0420	0.0090	1.000
9	6	0.0000	0.2080	0.0000	0.978
10	6	0.0000	0.5560	0.0000	0.969
9	11	0.0000	0.2080	0.0000	1.000
9	10	0.0000	0.1100	0.0000	1.000
12	4	0.0000	0.2560	0.0000	0.932
12	13	0.0000	0.1400	0.0000	1.000
12	14	0.1231	0.2559	0.0000	1.000
12	15	0.0662	0.1304	0.0000	1.000
12	16	0.0945	0.1987	0.0000	1.000
14	15	0.2210	0.1997	0.0000	1.000
16	17	0.0524	0.1923	0.0000	1.000
15	18	0.1073	0.2185	0.0000	1.000
18	19	0.0639	0.1292	0.0000	1.000
19	20	0.0340	0.0680	0.0000	1.000
10	20	0.0936	0.2090	0.0000	1.000
10	17	0.0324	0.0845	0.0000	1.000
10	21	0.0348	0.0749	0.0000	1.000
10	22	0.0727	0.1499	0.0000	1.000
21	22	0.0116	0.0236	0.0000	1.000
15	23	0.1000	0.2020	0.0000	1.000
22	24	0.1150	0.1790	0.0000	1.000
23	24	0.1320	0.2700	0.0000	1.000
24	25	0.1885	0.3292	0.0000	1.000
25	26	0.2544	0.3800	0.0000	1.000
25	27	0.1093	0.2087	0.0000	1.000
27	28	0.0000	0.3960	0.0000	0.968
27	29	0.2198	0.4153	0.0000	1.000
27	30	0.3202	0.6027	0.0000	1.000
29	30	0.2399	0.4533	0.0000	1.000
8	28	0.0636	0.2000	0.0428	1.000
6	28	0.0169	0.0599	0.0130	1.000

Table A. 4 – Bus data for the system.

Bus No.	Bus type	Generation (PU)		Load (PU)		Voltage Magnitude
		PG	QG	PL	QL	
1	Swing	2.602	-0.161	0.000	0.000	1.060
2	PV	0.400	0.500	0.217	0.127	1.043
3	PQ	0.000	0.000	0.024	0.012	--
4	PQ	0.000	0.000	0.076	0.016	--
5	PV	0.000	0.370	0.942	0.190	1.010
6	PQ	0.000	0.000	0.000	0.000	--
7	PQ	0.000	0.000	0.228	0.109	--
8	PV	0.000	0.000	0.300	-0.073	1.010
9	PQ	0.000	0.000	0.000	0.000	--
10	PQ	0.000	0.000	0.058	0.020	--
11	PV	0.000	0.162	0.000	0.000	1.082
12	PQ	0.000	0.000	0.112	0.075	--
13	PV	0.000	0.106	0.000	0.000	1.071
14	PQ	0.000	0.000	0.062	0.016	--
15	PQ	0.000	0.000	0.082	0.025	--
16	PQ	0.000	0.000	0.035	0.018	--
17	PQ	0.000	0.000	0.090	0.058	--
18	PQ	0.000	0.000	0.032	0.009	--
19	PQ	0.000	0.000	0.095	0.034	--
20	PQ	0.000	0.000	0.022	0.007	--
21	PQ	0.000	0.000	0.175	0.112	--
22	PQ	0.000	0.000	0.000	0.000	--
23	PQ	0.000	0.000	0.032	0.016	--
24	PQ	0.000	0.000	0.087	0.067	--
25	PQ	0.000	0.000	0.000	0.000	--
26	PQ	0.000	0.000	0.035	0.023	--
27	PQ	0.000	0.000	0.000	0.000	--
28	PQ	0.000	0.000	0.000	0.000	--
29	PQ	0.000	0.000	0.024	0.009	--
30	PQ	0.000	0.000	0.106	0.019	--